FLORIDA INTERNATIONAL UNIVERSITY

Miami, Florida

APPLICATIONS OF PAPER MICROFLUIDIC SYSTEMS IN THE FIELD DETECTION OF DRUGS OF ABUSE

A dissertation submitted in partial fulfillment of

the requirements for the degree of

DOCTOR OF PHILOSOPHY

in

CHEMISTRY

by

Ling Wang

2017

To: Dean Michael R. Heithaus
College of Arts, Sciences and Education

This dissertation, written by Ling Wang, and entitled Applications of paper microfluidic systems in the field detection of drugs of abuse, having been approved in respect to style and intellectual content, is referred to you for judgment.

We have read this dissertation and recommend that it be approved.

_____
Anthony DeCaprio

_____
Piero Gardinali

_____
Nelly Mateeva

_____
Anthony McGoron

_____
Yi Xiao

_____
Bruce McCord, Major Professor

Date of Defense: July 6, 2017

The dissertation of Ling Wang is approved.

_____
Dean Michael R. Heithaus

College of Arts, Sciences and Education

_____
Andrés G. Gil
Vice President for Research and Economic Development
and Dean of the University Graduate School

Florida International University, 2017

ACKNOWLEDGMENTS

I want to acknowledge the support of my parents, whenever I have a happiness or a sadness, you are always on my side, even you are in the other side of the earth, you are my home of everything. I want to thank my major professor, Dr. Bruce McCord, and the members of my committee: Dr. Anthony DeCaprio, Dr. Piero Gardinali, Dr. Nelly Mateeva, Dr. Anthony McGoron, and Dr. Yi Xiao. Their good advice throughout my graduate years was appreciated. I also want to thank Dr. Watson Lees, FIU Chemistry Department's Graduate Program Director. I would like to thank Dr. Giacomo Musile for his helping to improve my critical thinking and operations in the research.

Finally, I would like to thank the US Department of Justice of their funding of NIJ-DW-BX-K032, and the FIU Presidential Fellowship.

ABSTRACT OF THE DISSERTATION

APPLICATIONS OF PAPER MICROFLUIDIC SYSTEMS

IN THE FIELD DETECTION OF DRUGS OF ABUSE

by

Ling Wang

Florida International University, 2017

Miami, Florida

Professor Bruce McCord, Major Professor

Over the years, colorimetric reagents and immunology have been widely used in screening tests for illicit drugs; however, the test kits are not always convenient for field use and often require the user to mix and develop a specific set of reagents. In our project, we have been working on alternative platforms based on paper microfluidic devices (uPADs) for field testing. These devices utilize wax channels printed on paper to direct the analyte towards a specific set of chemical reagents. Using the procedure, we have developed a six-channel chip that adapts known colorimetric reagents targeting cocaine, opiates, amphetamines and ketamine for multiplex detection. For more sensitive and specific determinations than the colorimetric reagents, we have also developed a paper device that utilizes the interaction between gold nanoparticles and drug specific aptamers.

The μPADs using colorimetric reagent are designed as a six-channel multiplexed system. Sequences of different reagents applied to each channel to produce a series of reactions and the color changes appear at the end of each

channel. The entire process takes less than five minutes. The adjusted reagents produce specific color changes for seized drugs on the paper microfluidic devices. Procedures have been developed for the detection of cocaine, ketamine, codeine, ephedrine, morphine, amphetamine, methamphetamine, and MDMA. These devices have been tested for sensitivity, specificity and stability against a variety of potential interferences and test conditions.

Gold nanoparticles (AuNPs)/ aptamers μPADs were developed to detect cocaine. The presence of cocaine cause the binding with aptamers, and the gold nanoparitcles produced a salt-indicated aggregations and gave a color change of AuNPs from red to black. The absence of cocaine allowed the aptamers freely to bind gold nanoparticles, and no color change occured. The device had a preliminary validation of sensitvity and specificity against a variety of potential interferences.

The use of paper microfluidic devices permits the development of rapid, inexpensive and easily operated tests for drug samples in the field. They present a safe and convenient presumptive tool that can be used in the field.

TABLE OF CONTENTS

CHAPTER PAGE

LIST OF TABLES

LIST OF FIGURES

FIGURE PAGE

ABBREVATIONS

AKD	Alkyl ketene dimer
AuNPs	Gold nanoparticles
CE	Capillary electrophoresis
cm	Centimeter
CNS	Central nervous system
$Co(SCN)_4$	Cobalt(II) thiocyanate
CTAB	Cetrimonium bromide
d.i. water	Deionized water
DNA	Deoxyribonucleic acid
$FeCl_2$	Iron (II) chloride
$FeCl_3$	Iron (III) chloride
g	Gram
GC	Gas chromatography
H_2O	Water
H_2SO_4	Sulfuric acid
HAuCl4	Tetrachloraurte (III)
HCl	Hydrochloric acid
HNO3	Nitric acid
IMS	Ion mobility spectrometry
IN	Intranasal
IR	Infrared spectroscopy
IV	Intravenous
LC	Liquid chromatography
LFIA	Lateral flow immunoassay
LOD	Limit of Detection
LSD	Lysergic acid diethylamide
M3G	Morphine-3-glucuronide
M6G	Morphine-6-glucuronide
MDMA	3,4-methylenedioxyamphetamine
MDQ	Minimum detectable quantity
$MgCl_2$	Magnesium chloride
mM	Millimolar
MPC	Monolayer protected cluster
MS	Mass spectrometry
mV	Millivolt

Na_2SO_4	Sodium sulfate
NaOH	Sodium hydroxide
NIDA-5	National Institute on Drug Abuse
nM	Nanomolar
NMR	Nuclear magnetic resonance spectroscopy
PCP	Phencyclidine
PCR	Polymerase chain reaction
PEG	Poly(ethylene glycol)
PO	Oral
PVA	Polyvinyl alcohol
QD	Quantum dot
RGB	Red-Green-Blue
RNA	Ribonucleic acid
SELEX	Systematic evolution of ligands by exponential enrichment
SM	Smoking
SPR	Surface plasmon resonance
SWGDRUG	Scientific Working Group for the Analysis of seized Drugs
THC	Tetrahydrocannabionl
THC-COOH	11-nor-delta 9- tetrahydrocannabinol carboxylic acid
TLC	Thin layer chromatography
Tween 20	Polysorbate 20
Tween 80	Polysorbate 80
UV	Ultraviolet spectroscopy
v:v	Volume : Volume
w:v	Weight: Volume
µg	Microgram
µL	Microliter
µM	Micromolar
µPADs	Paper microfluidic devices

Chapter 1. Short History of Drugs of Abuse and Analysis

1. Introduction

Drug abuse has been a global problem for many years. The World Drug Report has estimated that up to 250 million people used illicit drugs in 2010. [1] In 2014, the report estimated that one in 20 adult individuals were drug users ,and over 29 million drug abusers suffered disorders such as HIV and hepatitis; however, only 4.83 million drug addicts with these issues were in treatment. [2] Drug users have higher risks of health problems than other non-drug users [3], and are often involved in antisocial behavior. Almost one in five sentenced prisoners are involved in a drug-related offense, and the estimated global drug-related deaths was 207,400 per year. [4] In the United States, abuse of illicit and prescription drugs cost millions of dollars in crime, health and productivity. [5]

The term ‘drug of abuse’ does not have the same meaning as the term ‘illicit drug’ despite the fact they are often mixed in daily life. [6] For example, alcohol and tobacco are commonly abused drugs but are legal. [6] Patterns of drug abuse change with the time and country. Even in the same country, there exists a diversity of drug consumption depending on the period, local government and financial status. [4, 6] For example, in Southeast Asia there is a higher consumption of ketamine than in northern Europe [7], while North America and Western Europe have a greater consumption of cannabis than other regions. In South America, increasing abuse of cocaine has become a great problem. [4]

Drug control programs have been established for many years. Since the 1980s, the U.S. government has yearly spent billions of dollars in an attempt to control the illicit drug market; however, the results are limited. [8] There is a continuing development of new drug analogs along with an increasing use of mixtures of synthetic and traditional drugs. The increasing availability of dangerous drugs creates problems in legislation, control, interdiction, and forensic analysis.

a. Overview of SAMHSA 5

There are an overwhelming number of drugs of abuse, therefore in our research project, we have focused on a list of important compounds promulgated by the National Institute on Drug Abuse (SAMHSA-5). The SAMHSA-5 does not cover the entire set of drugs of abuse, such as new "designer drugs", legitimate drugs, or other less prevalent illicit drugs. [9] The primary concern is to control amphetamines (amphetamine and methamphetamine), cocaine, marijuana, opiates (codeine, morphine, heroin) and phencyclidine (PCP). These compounds are commonly detected as part of a standard five-drug panel.

(1) Cocaine

Cocaine (methylbenzoylecgonine) is an alkaloid which consists an ester of benzoic acid combined with an amino alcohol methylecgonine. Cocaine hydrochloride is a white crystalline salt and it can precipitate to yield

cocaine free base when mixed with potassium permanganate and aqueous ammonia. [9] Cocaine can be prepared as either the purified product from the coca paste or a synthesized product from ecgonine via the Mannich reaction. [9,10]

Cocaine has been used as a topical local anesthetic in medicine. Its mode of action is to block sodium channels in the central nervous system and increase the threshold required to generate an action potential. [10]

Acute abuse of cocaine can cause cocaine intoxication, in which excessive stimulation occurs in the central nervous system. Chironic usage can cause psychological dependence.

The routes of administration of cocaine are via intravenous (IV), intranasal (IN), oral (PO) or smoking (SM). Comparing the drug bioavailability, the oral route has the lowest bioavailability (20%), the IN route is dose dependent with an estimated range of 25-94%, the SM route has a range of 57-70%, and the IV route has 100% drug bioavailability. [10] Cocaine and its metabolites can stay in urine or blood for up to 10 days. [9,10] The primary metabolites of cocaine are benzoylecgonine and ecogonine methyl ester. Cutoff concentrations of cocaine and its metabolites are 150ng/mL in screening tests and 100 ng/mL in confirmatory tests. [11]

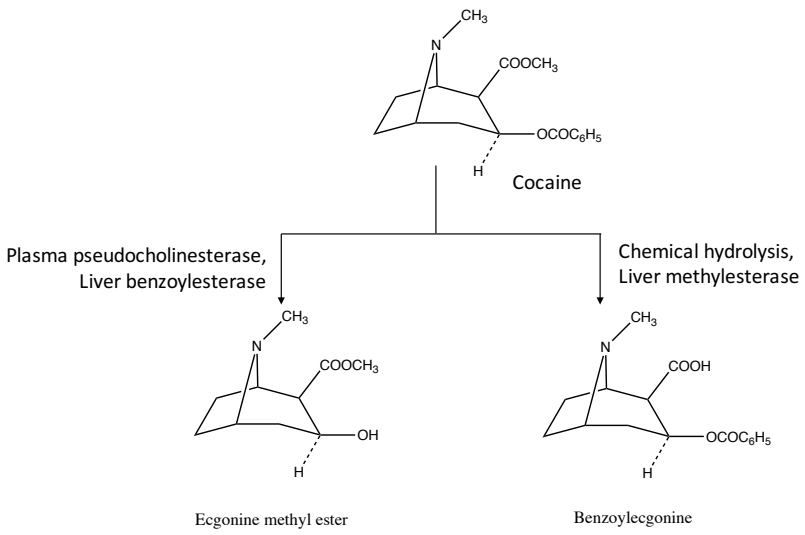

Figure 1.1. Main pathways in the primary metabolism of cocaine.

(2) Amphetamines

Amphetamines are central nervous system (CNS) stimulants that mimic natural hormones. Amphetamine and methamphetamine belong to the phenethylamine group, and are classified as Schedule II controlled substances. [9,10] Amphetamines can increase dopamine concentration at nerve endings and stimulate the CNS. Methamphetamine has a better CNS efficacy than amphetamine because the extra methyl group increases its lipophilicity and entry into the CNS. (Figure 1.2) In the urine samples, up to 45% of methamphetamine and 4-7% of amphetamine are excreted as the unchanged parent drugs in a 24-hour period. [9] For detection, the analytical cutoff is 500 ng/mL in screening tests and 250 ng/mL in confirmation tests. [11]

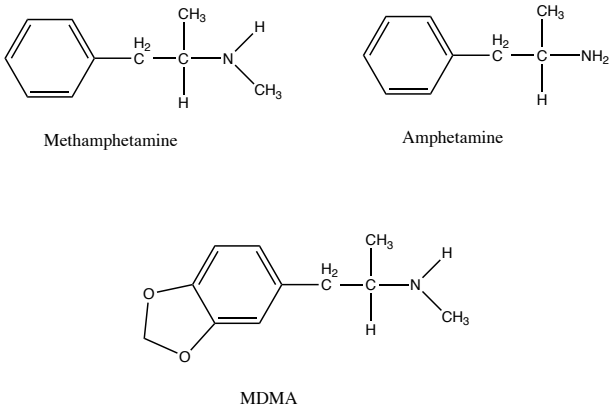

Figure 1.2. Structures of commonly abused phenethyl amines: methamphetamine, amphetamine, and 3,4-methylenedioxyamphetamine (MDMA).

3,4-methylenedioxyamphetamine (MDMA) is a designer drug of the phenethylamine class. It was previously used in therapeutic treatment, however today it is classed as a Schedule I controlled substance with no approved medical use. MDMA has a similar sympathomimtic activity to amphetamine, but its overdose can affect multiple organ systems. [10] MDMA has a cutoff level of 500 ng/mL in screening tests and 250 ng/mL in confirmation tests. [11]

(3) Phencyclidines

Phencyclidines(PCPs) are hallucinogens which interact with neurotransmitter systems and dopaminergic systems. Ketamine is an analog of PCP and its chemical structure is shown in Figure 1.3. Its salt form is ketamine hydrochloride and this form is used in medicines. Ketamine is structurally and pharmacologically related to PCP. It is

classified as a Schedule III controlled substance because it can be used as a drug for sexual assault because of its hallucinogenic properties. Phencyclidine has a cutoff of 25 ng/mL in screening tests and 25 ng/mL in confirmation tests. [11]

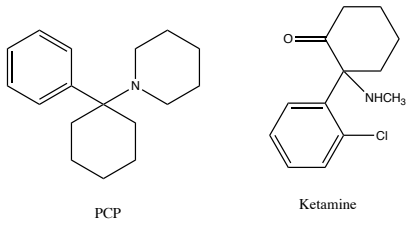

Figure 1.3. Structure of PCP and Ketamine.

(4) Cannabinoids

Cannabinoids are psychoactive products extracted from the *Cannabis sativa* plant complex. The products can come from whole plants or finely chopped leaves and buds. ∆9-Tetrahydrocannabinol (THC) is the main component of cannabis, and it has a low toxicity, however, chronic usage can cause damage to the liver and other organs and impairment of attention and memory. [9,10] The main metabolite of THC is 11-nor-delta 9- tetrahydrocannabinol carboxylic acid (THC-COOH) which can be found in blood, urine, hair, sweat, and oral fluids. (Figure 1.4) The drug is usually detectable from one to 10 days depending on the type of biological sample. [10] Marijuana metabolites have a 50 ng/mL cutoff in screening tests and a 15 ng/mL cutoff in confirmation tests. [11]

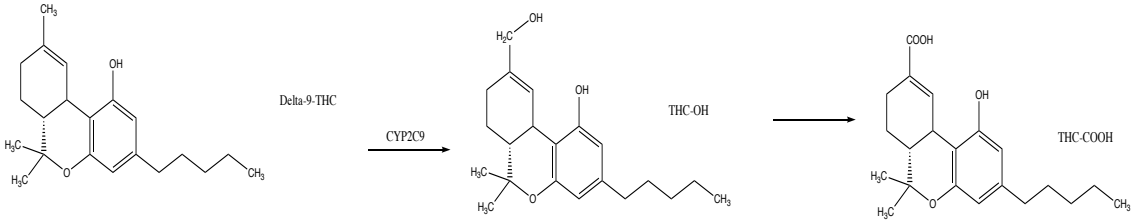

Figure 1.4. Pathway of THC metabolism.

(5) Opioids

The basic structure of opioids contains an aromatic core along with basic moieties. Codeine and morphine have a similar structure, and they are Schedule II controlled substances. (Figure 1.5) Both are extracted from the opium poppy as opiate alkaloids and are classified as phenanthrenes. Opioids have major pharmacologic effects on the CNS because they have selective binding sites at several receptors. Codeine is a weak μ and κ agonist, while morphine is a strong μ agonist and a weak κ and δ agonist. They both can block the transmission of painful stimuli. [10]

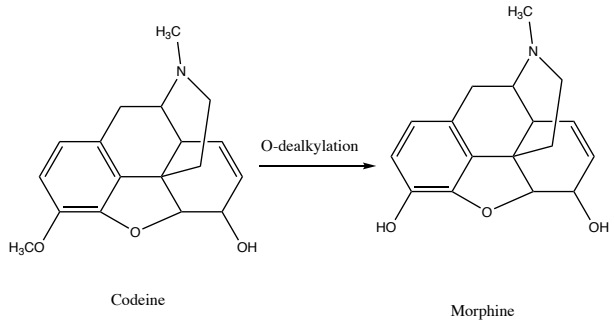

Figure 1.5. Structures and Metabolism of codeine to morphine.

The primarily metabolites of morphine are morphine-3-glucuronide (M3G) and morphine-6-glucuronide(M6G). Codeine converses to morphine in the liver via cytochrome P450 enzyme CYP2D6. [10] Approximately 10-20% of unchanged codeine is excreted in the urine in one day.[9] The analytical cutoffs for presumptive and confirmatory testing are 2000 ng/mL. [11]

b. Forensic Applications of Drugs Analysis

Typically, there are two steps involved in forensic drug analysis, presumptive and confirmatory testing. [14] A presumptive test is used to quickly identify the presence of a drug substance while a confirmatory test is used to identify and quantify the presence of a target drug. In general, a presumptive test is less specific and mainly detects drug classes while a confirmatory test utilizes spectroscopic and chromatographic methods for a compound specific determination. These tests are described and standardized by an official organization known as the 'Scientific Working Group for the Analysis of seized Drugs' (SWGDRUG). The SWGDRUG has published a list of recommendations to assist forensic analysts with analytical techniques, protocols and policies. The most recent version of these guidelines was updated in June 2016 as Version 7.1. [15] These recommendations cover the practices of sampling, drug identification, validation, quality assurance and education. In this recommendation, analytical techniques are classified into three types. Category A includes

infrared spectroscopy (IR), mass spectrometry (MS), nuclear magnetic resonance spectroscopy (NMR), Raman spectroscopy and X-ray diffractometry; Category B includes capillary electrophoresis (CE), gas chromatography (GC), ion mobility spectrometry (IMS), liquid chromatography (LC), microcrystalline tests, pharmaceutical identifiers, thin layer chromatography (TLC) and macroscopic/microscopic examination (only for cannabis); Category C includes color tests, fluorescence spectroscopy, immunoassays, melting point, and ultraviolet spectroscopy (UV). [15] In the forensic identification of seized drugs, the minimum standards are: (1) if an analytical scheme uses one validated analytical technique from Category A, at least another technique from Category A, B or C is required; (2) if any technique from Category A is not used, at least two techniques from Category B should be examined, and one additional test must be performed from Category B or C. [15] Depending on jurisdictional requirements, the analytes may be characterized as finished products, intermediates, precursors, key reagents, or reaction mixtures. [15]

(1) Presumptive Tests

The purpose of a presumptive test is to determine the potential presence of a substance at a crime scene, it is also called a screening test. [12] The test can produce a positive, negative, or inconclusive result. In drug analysis, different types of separate presumptive tests are used in the

determination of seized drugs and in toxicology. [13] According to SWGDRUG Recommendations, color tests and immunoassays from Category C, and thin layer chromatography from Category B are used in screening tests. [15] Spot tests and thin layer chromatography (TLC) are the most widely used methods in seized drug detection while immunoassays are generally applied to human toxicological samples. Spot tests utilize colorimetric reagents in drug analysis. These reagents are generally selected because of chemical interactions with reactive moieties present in the drug. Because of this fact, spot tests lack the specificity of spectroscopic methods [13,14] have a relatively high limit of detection [13], and can yield false positive and negative results. Despite these weak points, spot tests offer rapid answers under field conditions making them highly useful in drug interdiction. [14] The tests do not require a highly-trained individual to operate them and generally provide quick and useful results. A typical colorimetric reagent kit contains nine to fifteen reagents, and can identify more than 40 of the most common street drugs. [13] Once a positive result is obtained, subsequent analytical techniques from Category B and A are required to confirm the drug determinations. [15]

More sensitive presumptive detection of toxicological samples can be performed via immunoassay. Immunoassay is an analytical technique which can detect and qualify the target analyte based on binding to specific antibodies. In drug analysis, immunoassays are used to detect

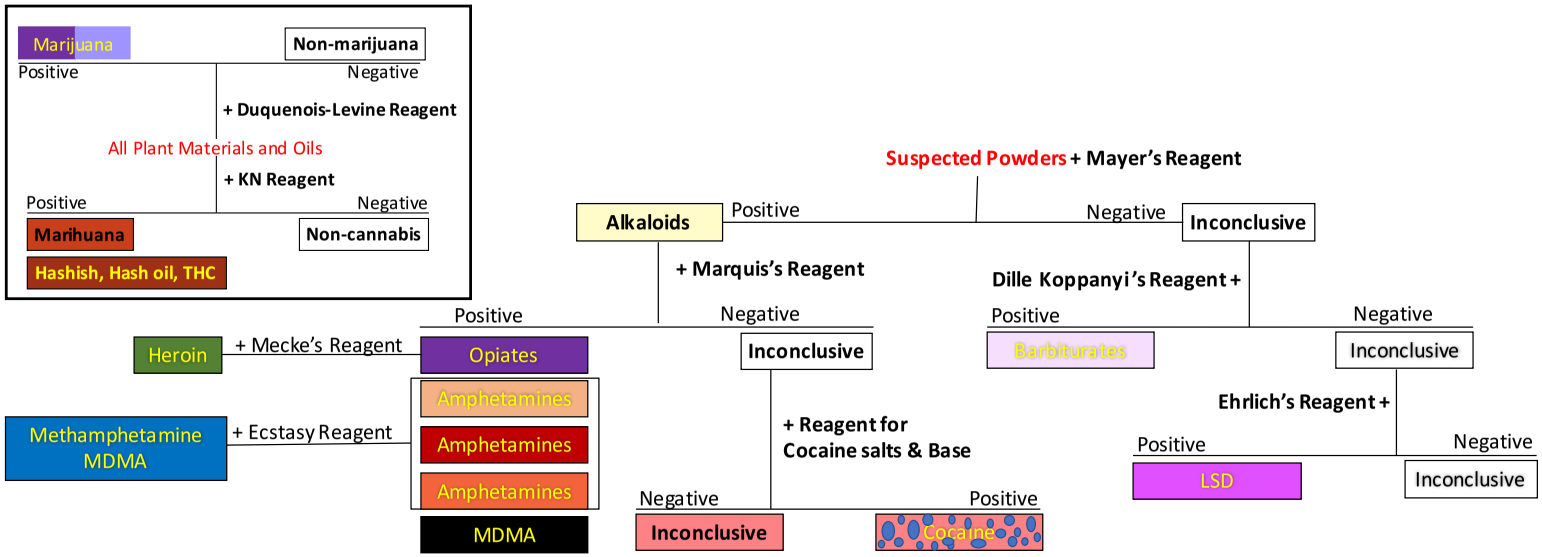

Figure 1.6. A typical set of colorimetric reagents used in narcotics testing. [16] The kits contain multiple plastic tubes which contains all chemical components required for each colorimetric reagent. The suspected materials are added to the tubes and colorimetric matching is used to screen for compounds of interest.

target drugs in biological matrices. [10] Although Immunoassays higher specificity and a lower limit of detection than spot tests, they have some shortcomings. Of most importance is the cross-reactivity, especially for the metabolites and drugs of similar structure. Cross reactivity can cause false positive results, particularly when non-controlled substances at high concentrations react weakly with the test. False negative results can also occur due to interfering substances in the sample matrix. Another problem with immunoassays is the administrative detection cutoffs. The response to each drug can vary depending on the design and manufacturer of the test. [13,17]

(2) Confirmation tests

All positive results from a screening test require further confirmation. Confirmation tests utilize a different analytical principle which has higher specificity and greater sensitivity than screening tests. [13] The tests commonly utilize separation methods to separate the drugs from samples, and spectroscopic methods to quantify and identify the components in the sample. [9] GC/MS and LC/MS are the most common methods used. For seized drugs, spectroscopic techniques such as FTIR may also be utilized. [10,15]

2. Research Goals

In forensic analysis, presumptive tests for drugs of abuse may be performed on-site or in a laboratory setting. On-site and point-of-care testing are important to prescreen samples because of the increasing laboratory backlogs for confirmatory testing. Colorimetric tests and antibody-based lateral flow immunoassay have been used for years, however they generally lack multiplex capabilities. Thus, several tests are required to determine the range of potential analytes.

The goal of the present project was to improve the specificity and sensitivity of screening tests through the development of a paper-based microfluidic device for drug detection. Such tests should be inexpensive, simple to use and rapid in response. Two different paper-based microfluidic devices were developed. The first device adapted colorimetric tests to a paper format. Potential analytes included seized drug samples such as opiates, cocaine and amphetamines. The second type of device developed for on-site detection of cocaine used a gold nanoparticle/aptamers complex based on the principles developed in lateral flow immunoassays.

The colorimetric reagent-based paper microfluidic devices utilized modified colorimetric reagents with paper chips. Since individually these tests do not produce high specificity, a multi-channel device can help to confirm the presence of the target compound through a simultaneous set of cross-comparisons. Multiple channel also permit a simultaneous

determination of different classes of drugs. For example, in such a device, a drug could react with 3 or more of the differing spot tests on a single device, greatly improving specificity. As current spot tests are solution based and often involve harsh acids reacting with metal salts, the experimental work also included the development of a set of reagents that utilize alternative oxidants. The overall goal of these studies was to produce reactions that enhanced the color changes on the devices without destroying the paper matrix.

A gold nanoparticle/aptamer based paper microfluidic device was also developed to utilize anti-cocaine aptamers as an alternative to the antibody based lateral flow immunoassays that are currently used. Aptamers are useful alternatives to antibody-based assays as they have high affinity and specificity to the target molecule. Aptamers are DNA or RNA based oligomers, and they can be chemically synthesized and modified for use with a variety of colorimetric schemes as biosensors. Gold nanoparticles change colors resulting from their morphology in solution (dispersion vs aggregation). Gold nanoparticles easily change from red to blue under salt-indicated aggregation. The principle of salt-induced color changes of gold nanoparticles can be used to increase specificity and decrease the limit of detection in the detection of cocaine and other drug targets. Overall these projects have great potential to provide improved forensic determinations in on-site drug detection, making the analyses simpler, more specific and easier to use.

3. References

1. UNODC, World Drug Report 2012. 2012 June.

2. UNODC, World Drug Report 2016. 2016 May.

3. Chriqui, J. F., Pacula, R. L., McBride, D. C., Reichmann, D. A.,
4. Vanderwaal, C. J., Terry-McElrath, Y. M. Illicit drug policies: Selected laws from the 50 states. Berrien Springs, MI: Andrews University. 2002.

5. Organization, W.H., Global tuberculosis report 2016. 2016.

6. National Drug Intelligence Center, The Economic Impact of Illicit Drug Use on American Society. 2011, Product No. 2011-Q0317-002

7. Wills, S., Drugs of abuse. Pharmaceutical Press, 2005.

8. UNODC, World Drug Report 2013, Drug and Alcohol Review, 2014. 33(2), 216-216

9. Poret, S., Téjédo, C. Law enforcement and concentration in illicit drug markets. *European Journal of Political Economy*, **2006**, *22*(1), 99-114.

10. Smith, F. Handbook of forensic drug analysis. Academic Press, 2004.

11. Levine, B. Principles of forensic toxicology. Amer. Assoc. for Clinical Chemistry, 2003.

12. Guidotti, T. L., Arnold, M. S., Lukcso, D. G., Green-McKenzie, J., Bender, J., Rothstein, M. A., Stecklow, M. *Occupational health services: A practical approach*. Routledge, 2012.

13. Knapp, N., Illegal Drugs: A Complete Guide to Their History, Chemistry, Use, and Abuse. Aorn Journal, **2005**, 82(2), 306-307

14. Ramirez, C.R., Parish-Fisher C.L. Crime Scene Processing and Investigation Workbook. CRC Press, 2011.

15. Brandenberger, H., Maes R.A. Analytical toxicology for clinical, forensic and pharmaceutical chemists. Vol. 5. Walter de Gruyter, 1997

16. SWGDRUG Committee, Scientific Working Group for the Analysis of Seized Drugs (SWGDRUG), Recommendations for: Education and Training. Quality Assurance, Methods of Analysis, US Department of Justice, Drug Enforcement Administration/Executive Office of the President, Office of National Drug Control Policy, Counterdrug Technology Assessment Center, 2016.

17. Lancashire, R.J. Unit 9. Crime http://wwwchem.uwimona.edu.jm/courses/CHEM2402/Crime/Reagent_Kits.html (accessed by May 1, 2017)

18. McClatchey, K.D., Clinical laboratory medicine. Lippincott Williams & Wilkins, 2002.

Chapter 2. Paper microfluidic devices

1. Introduction

Paper microfluidic devices (μPADs) are patterned paper based analyzers which are designed for use as point-of-care diagnostic devices. Hydrophobic barriers on the paper channel solvents and analytes to specific detection regions. Originally, these devices were developed for use in third world countries where the lack of refrigeration and power for instrumentation limited diagnostic capabilities. Instead, for μPADs, reagents are stabilized by being isolated and dried on the paper. They are then activated as the analyte solution moves up the paper, creating a system of coupled linear reactions which ultimately result in a color change as a positive response. No external power is needed. As a result, diagnosis can be performed at much lower cost. [1]

The development of such microfluidic systems for laboratory analysis has the potential to revolutionize analytical procedures, bringing laboratory operations to the field, and increasing convenience. Microfluidic platforms can be divided into five groups depending on the method of sample mobility and fluidic control. These include methods related to capillary action, hydrostatic pressure, centrifugal force, electrokinetic mobility and acoustic forces. [2] Paper microfluidic devices are one type of microfluidic platform, they use capillary and electrokinetic methods for the movement and analysis of the target of interest. [3]

Paper microfluidic devices utilize paper as a substrate material. The

development of paper-based chemical testing traced back the work of Műller and Clegg in the 1940s, who developed paper chromatography. The usage of paper did not get much attention until Martinez et al. developed the first paper microfluidic device for chemical analysis. [4] The first PAD took advantage of unique properties of the hydrophilic channels, permitting the movement of the sample in a designated direction, resulting in colorimetric detection at low cost. Since then, there has been an explosion in the development of applications for paper microfluidic devices, and many studies of the properties of the paper substrate. [4] Paper microfluidic devices are small, flexible, portable, and inexpensive to use. They consume minimal volumes of analytes and reagents and can be easily stored for long periods of time. The devices have been used in spot tests and lateral flow analysis methods with chemical and biochemical targets. [3]

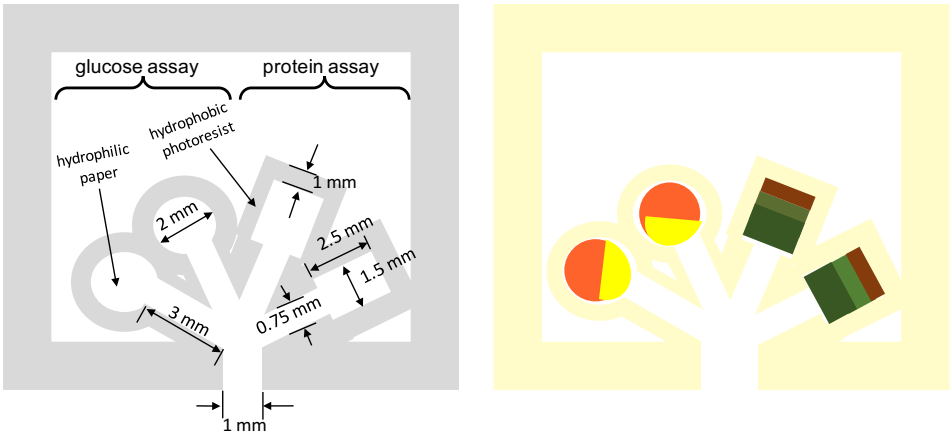

Figure 2.1 An early design for a paper microfluidic device used in bioanalysis. The device contained detection systems for both glucose and protein, with each assay having two detection channels. (A) The multi-channel design of a μPAD used to detect glucose and protein in urine. The

figure shows the design of channels and barriers. (B) The color changes produced by urine applied to the paper-based microfluidic device. When the urine sample contained glucose and protein, the channel of the glucose assay turned reddish brown and that for the protein assay turned green. [1]

A. Paper

Paper can perform capillary action without pumping, improve detection limits resulting from its high surface area-to-volume ratio, and retain chemicals within the fiber network. [3] The capillary flow that moves through a μPAD is a wicking-based flow, so the wicking rate of paper is an important parameter. Chemicals prepared on μPADs consist of different types of materials and the durability of the paper is also important. Therefore, the choice of paper depends on the application and the target of analysis.

B. Types of μPADs

There are two types of paper-based microfluidic devices: on-demand devices which are blank platforms without pre-deposited reagents; or ready-to-use devices, which are designed as complete systems by prior deposition of reagents into the designed zones of the device. [3] The ready-to-use devices are used to detect specific analytes in samples.

C. Preparations and Applications of uPADs

Manufacturing of paper microfluidic devices is very simple and cheap with an estimated price is < $10 per square meter, even using high-quality chromatography paper.[1,3,5] Recently published methods include photolithography, plotting with an analogue plotter, ink jet etching, plasma treatment, paper cutting, ink jet printing, flexography printing, screen printing, laser treatment and wax printing.[3] Although each method has its strengths and weaknesses, wax printing followed by heat based lamination can quickly and easily produce usable devices using a wax printer and a laminator.[3,6]

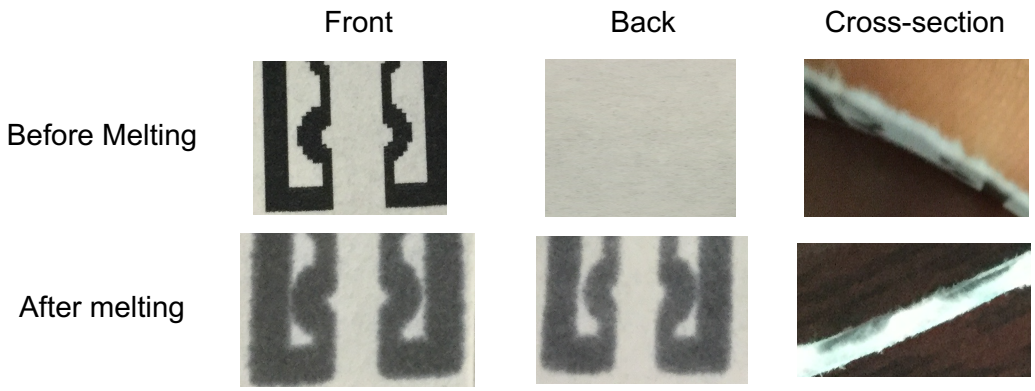

Figure 2.2 A comparison of the result from melting of wax ink barriers on chromatographic paper viewing the “front”, “back” and “cross-section” of the paper. Before melting, the wax ink only appeared on the front side of the paper; after melting, the wax flowed into the paper (cross-section) and was visible passing through the paper onto the opposite side. This created a barrier to the movement of the liquid sample.

The wax printing method was invented in 2009 and takes advantages of the physical deposition of the wax onto fibrous surfaces for later selective

hydrophobization [6]. Figure 2.2 demonstrates an example of wax printed lines. The devices' patterns can be easily designed and adjusted, producing devices that are portable, small, and inexpensive. The procedure used to create these devices are divided into two steps: (1) the wax patterns are printed on the paper, (2) the wax is melted so that it spreads horizontally and vertically into the paper. The vertical spreading creates a hydrophobic barrier within the paper. A byproduct of the process is a horizontal spreading that decreases the resolution of the printed pattern, and leads to the wider hydrophobic barriers than the original printed patterns. (Figure 2.2) This wax printing method has been successfully used in screening for metal ions [7] and pharmaceuticals [8,9].

Capillary flow is the basis of the mobility of fluids in μPADs. The movement can be adjusted by changing the spatial structures and raw materials during manufacturing. For example, Li and co-workers (2008) used plasma treatments on μPADs for use in cellulose-based mechanical switches, filters and separators. [10] The authors prepared chemically treated filter paper, then used metal masks to produce hydrophilic patterns via plasma treatments. The plasma treated areas then permitted capillary flow.

μPADs have been mostly used in biochemical analysis, as well as in medical and forensic diagnostics. The latest tendency in the development of these devices is the production of three-dimensional μPADs which can

be utilized in colorimetric detection and electrochemical detection in the same paper chip. [11] The application of lateral flow paper chromatography increases the specificity of μPADs. [4] Most μPADs utilize colorimetric assays, while others focus on chemiluminescence and electrochemiluminescence detection techniques. [3]

Above all, paper-based microfluidic devices have many advantages, such as low material costs, a simple production process, simple designs and easy interpretations of test results. There is often no requirement for external instruments or instrumentation. These devices are useful in point-of-care detection of disease, in forensic analysis and in environmental monitoring.

D. Color Detection

In this project, all tests involved colorimetric detection and the results were recorded as the pictures for the later instrumental analysis. The color of a substrate is dependent on the pigments used and the diffuse reflectance of the colored substrate. The measured signal is produced by the quantity of incident light that is diffusely reflected by the colored reagents in the visible range. [12] The observed color is the wavelength of incident light that is reflected from the substrate, the other visible wavelengths are absorbed.

Absorbance measurements are described by the Lambert-Beer law for the determination of quantities of a sample in solution. When paper is used as

an alternative to solution measurements, the Lambert-Beer law is modified to predict the diffuse reflectance of a light beam on a surface as a function of the quantity of a colored species detected. The equation [13] is shown below:

$$\mathrm{R} = I_r/I_0 = R_w e^{-k_1 m}$$

$$I_r = I_s + I_c + I_p$$

in which, R = the reflectance of the incident light by the surface; I_r = the intensity of the reflected light which depends on the surface of the carrier; I_0 = the intensity of the incident light; R_w = the reflectance of the reference white surface; k_1 = a proportionality constant; m = the mass per unit area of the substance of interest; I_s = the reflection on the surface of the solution, in the paper test, the value is assumed as a constant; I_c = the reflection on the white surface of the paper; I_p = the reflection on the surface of the colored reagent.

Visual identification is dependent on the perception of color by human beings. Humans have three cone cells in the eyes reflecting short, middle and long wavelengths. [14] Paper is a scattering material, thus when colored ink is placed on paper, people observe color because the light is reflected through the fibers and produces a diffusely-scattered result. [14] The perceived color of the dyes on the paper results from the wavelengths of incident light that are reflected following the absorbance of the analyte. [15]

For color detection methods utilizing cell phones, digital cameras, or

scanners, quantitative detection is based on reflectance. [16, 17] Usually the entire sensing area is used to measure the digital color values for the calculation of calibration curves [18]. RGB intensities are the most common values used in quantification [19] while chromaticity (hue and colorfulness) is another choice [20].

It is important to note that humans have varying sensitivity to the color. Thus to standardize color detection, the idea of a RGB color space was created to describe the physical color perceived by human eyes with normal vision.[16] In general the value for red, green and blue as well as the brightness are used to describe the color components in an image. [16] In this work, the estimation of the RGB values in a colored image, was performed using Image J software. Image J software is an open source software program used to analyze images based on color, pixel value, angles, and distance. In particular, Image J RGB Measure Plus software was developed to measure the value of single components of red, green and blue with a user selected area from a colored image. [17] This software permits a computer based verification of images taken during the user's observation of a color change on the device. It also provides an instrumental based confirmation of detection.

2. Goals

The overall goal of the current project was to develop multiplexed paper-based microfluidic devices for forensic drug detection. The novel development of paper microfluidic devices for drug screening can serve as a replacement for current colorimetric detection techniques. The key issue in this project was to modify existing solution-based colorimetric methods to permit paper-based detection. In addition, tests for interfering compounds and drug diluents were performed as well as an estimation of instrumental minimum detectable quantity (MDQ) for the multiple channel design.

3. Chemicals and Methods

A. Chemicals

All chemicals were analytical grade. Cobalt thiocyanate was purchased from Aldrich. Cocaine and ketamine were purchased from Sigma (St Louis, MO). Gold (III) chloride trihydrate (≥ 99.9%) was purchased from Sigma-Aldrich (St Louis, MO). Sucrose, acetone, chloroform, methanol and methylene chloride were purchased from Fisher Scientific (Fair Lawn, NJ). Solid wax inks were purchased from Xerox (Norwalk, CT)

B. Preparation and operation of μPADs

The paper microfluidic devices were printed on chromatographic paper using a Xerox wax-ink printer (Xerox ColorQube 8570). The paper was next wrapped in aluminum foil and allowed to pass through a laminator at

160˚C from two to five times to infuse the ink into the paper and create hydrophobic fluidic barriers. The colorimetric reagents are then placed at the designed positions along the fluidic path, and the drugs are spotted in organic solvents at the bottom of the chip. (Figure 2.3)

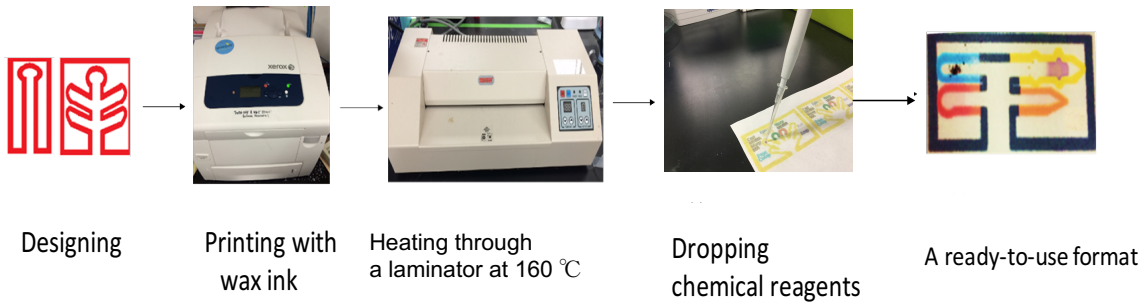

Figure 2.3. Preparation of μPADs. Step 1: Designing via a software Drawer in Windows system. Step 2: Printing with a chromatographic paper through a wax-ink printer. Step 3: Heating through a laminator at 160°C for several times. Step 4: Depositing reagents in the designed positions. Step 5: A ready-to-use μPAD.

The analysis was performed by spotting the dissolved drug onto the chip or by placing the chip into a solution of the dissolved drug to allow capillary action to carry it up to the various reaction zones as depicted in Figure 2.4.

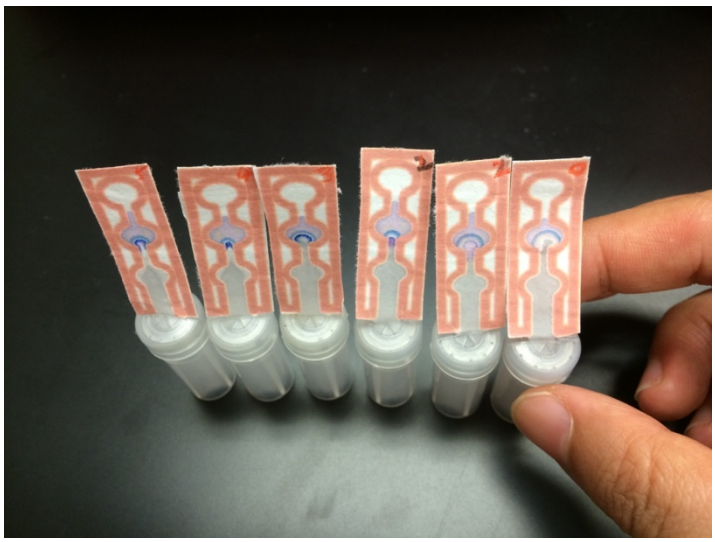

Figure 2.4. Operation of ready-to-use μPADs. The μPADs sat in the vial containing the moving solution and drug samples. The test stops when the solution moves to the end of a channel, the operation takes five to ten minutes.

4. Results and Discussion

A. Effects of μPADs

The channel size and length strongly affects colorimetric development on μPADs. In this work, it was important to adjust these parameters to optimize sensitivity and development time. For example, the size of the chip was important in optimizing analysis time. The longer the channel, the longer the running time of the paper chip with the same moving solution. Furthermore, channels facing in a direction counter to the upwards liquid flow took much longer for the analyte solution to reach the end of the channel. Depending on the mobility of the solvent, the resulting analytes may not reach the reaction zone in such designes. These design considerations must be combined with the chromatographic retention and

mixing effects as the solvent front hits each reagent zone. Thus, there are many critical design issues to consider when optimizing μPAD development. Figure 2.5 is an example of the effect of the width of channel on the mobility of the solvent as it delivers the colorimetric reagent. Gold nanoparticles moved in the desired channels and crossed the barriers when the top channel was much thinner in Figure 2.5, A and B. The same gold nanoparticles moved through the channel but these nanoparticles did not cross the barriers when the channel was wider as shown in Figure 2.5, C and D.

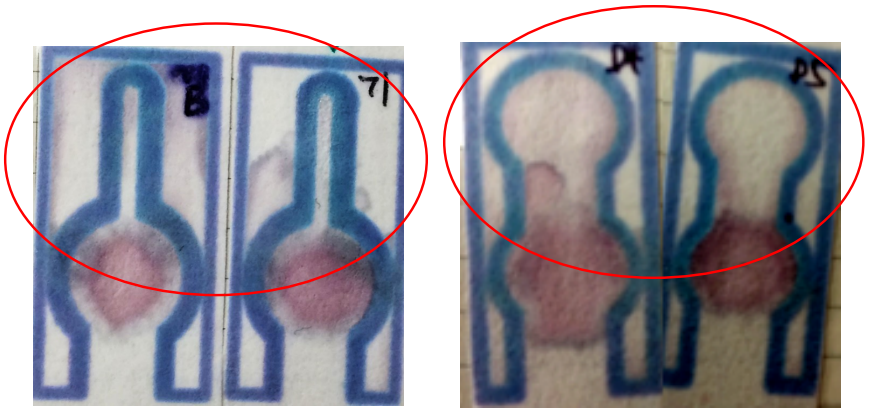

A B C D

Figure 2.5. The width of moving channels affects the mobility of gold nanoparticles on μPADs. Left: A thinner channel permits movement of nanoparticles in 0.3M sucrose solution, the gold nanoparticles crossed the barriers to the white part on μPADs. Right: A wider channel reduces the crossing of gold nanoparticles on μPADs.

The saturation of the melted wax into the paper creates a hydrophobic barrier on the μPADs. Insufficient melting decreases the hydrophobic properties of the barriers and the moving solution will again cross the

barrier (Figure 2.6) Therefore, it is critical to optimize the heat of the laminator.

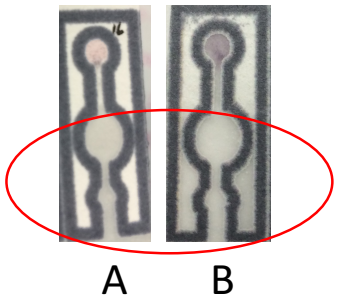

Figure 2.6. Effect of melted wax barriers on μPADs design. A: Fully melted wax barrier. When the moving solution passed through the channel, the solution did not cross barriers in a properly prepared μPAD. B: Incompletely melted wax barrier. When the moving solution passed through the channel, the moving solution leaked across the barrier, affecting the signal.

The width of the melted ink barriers is also critical. The purpose of the wax barrier is to prevent the solvent flow outside of the barriers, however when the barrier was thinner than 0.5mm, the solution crossed over the barrier and spread over the surface of chips. (Figure 2.7) Optimal widths ranged from 0.8mm to 1mm.

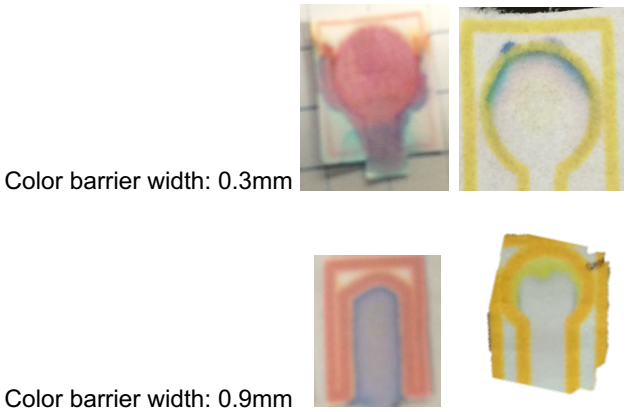

Figure 2.7. The width of barriers affect the control of solvent movement on the μPADs. When the width of barrier is less than 0.5 mm, the moving solution can cross the barrier.

B. Paper

The whiteness of chromatographic paper is a good background for colorimetric detection. However, chromatographic paper is quickly degraded by concentrated acids, creating burned areas and dark spots. Only diluted acids are compatible with chromatographic paper. For example, 96% sulfuric acid must be diluted to a concentration of 60% or lower, 56% nitric acid to a concentration of 50% or lower and 37% hydrochloride acid must be diluted to 35%. However, when these concentrated acids were diluted with water, most colorimetric reagents containing strong acids did not produce a chemical reaction. To avoid this problem, we attempted to use glass fiber filter paper (GF/A, GF/C and 934-AH.) While concentrated sulfuric acid still digested glass fiber paper, concentrated hydrochloride acid and nitric acid could be used. However, these three glass fiber filters were too soft to print wax ink on them, and capillary flow was not optimal. Thus, we needed to develop alternative reagents/compositions for this application instead of the standard reagents used in forensic and TLC analysis.

C. Solutions

Traditionally, spot test analysis involves the analysis of target drugs dissolved in chloroform or methylene chloride in spot tests. To transfer the colorimetric tests to μPADs, methylene chloride and chloroform were initially used as carrier solvents. However, the wax on μPADs dissolves

and spreads when acetone, methylene chloride and chloroform move through the channel. Methanol dissolves much less ink wax, but it evaporated before moving to the end of a long channel. Water is the best solvent so we examined the potential of aqueous/organic solvent mixtures. When acetone is mixed with water at a ratio of 50% and 25%, the wax barriers remained stable. Acetone was preferable as unlike methanol it did not produce color changes in the colorimetric test results. Therefore, paper-based microfluidic devices can utilize wax-inked chromatographic paper and solutions of acetone/water. Moving solutions used with gold nanoparticle/ aptamer based paper microfluidic devices were aqueous, containing only salt and sugar as additives. These mixtures did not affect the solubility of wax ink on the paper chips.

D. Flow rates

Flow rates on μPADs are dependent on the width of the channel and the type of moving solution. Four different sizes of chromatography paper were tested to determine the range of flow rates using a variety of solutes. (Figure 2.8) In general, the wider the channel, the faster the flow rates on paper. Pure water has the fastest flow rate on paper chips. When salts and sugars were dissolved in the moving solutions, the flow rates decreased. The solutions at higher concentrations produce lower flow rates.

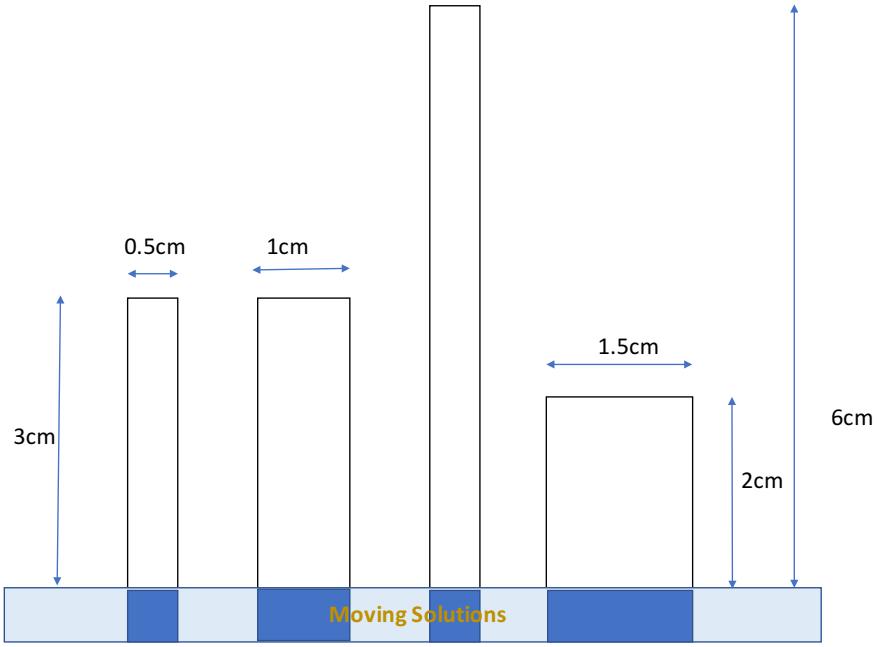

Figure 2.8 Tests of flow rates with different sizes of paper chips and different moving solutions.

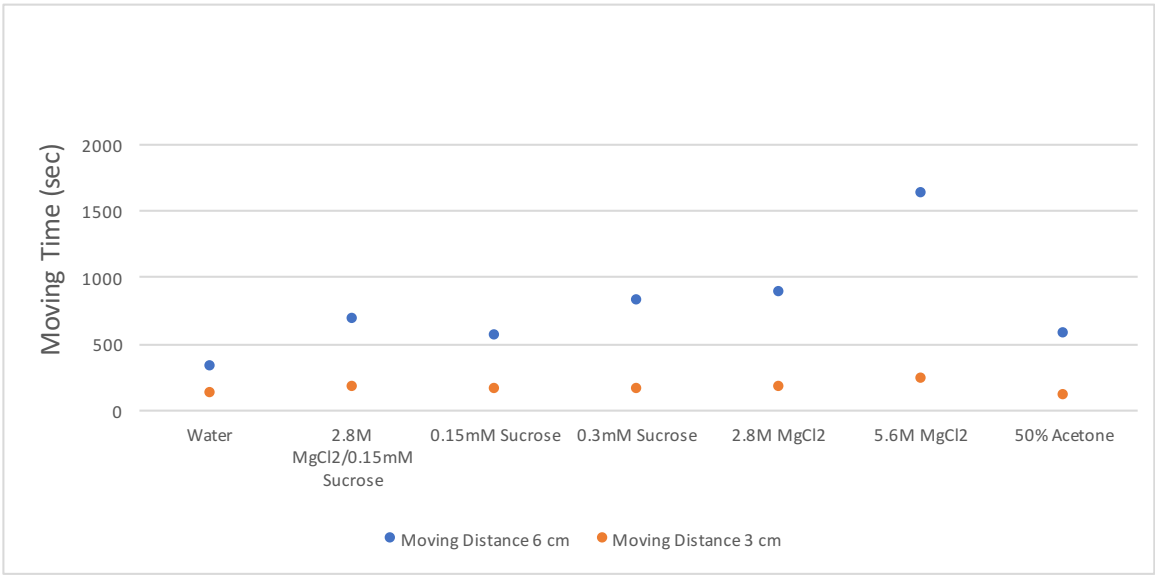

Figure 2.9 Run time of different moving solutions on a channel with a width of 0.5 cm. Water produced the lowest moving time on the paper.

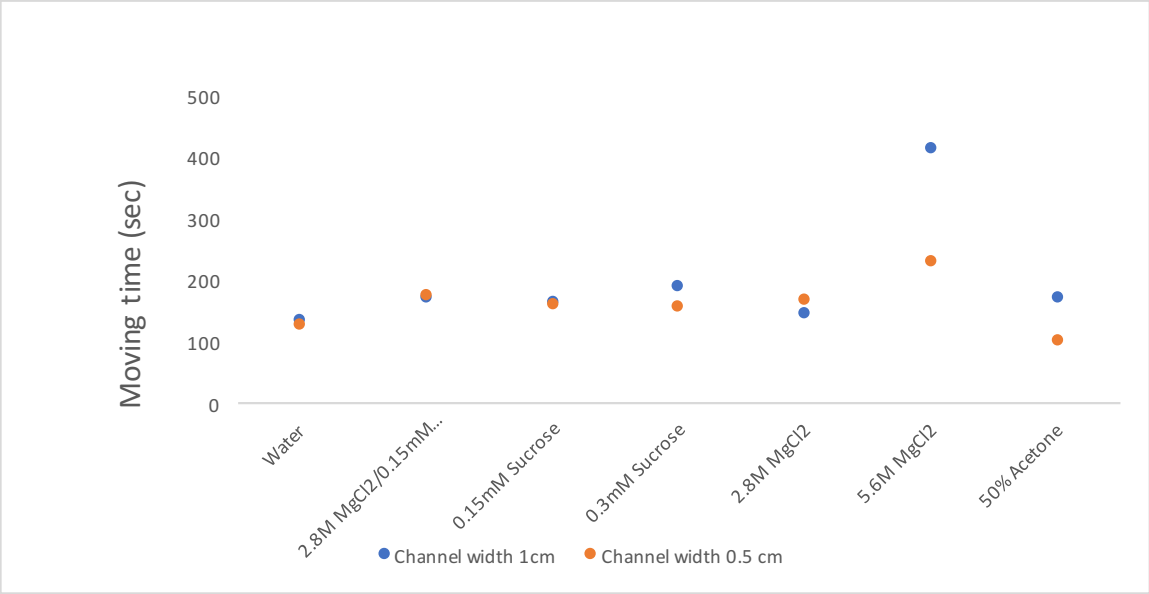

Figure 2.10 Run time of different moving solutions as channel width was changed from 1 to 3 cm. The greatest effect was seen at for the solution containing the highest salt concentration.

E. Capillary action

To enhance color developments on the μPADs, colorimetric reagents are used at a much higher concentration on the μPADs than in solution tests. The solvent migrates via capillary action in a forward direction and the color changes occur as reagents are mobilized and mixed together with the analyte in the reaction zone. However, when concentrated reagents are used it is possible that osmosis can occur, with the result that reagents may also flow counter to the moving channel. This effect can produce color changes in the solution channel instead of the detection zone. (Figure 2.11, Left) A wider solution channel can decrease the backflow of the reagent to the solution channel. (Figure 2.11, right) Therefore reagent concentration is a critical parameter to avoid backflow

due to osmotic effects, and the effect of backflow can be decreased through modification of the width of moving channel.

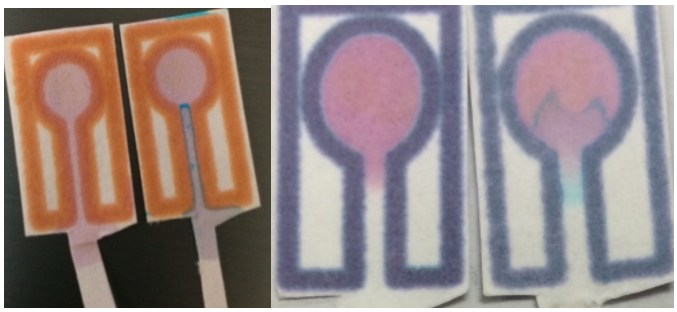

(a) **(b)**

Figure 2.11 Backflow of colorimetric reagents. (a) Left: The pink reagent moved from the top ball back to the end of the moving channel; Right: the color change reaction occurred in the moving channel instead of in the reagent ball; (b) Left: The pink reagent moved little from the top ball into the moving channel; Right: The color change again occurs in the solvent channel. The thinner channel (Left) has a greater backflow effect than the wider channel (Right).

5. Conclusions

A number of different factors affect the colorimetric detections on μPADs. The optimization of ready-to-use formats and the applications are related to the designs, ink wax, moving solutions and reagents. The optimal format considers the shape, size, direction of channels. Chromatographic paper is a good substrate to the colorimetric detection, and a well-prepared pattern contained a fully melted wax ink. The moving solution should be safe to the melted wax on μPADs. To minimize the moving time, the main moving channel should be as wide as the design possible, meanwhile, the moving solutions should have a low concentration; the barriers keep 0.5 mm or higher.

6. References

1. Martinez, A. W., Scott T. P., George M. W., Emanuel C. Diagnostics for the developing world: microfluidic paper-based analytical devices. **2009,** 3-10.

2. Mark, D., Stefan, H., Günter, R., Felix, V. S.,Roland, Z. Microfluidic lab-on-a-chip platforms: requirements, characteristics and applications. In *Microfluidics Based Microsystems*, **2010**, 305-376.

3. Cate, D. M., Adkins, J. A., Mettakoonpitak, J., & Henry, C. S. Recent developments in paper-based microfluidic devices. *Analytical chemistry***, 2014**, *87*(1), 19-41.

4. Martinez, A.W., Phillips, S.T., Butte, M.J. and Whitesides, G.M., Patterned paper as a platform for inexpensive, low-volume, portable bioassays. *Angewandte Chemie International Edition,* **2007**, *46*(8), 1318-1320.

5. Lisowski, P., & Zarzycki, P. K. Microfluidic paper-based analytical devices (μPADs) and micro total analysis systems (μTAS): development, applications and future trends. *Chromatographia*, **2013**, *76*(19-20), 1201-1214.

6. Carrilho, E., Martinez, A. W., Whitesides, G. M. Understanding wax printing: a simple micropatterning process for paper-based microfluidics. *Analytical chemistry*, **2009**, 81(16):7091-7095.

7. Nie, Z., Nijhuis, C. A., Gong, J., Chen, X., Kumachev, A., Martinez, A. W., Whitesides, G. M. Electrochemical sensing in paper-based microfluidic devices. Lab on a Chip, **2010,**10(4), 477-483.

8. Weaver, A.A., Reiser, H., Barstis, T., Benvenuti, M., Ghosh, D., Hunckler, M., Joy, B., Koenig, L., Raddell, K. and Lieberman, M., Paper analytical devices for fast field screening of beta lactam antibiotics and antituberculosis pharmaceuticals. *Analytical chemistry,* **2013**, *85*(13), 6453-6460.

9. Martinez, A. W., Phillips, S. T., Carrilho, E., Thomas III, S. W., Sindi, H., & Whitesides, G. M. Simple telemedicine for developing regions: camera phones and paper-based microfluidic devices for real-time, off-site diagnosis. *Analytical chemistry*, **2008**, *80*(10), 3699-3707.

10. Liu, J., Mazumdar, D., Lu, Y. "A Simple and Sensitive “Dipstick” Test in Serum Based on Lateral Flow Separation of Aptamer-Linked Nanostructures." *Angewandte Chemie,* **2006,** 118(47), 8123-8127.

11. Li, X., Tian, J., Nguyen, T., Shen, W. Paper-based microfluidic devices by plasma treatment." *Analytical chemistry,* **2008**, 80(23), 9131-9134

12. Li, X., Zwanenburg, P., Liu, X. Magnetic timing valves for fluid control in paper-based microfluidics. *Lab on a Chip,* **2013,** 13(13), 2609-2614.

13. Matias, F. A., Vila, M. M., & Tubino, M. A simple device for quantitative colorimetric diffuse reflectance measurements. *Sensors and Actuators B: Chemical*, **2003**, *88*(1), 60-66.

14. Neitz, M. and Neitz, J., Molecular genetics of color vision and color vision defects. *Archives of Ophthalmology*, **2000**, *118*(5), 691-700.

15. Juds, S. *Photoelectric sensors and controls: selection and application*. Vol. 63. CRC Press, 1988. pp 29

16. Evans, E., Gabriel, E. F. M., Coltro, W. K. T., & Garcia, C. D. (2014). Rational selection of substrates to improve color intensity and uniformity on microfluidic paper-based analytical devices. *Analyst*, **2014**, *139*(9), 2127-2132.

17. Abe, K., Suzuki, K., & Citterio, D. Inkjet-printed microfluidic multianalyte chemical sensing paper. *Analytical chemistry*, **2008**, *80*(18), 6928-6934.

18. Introduction to Colour Science, http://www.techmind.org/colour/, (accessed by July 10, 2017)

19. Shen, L., Hagen, J. A., & Papautsky, I. Point-of-care colorimetric detection with a smartphone. *Lab on a Chip*, 2012, *12*(21), 4240-4243.

20. Image J User Guide, https://imagej.nih.gov/ij/docs/guide/user-guide-USbooklet.pdf (accessed by July 10, 2017)

Chapter 3. Colorimetric reagent based multiple channel paper microfluidic devices

1. Introduction

A. Spot Tests

Colorimetry is defined as a method in which the analyte reacts with a proper reagent and produces a unique and visible colored product. [1] It is used in qualitative analysis to identify the presence of analytes in simple and complex matrices. The observation of colors is subjective, so the operators usually require reference standards to compare with the results. A spot test is an important type of the colorimetric measurement used in the preliminary identification of seized drugs. [2] A series of reagents are used to react with a single atom or functional group. For example, the Marquis test causes a yellow-brown color with nitrogenous bases and the Simon's test produces a blue color with a secondary amine. [1] Colorimetric reactions have been known for many years, many of which have been developed for 30, 40 [3] or even up to 70 years [4]. Some reagents were developed to detect a single chemical, but they more often react with multiple compound or materials.

In 1987, the Division of Narcotic Drugs invited an expert group to summarize a list of colorimetric tests with seized drugs, including details on the mechanisms and cross reactants. [5] The listed procedures include methods for the detection of opium, morphine, codeine, methadone, amphetamines, cannabis, barbiturates, diazepam and benzodiazepine

derivatives, lysergide, cocaines, phencyclidine, and others. [5] Later in 2000 the National Institute of Justice, Law Enforcement and Corrections Standards and Testing Program published a standard of the Color test reagents/ kits for preliminary identification of drugs of abuse. [6, 7] The standard listed the preparation of 12 colorimetric reagents (Table 1) and the color changes that occur in the presence of illicit drugs and adulterants, the drug detection limit, and the safety of the chemicals. The in-laboratory preparation of spot tests is more common in research labs than in government labs where, because of the necessity for validated, on-site measurements, the operators use colorimetric reagents from kits sold by various manufacturers. The reagents are stored in closed tubes or vials and the operator follows specified procedures, adding the samples to two or three tubes and observing the color changes. Results are read using the colorimetric charts to minimize the possibility of false positive detection of the drugs. (Figure 3.1)

Spot tests have been used for years in presumptive drug testing because they are rapid and inexpensive, however, they have several disadvantages. Most importantly, spot tests have low specificity as they mainly react with functional groups on the compound of interest [1, 6, 7, 9]. This characteristic can result in false positive results with other members of a drug class or common powders. [7] Thus it is important that the results of these tests be verified using more specific techniques to avoid improper prosecution of innocent individuals. [10] Because these tests

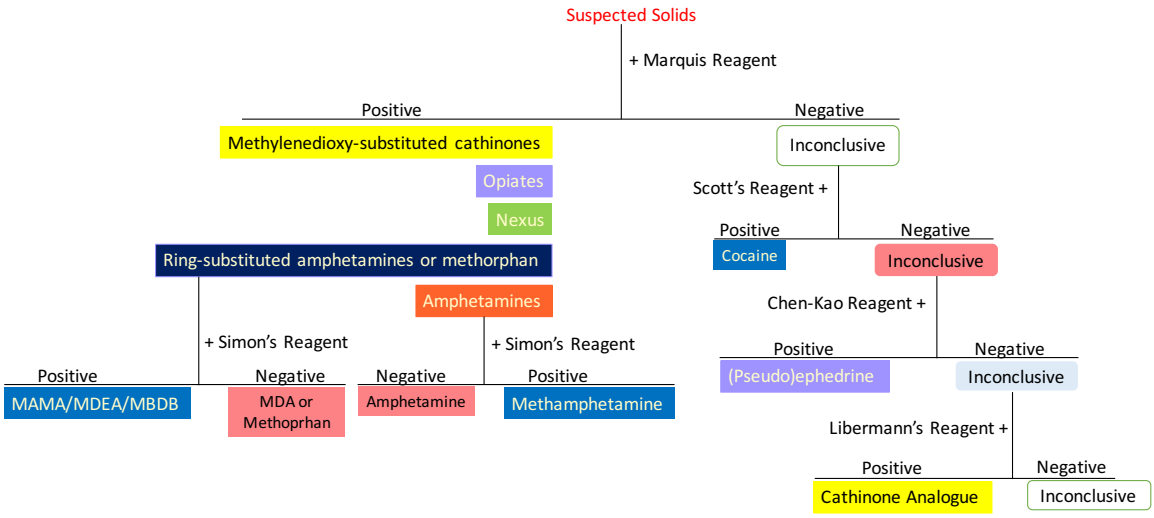

Figure 3.1. A flow chart for colorimetric drug analysis. [8] The boxes indicate the color change possible with each specific drug. The Marquis reagent is used in the first step which produces a specific color change for five different drugs, while the white boxes indicate negative results. Scott's reagent is used in the second step, with a pink color indicating negative results, and a blue color indicating a positive result. The Chen-Kao reagent is the third test, with a purple color indicating a positive result and a blue color indicating a negative result. Libemann's reagent is used in the fourth test, and the yellow color indicates a positive result. Simon's reagent is used to further differentiate compounds which are positive for the Marquis reagent.[

also have a lower sensitivity than other screening methods, most applications focus on seized drug analysis instead of toxicological detection. [2, 7] Many colorimetric reagents contain concentrated acids (96% H_2SO_4, 68% HNO_3, 37% HCl) and toxic organic solvents (Table 1) [6, 7]. For example, in the Duquenois -Levine test, chloroform, a suspect carcinogen and liver toxin is used to extract drugs from the reagent to display a color change [6]. Because such tests are often accessed by poorly trained individuals, more convenient and safer procedures are needed.

B. Drug detection

Each colorimetric reagent has their mechanism and targets. Some reagents are designed to detect a single drug; others are available to several drugs Commonly, Mayer, Wagner, and Dragendorff reagents can detect alkaloids. For example, the Marquis reagent detects opiates, the cobalt thiocyanate reagent detects cocaine, Duquenois reagent and the Fast Blue B reagent detect Marijuana. [9] In this project, an effort was made to produce colorimetric detection on a heterogeneous paper based device by modifying and applying these solutions based reagents to the solid support. Key issues included optimization of reactants to permit drug determination without damaging the paper substrate, as well as producing a format where the reagents can be isolated and stabilized prior to analysis.

a. Cocaine detection

In spot tests, cocaine HCl in chloroform produces a greenish blue color with cobalt thiocyanate and HCl, or produces a dark orange-yellow color with cobalt thiocyanate dissolved in water. These tests are performed using the Scott reagent, a mixture of 2% cobalt thiocyanate in water and glycerine (v:v=1:1). Cocaine reacts with both cobalt thiocyanate reagents

Table 3.1. Twelve Common colorimetric reagents used in the spot tests. [7]

Colorimetric reagents	Components	Examples-Analytes	Possible Color changes
Cobalt thiocyanate	Cobalt (II) thiocyanate in methanol (10% w/v)	Cocaine HCl	Strong greenish blue
Dille-Koppanyi reagent	Cobalt thiocyanate in methanol (0.1%, w/v) and glacial acetic acid (100:0.2, v:v)	Cobalt (II) thiocyanate in methanol (10% w/v)	Light purple
Duquenois-Levine reagent	Vanillin in acetaldehyde and ethanol (2%, w/v, v:v=2.5:100)	Tea	Light yellow green
Mandelin reagent	Ammonium vanadates in concentrated sulfuric acid (0.5% w/v)	Codeine	Dark olive
Marquis reagent	96% sulfuric acid: 37% formaldehyde (9:1, v:v)	Codeine	Very dark purple
Nitric acid	Concentrated nitric acid	Codeine	Light greenish yellow
Ehrlich's reagent	Para -dimethylaminobenzaldehyde in 95% Methanol (4%, w/v) and concentrated HCl	LSD	Deep purple
Ferric chloride	Ferric chloride (5% w/v)	Baking soda	Dark orange
Froehde reagent	Sodium molybdite in hot concentrated sulfuric acid (5% w/v)	Codeine	Very dark green
Mecke reagent	Selenious acid in concentrated sulfuric acid (1% w/v)	Codeine	Very dark bluish green
Zwikker reagent	Solution 1: Copper sulfate (0.5% w/v) Solution 2: 1:19 pyridine & chlorofom	Tobacco	Moderate yellowish green
Simon's reagent	Solution 1 : Acetaldehyde (10% v/v) Solution 2 : Sodium nitroprusside (10% w/v)	MDMA HCl	Pale violet

to produce a blue complex from an initially pink solution. The chemical mechanism [5] is as follows:

[Co(SCN)(H2O)5]+ + 3SCN- + cocaine ↔ Blue complex

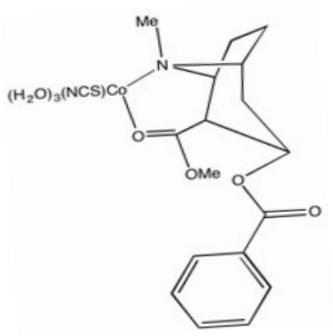

The generic cobalt thiocyanate produces a similar greenish blue color with heroin HCl, propoxyphene, hydrocodone tartrate, and another 54 drugs in the chloroform solution. [3] Therefore, the Scott reagent was developed which is more specific for with cocaine. [11] Houck has mentioned that the blue-color changes can turn back to pink after adding concentrated hydrochloride acid, and will turn to blue again if a chloroform extraction is performed. [11] Deakin reported that cobalt thiocyanate produced a blue color with cocaine HCl, but no color changes with cocaine free base. [12] Only the addition of concentrated acids lead to a blue color for free base cocaine using this cobalt thiocyanate reagent.

The Mandelin reagent is a mixture of ammonium metavandate and concentrated sulfuric acid. The fresh reagent has a strong yellow color. It reacts with more than 100 drugs and the resulting final products yield a variety of colors. For example, a brilliant orange-yellow color is produced with methylphenidate and an orange color with ketamine. [3]

b. Ketamine detection

The Mandelin reagent also works with ketamine and the color change is from yellow to orange [7], but the Mandelin reagent has a high toxicity. In 2013 Gupta et al. modified the cobalt thiocyanate complex with bases to permit the colorimetric detection of ketamine hydrochloride. [13] The cobalt (II) complex reacts with the thiocyanate to an octahedral complex of $[Co(SCN)_4]^{2-}$, and the complex is stabilized by the two hydrophobic cations in the coordination sphere. (Figure 3.2)

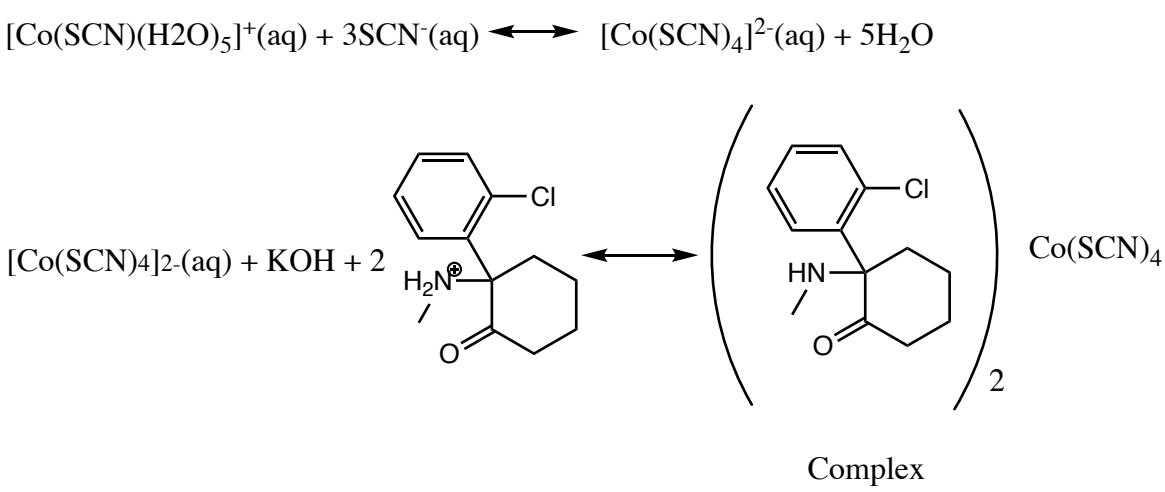

Figure 3.2. Mechanism of Cobalt thiocyanate complex reacting with ketamine. [13]

c. Codeine/ morphine detection

Both Codeine and morphine are alkaloids extracted from opium. The most common spot tests for these opioids include concentrated nitric acid, ferric sulfate, Marquis reagent, Mecke's reagent [5], and Froehde reagent [6]. Opioids can react with concentrated nitric acid and the final products are

nitrated opioids which form a hydrogen bond between the nitro group and the hydroxyl group. [5] Nitrated morphine produces an orange-red color while nitrated codeine produces an orange color.[5] Ferric sulfate has a positive reaction with the meconic acid in opium resulting in a purple color change. [5, 6] The Marquis reagent produces a purple color with both morphine and codeine. [6] (Figure 3.3) Mecke's reagent when mixed with codeine and morphine produces a dark bluish green color. [7] (Figure 3.4)

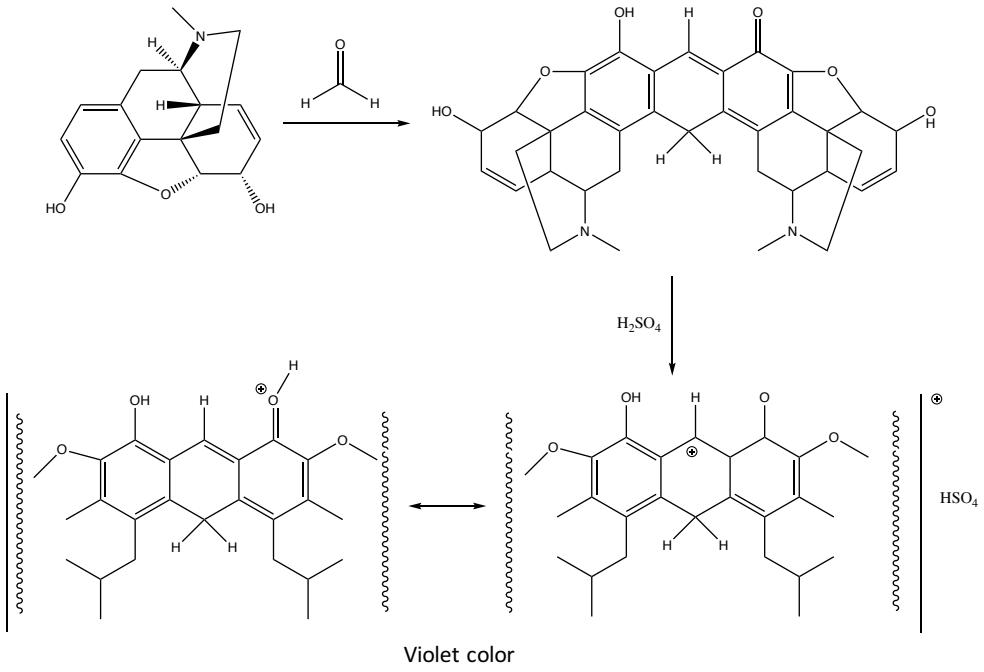

Figure 3.3. Mechanism of Morphine reacting with Marquis reagent.[14]

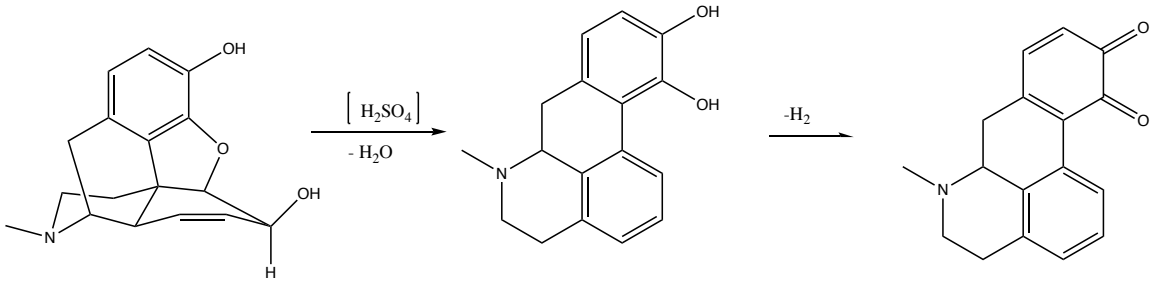

Figure 3.4. Mechanism of Morphine reacting with Mecke's reagent.[5]

Froehde's reagent (Table 3.1) is used to detect the benzomorphan class of alkaloids, especially opioids. It turns a dark green color with codeine and a dark purplish red with morphine. [6] The mechanism is not well studied, but it produces a color change that ranges from pink to purple when applied to alkaloids. [7] Ipecac alkaloids and opium alkaloids react to a purple-bluish-violet color using this test. [15]

d. Amphetamine/ Methamphetamine detection

The Marquis' Reagent, sulfuric acid, Simon's reagent, Simon's reagent with acetone and Vitali-Morin's reagent are common colorimetric reagents for the detection of amphetamines and other amphetamine derivatives. The Marquis' reagent gives an orange color with amphetamine and a yellowish green color with methamphetamine. [5, 6] (Figure 3.5) Simon's reagent reacts with secondary amines (Figure 3.6) and gives a blue Simon-Awe complex with methamphetamine. [5, 6] Acetone can replace acetaldehyde in the Simon's reagent, this alternative works selectively with primary amines. [5] (Figure 3.7)

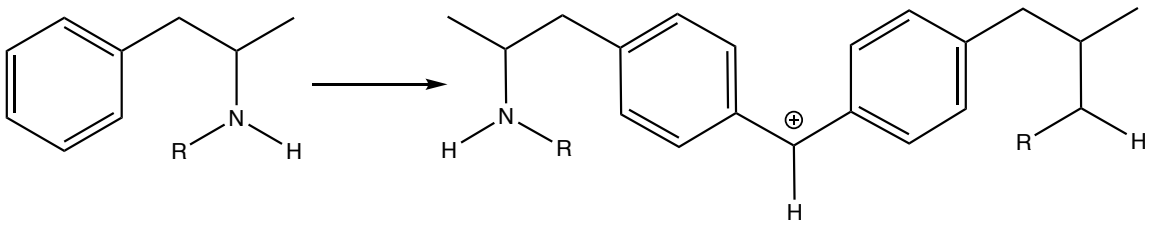

Figure 3.5. Mechanism of Amphetamine (R = H) and methamphetamine (R = CH_3) reacting with Marquis' reagent.[5]

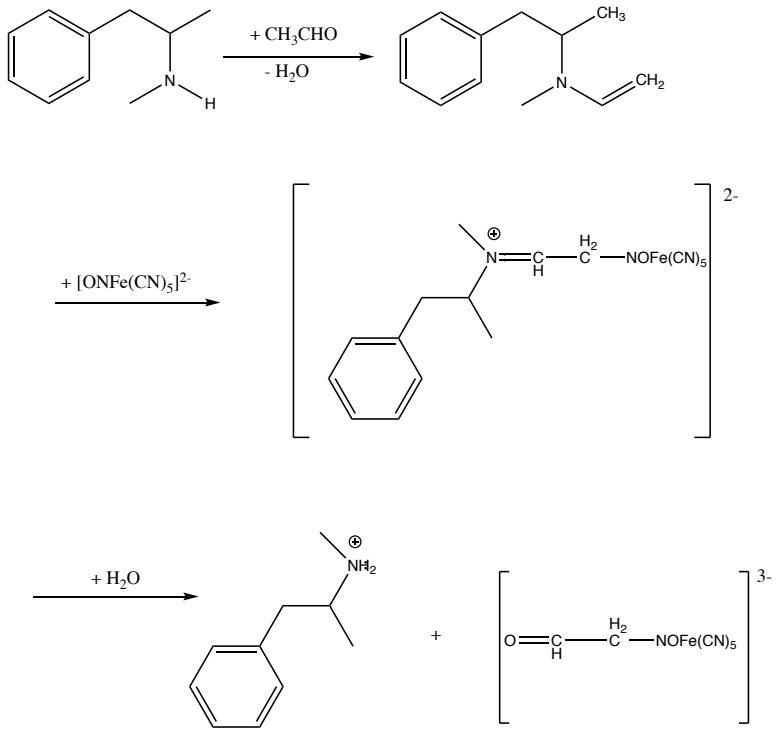

Figure 3.6. Mechanism of methamphetamine reacting with Simon's reagent of aldehyde. [5]

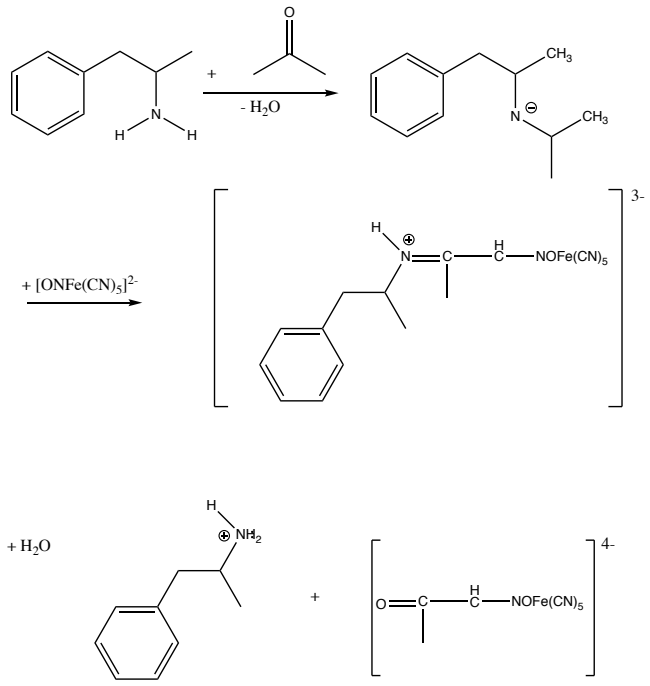

Figure 3.7. Mechanism of Amphetamine reacting with Simon's reagent of acetone. [5]

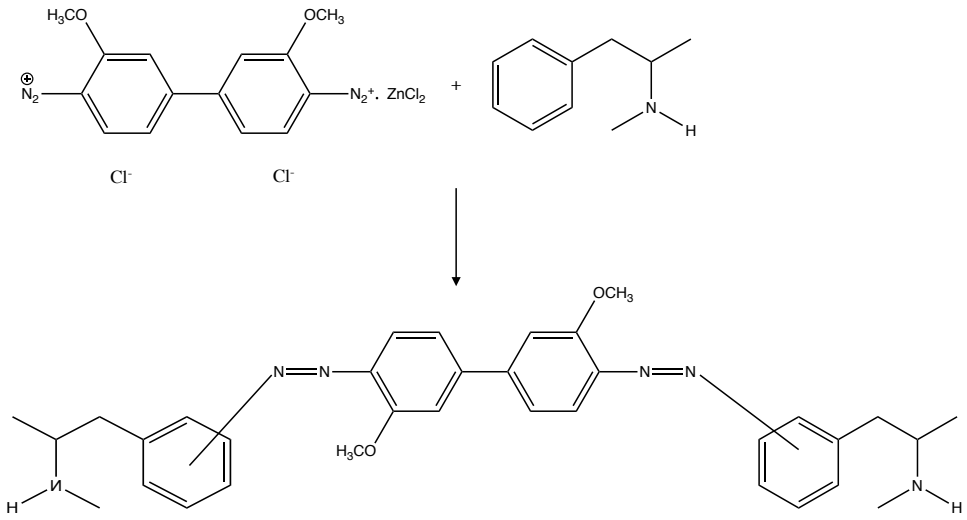

Figure 3.8. Mechanism of methamphetamine reacting with Fast Blue B reagent. [5]

Additional test reagents include Fast Blue B reagent which has been used to detect THC in marijuana [16] (Figure 3.8) and $FeCl_3$ which gives a color change from yellow to green with amphetamine. [17]

Colorimetric reagents are designed to for use with liquid solutions. When these same reagents are applied for use with paper microfluidic devices, many are not suitable. As shown in Table 3.1, most colorimetric reagents used in drug testing, such as Mandelin and Marquis reagents, use concentrated acids in the solution tests. However, these acids can degrade chromatography paper. Thus, it is necessary to develop an alternative to these strong acids. Some reagents, like the Zwikker reagent, require mixing two solutions to create new complex which gives a color change with the addition of specific drugs. However, this type of complex is unstable and typically requires fresh preparation prior to use. Other reagents use organic solvents, such as acetaldehyde and chloroform. These organic rapidly evaporate in air, and will also not work with paper chips. The reagents also require modification before they can be applied to the paper devices.

2. Goals

The goal of this project was to prepare a multiple-channel paper chip for the presumptive determination of seized drugs. The project was separated into four tasks. First, the colorimetric reagents had to be modified to permit their use with chromatographic paper instead of liquid

solutions. Second, the cross-reactivity and interferences of the modified colorimetric reagents on μPADs needed to be cataloged. Third, an estimation of figures of merit including instrumental minimum detectable quantity (MDQ) needed to be determined. Fourth, the final development and validation of a multi-channel device for drug detection needed to be completed.

3. Chemicals and Methods

A. Chemicals

All chemicals were analytical grade. Cobalt thiocyanate was purchased from Aldrich; iron (III) chloride and glycerol were purchased from Acros Organics (Waltham, MA, United States); fast blue B, molybdic acid and ninhydrin were purchased from Sigma-Aldrich (St. Louis, MO, Unites States); potassium permanganate, sodium hydroxide, hydrochloric acid, and acetone were purchased from Fisher (Pittsburgh, PA, United States). Amphetamine, methamphetamine, cocaine, ketamine, ephedrine were purchased from Sigma (St Louis, MO, United States). Morphine, codeine and thebaine were purchased from RBI (Natick, MA, United States). The standard solutions of drugs were prepared as 100mg/mL in 50% acetone/ 50% deionized (d.i.) water.

B. Designs of Paper Microfluidic Devices

A six-channel paper microfluidic device was designed to detect several psychotropic compounds as followed: cocaine, ephedrine, morphine, ketamine, amphetamine, methamphetamine and MDMA.

The paper chip was developed following single tests, and each channel contained different amounts of the reagent area. (Figure 3.9) According to the final colors, the format used the color of yellow, other colors like black, blue, green and red could produce misleading phenomena to the naked eyes. The words next to each channel indicated the possible drugs with the positive results for each channel, the color of the terms described the positive color changes.

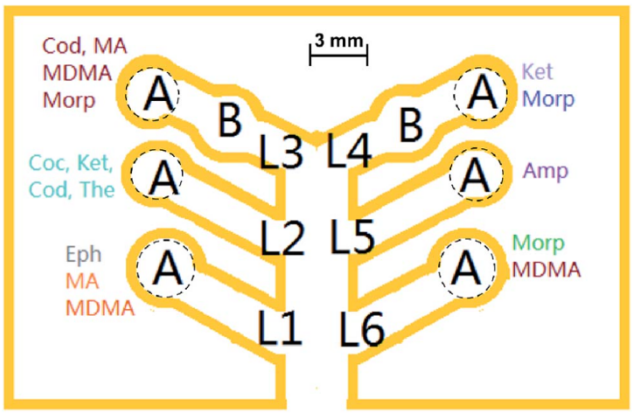

Figure 3.9: Six channel device developed for sample analysis. The device consists of six channels with one or two zones for placing reagents. The solid sample is dissolved in solvent and introduced at the bottom of the device using a paper tab placed in a vial. Alternatively, the solids can be added to the middle channel. Capillary action mobilizes the drug and the solvent mixture up into the reaction zones. Dashed areas indicate the image region used for the colorimetric detection by eye or cell phone camera. Cod = codeine, Coc = cocaine, Ket = ketamine, Morp = morphine, Amp = amphetamine, MA = methamphetamine, Eph = ephedrine, The = thebaine.

After the final design was obtained, the format was printed on chromatographic paper (Whatman No.1, GE Healthcare, UK) using a commercial wax printer (Xerox Color Cube 8570, Xerox, US). Next, the paper was wrapped in an aluminum foil package and passed three to five times through a laminator at 160 °C, at a speed of 1.6 cm/sec (Tamerica Tashin Industrial Corp, TCC-6000). The wax melted from the surface to the back of the chromatographic paper and created the hydrophobic barriers.

The design of each channel can detect a different set of compounds with unique colored responses depending on the modified reagents. Figure 3.9 illustrated the design of the chip, and the number indicated each channel, and the letters identified the potential locations for each reagent. Samples and reagents were prepared in different locations to optimize the color generation, sensitivity, reaction time and system stability.

Lane 1 (L1 in Figure 3.9) prepared to detect ephedrine, MDMA and methamphetamine in unknown samples. In this lane, 0.5 μL of a mixture containing 100 mg/mL sodium sulfate and 10 mg/mL Fast Blue B were deposited to zone A. Lane 2 (L2 in Figure 3.9) was used to detect four compounds, cocaine, codeine, thebaine, and ketamine. Also, 0.5 μL of a mixture containing 100 mg/Ml cobalt (ii) thiocyanate and glycerol (v:v=3:2) added to zone A. Lane 3 (L3 in Figure 3.9) could identify codeine, MDMA, morphine and methamphetamine. One mg of potassium permanganate was crushed by a spatula onto L3 zone A and 2 μL of 1 mg/μL molybdic

acid were added to L3 zone B. Lane 4 (L4 in Figure 3.9) detected ketamine by using 0.5 μL of 0.02 mg/mL of sodium hydroxide in zone B and 0.5 μL of 12.5 mg/mL cobalt thiocyanate in zone A. Lane 5 (L5 in Figure 3.9) was designed to detect amphetamine with the separate deposition of 0.5 μL of 50 mg/mL ninhydrin in 50% acetone and 1M NaOH in zone A. Lane 6 (L6 in Figure 3.9) detected morphine and MDMA. 0.5 μL of 100 mg/mL $FeCl_3$ added to zone A. Finally, the bottom tip of the device would be placed in a carrier solution of 300 μL of 50% acetone in water, and capillary action would move the drug and the solute to the end of each channel.

C. Estimation of instrumental MDQ and visual LOD

For the solution limit of detection by eye, single lane paper microfluidic devices were set in the sample bottles. The drugs were dissolved in acetone:water (v:v=50:50). When the paper devices were place in the bottles, the solutions moved through the channels and produced the color changes at the end of the channels. (Figure 3.10)

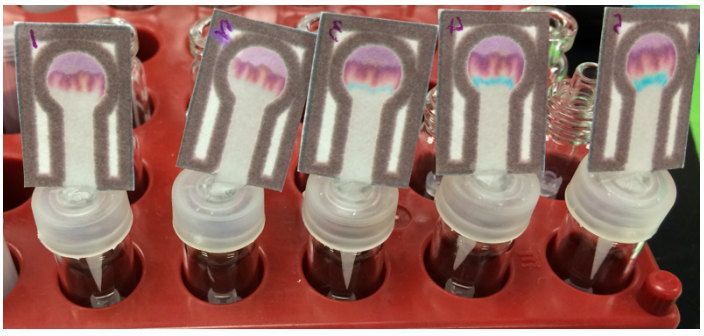

Figure 3.10. A solution test for determination of limit of detection. The cocaine concentrations used in this test were 0, 200 µg/mL, 400 µg/mL, 600 µg/mL, 800 µg/mL, 1000 µg/mL from left to right.

The calculation of MDQ was carried out using the single lane devices and the analysis by software Image J. The sample bottles contained acetone/water solvent. The drugs were dissolved in acetone/water, and were placed on the middle of the channel. When all solutions on the paper chips dried, the paper chips were placed in the carrier solution vials and the drugs on the paper moved up the chip via capillary flow. When the drug reached the terminal end of channel, the color change immediately occurred. The calculation of minimum detectable quantity (MDQ) was performed using pictures recorded by an 8-megapixel camera attached to a Nexus 5 (LGE) smartphone. The microfluidic devices were photographed on a white background and with a flash from the smartphone camera to avoid the external light contamination. All paper microfluidic devices were kept at a distance of 6 cm between the camera and the background.

The intensity of the red (R), green (G), blue (B) and RGB components was used in data analysis by Image J software version 1.48. Equation (1) calculated the proportionality between the color components and the absorbance:

$$A_X = -log \frac{I_x}{I_{x,w}} = - logR_x \quad (1)$$

in which A_x was the absorbance of X, I_x was the intensity of color

component, $I_{x,w}$ was the intensity of the blank spot, R_x was the reflectance of light X and C was the concentration of X.

Estimation of MDQs was performed using a modified device in which an additional Position A was added to permit the deposition of 0.5 μL of a standard sample upstream of the colorimetric reagents. 0.5 μL of a variety of standard solutions containing 1 to 100 mg/mL of each drug was added to the sample area of each lane (A zones – Figure 3.11) Each test was repeated three times. Quantitative measurements were taken at the end of each channel (Position D in Figure 3.11). The absorbance of each drug sample was proportional to the quantity of the drug, and the minimum detectable quantity was estimated as three times the standard deviation of the intercept divided by the slope of the calibration line.

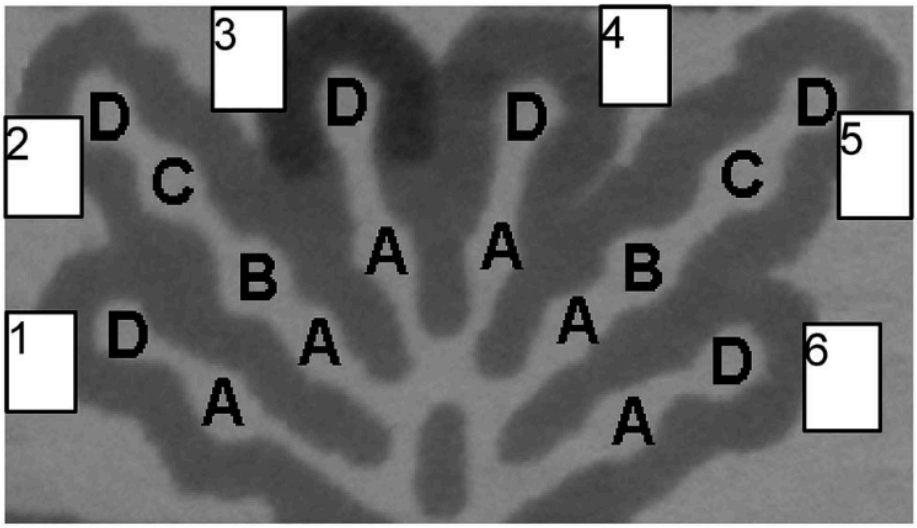

Figure 3.11. Multi assay presumptive test of a six-lane device for MDQ estimation. Position A: Sample area; Position B, C: Reagent areas. Position D: End part. Lane 1: Modified Fast Blue test. Line 2: Modified

Frohdles test. Line 3: Modified Scott reagent test. Line 4: Ninhydrin test. Line 5: Cobalt thiocyanate/ NaOH test. Line 6: Modified iron (III) chloride test.

D. Interference tests

Lidocaine and procaine were purchased from Acros Organics (Waltham, MA, United States), quinine was purchased from J. T. Baker Inc. (Philipsburg, NJ, United States) and caffeine was purchased from Sigma-Aldrich (St. Louis, MO, United States). Dimethylsulfone, lactose, mannitol and inositol were obtained from Fisher (Pittsburgh, PA, United States). King Arthur gluten-free flour, Arm & Hammer baking soda, Publix granulated sugar, Rumford aluminum free baking powder, Shower Bath Salt absorbent body powder, iodized salt, (Publix antacid tablets), and Argo 100% pure corn starch were purchased from supermarkets in Miami, FL, United States. Before analysis a solution or slurry of each interference was prepared at a concentration of 100 mg/mL in 50% acetone /50% deionized water.

The device used in interference tests used the design in Figure 3.11. Each sample was deposited in zone A, and the moving solution of 50% water transferred the sample to the end of the channels and produced positive/negative results

4. Results and Discussion

A. Modifications of Reagents for SAMHSA-5 drugs

(a) Modifications of Scott's reagent for cocaine detection

The Scott reagent was designed for specific detection of cocaine, but we found the reagent produced an incomplete result with cocaine free base in the solution test. The original method required the addition of concentrated hydrochloric acid and chloroform to create a bilayered extraction and the positive color blue color change appeared in the organic phase. Deakin found that cocaine free base itself did not produce a blue color with Scott reagents, and cocaine in both its acidic and free base phases produced a blue color change with the addition of concentrated acids.[12] However, concentrated acids, from 98% sulfuric acid, 68% nitric acid to 37% hydrochloride, degrade chromatographic paper and cannot be directly applied to paper microfluidic devices. Dilution of the acid was one option. Experiments were performed using concentrated hydrochloric acid diluted to 24%, 13.5%, 6.5%, and 3.7% with d.i. water. The result was then examined for use on the paper devices. All solutions produced a blue color change with the Scott reagent in the solution tests when cocaine was added. However, when the modified Scott reagent was mixed with 3.7% hydrochloride, it produced a positive result with several psychotropic compounds including Morphine, MDMA, amphetamine, methamphetamine, ketamine, ephedrine, cocaine, codeine, quinine, and procaine.

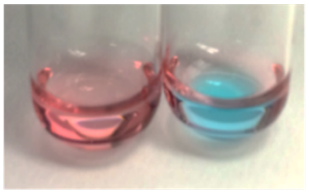

Figure 3.12. Blank (left), cocaine (right, 1 mg/mL) was added to the Scott reagent (2 g $Co(SCN)_2$, 48 mL glycerol, 50 mL H_2O).

In the original Scott reagent test, chloroform is the solvent for the cocaine solid. Chloroform is toxic and a carcinogen, and is a poor choice for usage in the field test. Furthermore, chloroform dissolve the wax on paper microfluidic device. An alternative method involves the use of methanol and acetone as a solvent. These solvents can be mixed with water, eliminating problems with dissolution of the wax barriers of the hydrophilic channels. In our design, we utilized organic solvents to adjust the capillary action of solutions of drugs on paper microfluidic device. In our work, it was important to catalog differences in color development caused by changes in organic solvent composition. When solid cocaine was dissolved in 50% acetone and 50% methanol, the acidified Scott reagent still produced a blue color from the red reagent. An interesting result was obtained when the reagent was used with ephedrine. Deakin reported that ephedrine HCl produced a quickly-disappearing light blue color with the Scott reagent, and the presence of concentrated hydrochloride can make the color change stable in aqueous solution. [12] We examined the results of this test with ephedrine hydrochloride in 50% acetone. The result was a green color, however, when dissolved in 50% methanol, the same

reagent produced a purple color.

Figure 3.13. Color change observed for the modified Scott reagent. Left: ephedrine/methanol; Right: ephedrine/acetone. Ephedrine: 1mg/mL

This reagent did not work with cocaine free base in solution but it did work on paper microfluidic devices. However, the color produced was light and difficult to distinguish from the paper background. As a result, a set of solutions including 2%, 4%, 6%, 8%, 10%, 12%, 15%, 20% (w/v) cobalt (II) thiocyanate were examined for color changes, when the concentration increased to 8%, the blue color changes were easy to observe (Figure 3.14); but when the concentration were higher than 12%, the blue color was hidden in the original dark red color.

Figure 3.14. Color change observed for the modified Scott reagent on paper microfluidic device. Left: Blank test. Right: Cocaine test, cocaine 1mg/mL in 50% Acetone.

(b) Modifications of basic Scott reagent for ketamine detection

The published method for detection of ketamine hydrochloride used 0.1M cobalt tetrathiocyanate/ ethylene glycol and 0.1 KOH solution. [12] In the solution tests, we prepared a mixture of cobalt thiocyanate and sodium hydroxide, and the tests did not work with ketamine hydrochloride. The cobalt thiocyanate appeared as red in the aqueous solution, and it changed to green following the addition of NaOH. Ketamine hydrochloride was continually added to the mixture, and the solution remained green. We found that additional hydrochloride was necessary to produce the same purple color change in the solution tests as the paper described. [13] A higher concentration of reagents was next used to increase the intensity of the color on paper chips. The modified thiocyanate reagent was used at a concentration of 125 grams/L; the sodium hydroxide was 2% (w/v). When the test was applied to paper microfluidic devices, a solution containing 10% $Co(SCN)_2$/ NaOH was deposited on the paper (Figure 3.15, Mid, Zone B), and when the ketamine solution moved up the channel to the reagent position, no color change occurred. A modified design incorporating three sequential zoned for reagents was developed to optimize this process, (Figure 3.15). When the $Co(SCN)_2$ was added to position C and the NaOH added to Position B, the ketamine sample moved through the channel and no color change occurred. When the NaOH solution was deposited on position C and the $Co(SCN)_2$ deposited on position B, the ketamine produced a unique purple-blue color in the $Co(SCN)_2$ zone. (Figure 3.15, Mid) Dubey et al. described a ketamine test

reagent based on the use of a basified Scott reagent.[13] In this test, the order of addition of the chemicals did not impact the color change. However, when used in the μPADs, the ketamine must react with NaOH before moving to the $Co(SCN)_2$ area. The presence of 3.7% hydrochloride created a blue-color change under the same conditions. (Figure 3.15, Right)

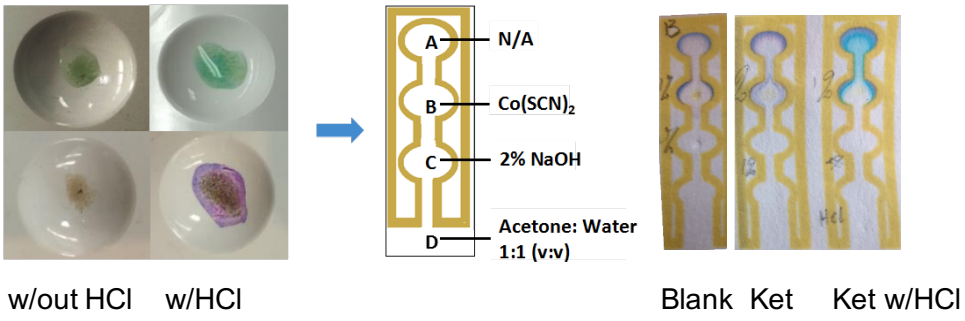

Figure 3.15. Color change observed for the ketamine test. Ketamine (Ket): 50 mg/mL.

(c) Modifications of Frohde's reagent for codeine detection

The original Frohde's reagent consists of concentrated sulfuric acid and molybdic acid. Chromatographic paper cannot survive from the presence of concentrated sulfuric acid. Dilution of the 96% H_2SO_4 to a lower concentration eliminated the colorimetric response. In general, this test did not work when the concentration of acid was lower than 96%. Concentrated sulfuric acid is commonly used as an oxidizer or a strong acid. To test the potential that the role of sulfuric acid was as an oxidizer and not a proton source, molybdic acid was treated with concentrated

nitric acid and concentrated hydrochloride acid and used in the test format with codeine. Since neither acid produced a color change, it was likely that concentrated sulfuric acid was acting as an oxidizer in the reagent. Several strong oxidizers were next examined, however only potassium permanganate combined with molybdic acid produced a color change when combined with different drugs. The blank test produced a purple-red color which results from the permanganate in the solution. Following the addition of codeine, the color of the solution changed to a brown-yellow color. This brown-yellow color likely results from a complex of molybdate-oxidized codeine coupled with the manganese ion (Mn^{2+}). The mechanism was assumed as follows:

Morphine + $KMnO_4$ + MoO_3

–> Mn^{2+} + MoO_4^{2-} + Product from oxidation/complexation with codeine

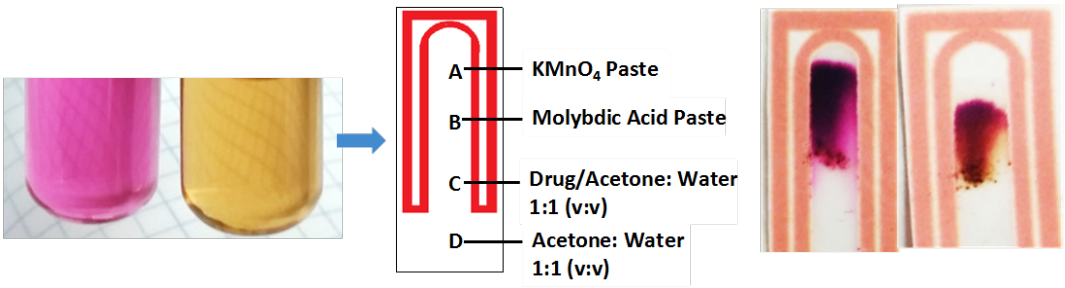

Figure 3.16. Color change observed for the codeine test. Blank (left), codeine (right,2.5 μM) was added to molybdic acid dissolved in $KMnO_4$/acetone at 5 μM - 2.5 μM). On the paper, oxycodone in acetone: H_2O (10 mg/mL) was screened using $KMnO_4$ and molybdic acid pastes.

When the test was transferred to the paper microfluidic device, the reagent produced a purple-red color. However, this mixture oxidized in air when

deposited on paper changing to red in ten minutes and then continuing to oxidize to brown color over a period of one hour. Even when prepared and protected in the sealed packages oxidation occurred within a day. However, when the reagent was prepared as a paste, the test worked. The order of placement of the reagents on the paper chip was also important.

In these experiments a sample of codeine was dissolved in 50% acetone and was placed at the bottom of the chip. It then moves up the lane via capillary action towards the reagent zones. When the chip was prepared by deposition of permanganate upstream of the molybdic acid, the purple-red color migrates upward, covering all spaces in the chip, making it difficult to detect the color change produced by the molybic acid. However, if molybdic acid was deposited upstream of permanganate, a proper color change was observed.

(d) Modification of Iron (II) Chloride for the morphine test

The original iron chloride test involves the reaction of ferric chloride with morphine which produces a color change from yellow to green. Ferric chloride was dissolved in water at concentrations of 10mg/mL, 30mg/mL, 50mg/mL, 700mg/mL, 100mg/mL and applied to μPADs, with the deposited reagent appearing as yellow spots at the end of channel (Figure 3.17, Left). A concentration of 100mg/mL produced the darkest green with a morphine sample of 1mg/mL. (Figure 3.17, right)

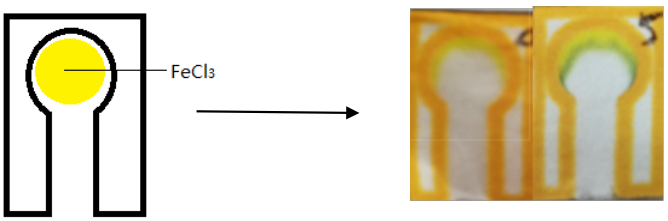

Figure 3.17: Color change observed for the morphine test (right) and a blank (mid)

(e) Modification of Ninhydrin for the amphetamine test

The ninhydrin /NaOH test designed for amphetamine included three steps: (1) ninhydrin was dissolved in acetone/water at a concentration of 50mg/mL and the solution was dropped to the end of the channel and dried; (2) a sodium hydroxide solution of 1M was spotted on top of the ninhydrin; (3) amphetamine was dissolved in an acetone/water (v:v=50:50) 1mg/mL of amphetamine in 50% acetone of 300 µL was prepared in the carrier vials. When the paper chip dried, it was placed in a vial, and capillary action moved the sample to the end of the channel. The color change of amphetamine was from light yellow to purple.

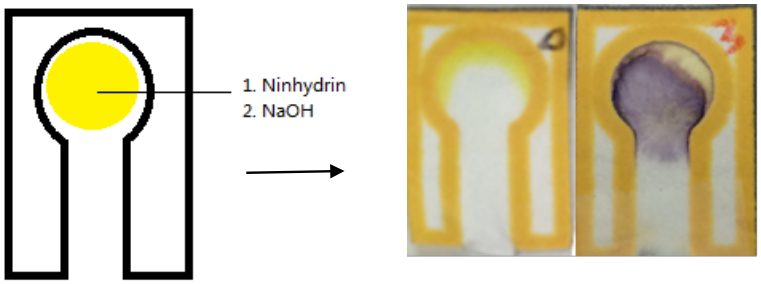

Figure 3.18: Color change observed for the amphetamine test (right) and a blank (mid)

(f) Modification of Fast Blue B for the MDMA and methamphetamine test

The Fast Blue B/ Na_2SO_4 test designed for methamphetamine and MDMA

included three steps: (1) 1μL of a Fast Blue B solution of 10mg/mL was spotted on the end of the channel and dried; (2) 1μL of a Na_2SO_4 solution of 100mg/Ml was dropped to the position of Fast Blue B; (3) MDMA and methamphetamine were separately dissolved in a acetone/water (v:v=50:50) solution. A 300 μL of 1mg/mL methamphetamine in 50% acetone was prepared in the carrier vials. When the paper chip dried, the paper chip sat in the vials and capillary action moved the sample to the end of the channel. The color change of methamphetamine was from yellow/brown to orange. (Figure 3.19, upper) 1 μL of 1mg/mL MDMA added in the middle channel under the Fast Blue B spot, 50% acetone moved the sample to the end of the channel and produced a color change from yellow/brown to red/brown. (Figure 3.19, bottom)

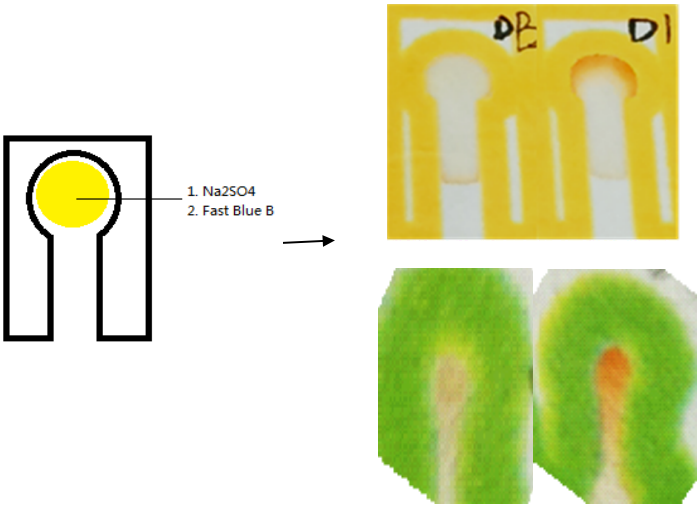

Figure 3.19: Color change observed for the detection of Methamphetamine (top) and MDMA test (bottom) a modified Fast Blue B reagent was used.

B. Estimation and Determination of MDQ and LOD

The minimum detectable quantity (MDQ) for the drug detection was

calculated using the amount of drug necessary to produce a color change on each μPAD. Each test was repeated three times. Image J software was used to calculate the intensity of the red, green, blue and RGB components of the area of each reaction (end of each lane – Figure 3.11) from the images produced by a Nexus 5 (LGE) smart phone. The resultant signals were plotted as a function of the quantity of drug using eqn (1), Figure 3.20. Ephedrine, methamphetamine and MDMA produced the best linear relationship using the absorbance of blue components and the drug quantity. Amphetamine, ketamine and morphine respectively produced an optimal response with the green, RGB and red component. The value of the instrumental MDQ was estimated as three times the standard deviation of the intercept divided by the slope of the calibration curve.

C. Cross-reactivity and interferences

Cross-reactivity tests were designed to test the response of the colorimetric reagent paper chips with cocaine, ketamine, ephedrine, MDMA, amphetamine, methamphetamine, codeine, morphine and thebaine. All color changes were labeled in Table 3.3, and the false-positive tests of common powders and controlled substances were listed in Table 3.4. The paper chips containing the modified Scott's reagent and the modified Morris reagent reacted with almost all drugs listed in Table 3.4. Only ketamine produced a distinct purple color, while the rest of the drugs produced a blue color. Since these two paper chips did not react with common powders, they could only be used to narrow the range of

types of drugs, but they cannot identify a single drug. Fast Blue B reagent based paper chips only produced results with MDMA, methamphetamine,

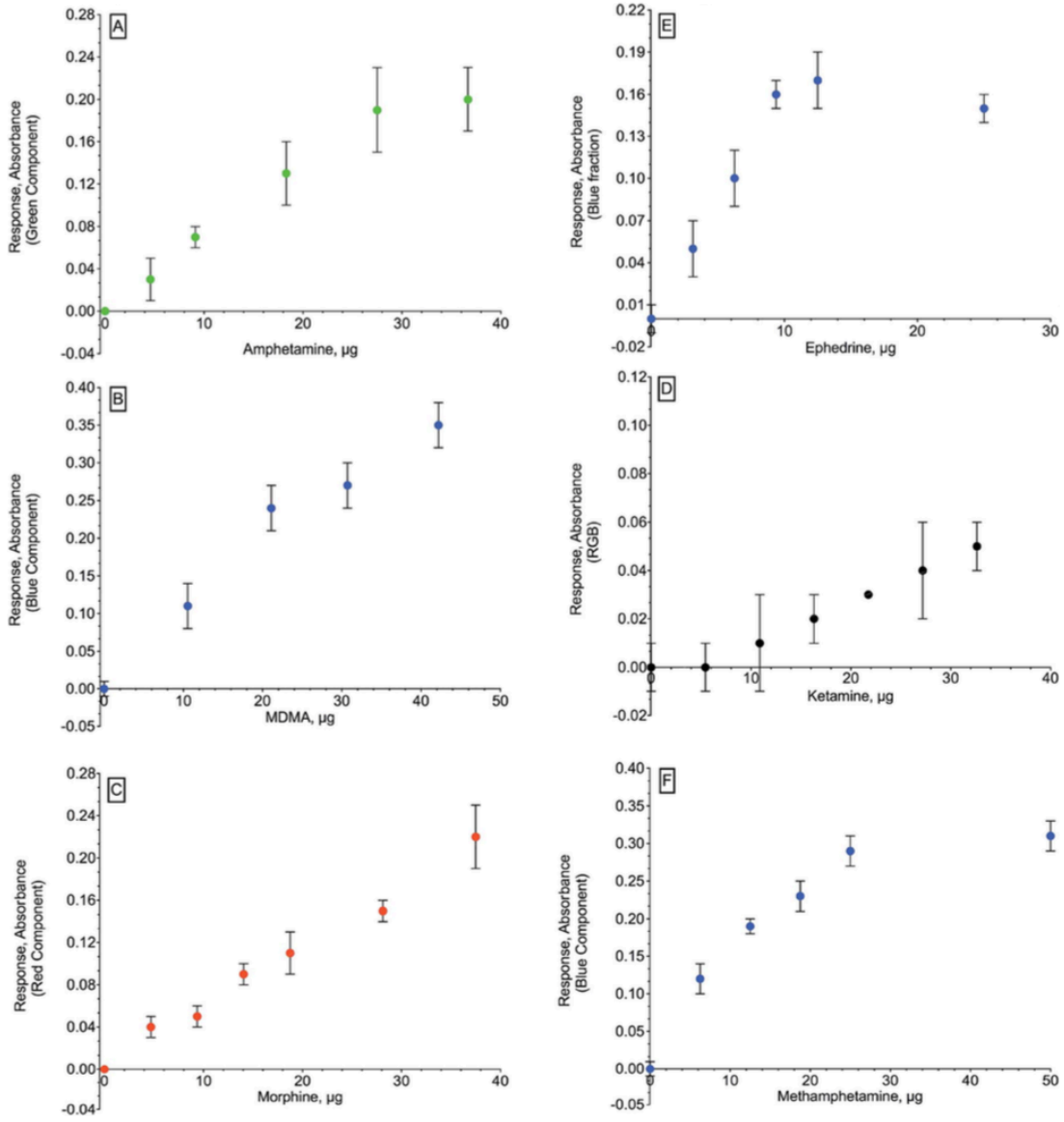

Figure 3.20. Application of ImageJ software for the detection of various drugs on the μPAD device. Pixel colors are indicated on the Y axis. Linearity ranges: (a) amphetamine; (b) ephedrine; (c) MDMA; (d) ketamine; (e) morphine; (f) methamphetamine. (n=3)

Table 3.2. Limit of detection.

Drugs	Reagent	µPADs MDQ, µg	Drugs	Reagent	Solution LOD, µg
Morphine	$FeCl_3$	3.2	Morphine	FeCl3	200
MDMA	$FeCl_3$	8.7	MDMA	- -	N/A
Amphetamine	Ninhydrine	1.2	Amphetamine	Marquis	10
MA	Fast Blue B	5.6	MA	Marquis	5
Ketamine	Morris R.	4.1	Ketamine [25]	Morris R.	1250
Ephedrine	Fast Blue B	2.4	Ephedrine	- -	N/A
Cocaine*	Mod. Scott R.	1.4	Cocaine	Scott R.	60
Codeine*	Mod. Froehde R.	2.0	Codeine	Froehde R.	50

ketamine and procaine. All gave the same orange color. The $FeCl_3$ reagent based paper chips produced different color changes when treated with MDMA, ephedrine and morphine. Ninhydrin reagent based paper chips produced results with amphetamine.

In order to test for interferences, nine commercial products including flour, baking soda, sugar, baking powder, bath salt, body powder, table salt, antacid and corn starch were tested to determine if false positive responses occur. Among the tested products, the baking soda reacted with Fast Blue B reagent, turning to brown. Most of the common diluents used to cut illicit compounds (quinine, lidocaine, procaine, caffeine, dimethylsulfone, lactose, sucrose, mannitol, and inositol did not react with test reagents. However, procaine did produce a combination of colors close to that of methamphetamine (Table 3.4)

Additional tests of drugs and interferences with the multiple channel chip design were performed by Giacomo Musile (Figure. 3.21). [17]

Figure 3.21 A demonstration of the μPAD developed to detect interferences: From left to right: Modified Scott's reagent channel, ninhydrin reagent channel, Fast blue B reagent channel, ferric chloride channel, permanganate/ molybdic acid channel. The results show a comparison of a blank chip (left) and a chip exposed to a sample of quinine (right), with a resulting change in the color of the modified Scott's reagent.

Table 3.3. Cross-reactivity of six reagents

	R#1	R#2	R#3	R#4	R#5	R#6
Blank solution						
Amphetamine	NCC	NCC		NCC		NCC
MDMA			NCC	NCC		
Methamphetamine		NCC	NCC	NCC		
Cocaine	NCC	NCC	NCC			NCC
Codeine	NCC	NCC	NCC			
Ketamine		NCC	NCC			NCC
Ephedrine			NCC	NCC		NCC
Morphine	NCC		NCC	NCC		
Thebaine	NCC	NCC	NCC			NCC

*R#1: Fast Blue B Reagent; R#2: $FeCl_3$ Reagent; R#3: Ninhydrin Reagent; R#4: Modified Scott's Reagent; R#5: Modified Morris Reagent; R#6: Modified Froehde's Reagent. NCC: no color change.

Table 3.4. False positives: Common powder, diluents and adulterants

	R#1	R#2	R#3	R#4	R#5	R#6
Blank Solution						
Positive Solution						
<u>Common Powder</u>						
King Artur Flour Gluten Free Multipurpose Flour	NCC	NCC	NCC	NCC	NCC	NCC
Arm & Hummer Pure Baking Soda		NCC	NCC	NCC	NCC	NCC
Publix Pure Granulated Sugar Extrafine	NCC	NCC	NCC	NCC	NCC	NCC
Publix Confectioners Sugar	NCC	NCC	NCC	NCC	NCC	NCC
Rumford Aluminium Free Baking Powder	NCC	NCC	NCC	NCC	NCC	NCC
Shower Bath Salt Absorbent Body Powder	NCC	NCC	NCC	NCC	NCC	NCC
Winn Dixie Iodized Salt	NCC	NCC	NCC	NCC	NCC	NCC
Antacid Tablet	NCC	NCC	NCC	NCC	NCC	NCC

	R#1	R#2	R#3	R#4	R#5	R#6
Adulterants						
Quinine	NCC	NCC	NCC		NCC	NCC
Lidocaine	NCC	NCC	NCC	NCC	NCC	
Procaine		NCC	NCC			
Caffeine	NCC	NCC	NCC	NCC		NCC
Diluents						
Dimethylsulfone	NCC	NCC	NCC	NCC	NCC	NCC
Lactose	NCC	NCC	NCC	NCC	NCC	NCC
Sucrose	NCC	NCC	NCC	NCC	NCC	NCC
Mannitol	NCC	NCC	NCC	NCC	NCC	NCC
Inositol	NCC	NCC	NCC	NCC	NCC	NCC
Starch	NCC	NCC	NCC	NCC	NCC	NCC

*R#1: Fast Blue B Reagent; R#2: FeCl3 Reagent; R#3: Ninhydrin Reagent; R#4: Modified Scott's Reagent; R#5: Modified Morris Reagent; R#6: Modified Froehde's Reagent. NCC: no color change.

Although some of the drugs had the same color change with one reagent on the paper chips, the multi-channel paper chips permitted a far more specific determination of the unknown compounds through the use of the cross-reactivity chart. Figure 3.22 is an example of an application involving the determination of morphine. For this chip, Lane 3, the modified Froehde turned red; Lane 4, the basified cobalt thiocyanate turned blue, and lane 6, Fast Blue B turned green. The rest of the channels produced negative results. Because the chips are printed with colored wax, it was easy for the user to determine the result, by simply comparing the developed color with that color printed on the device.

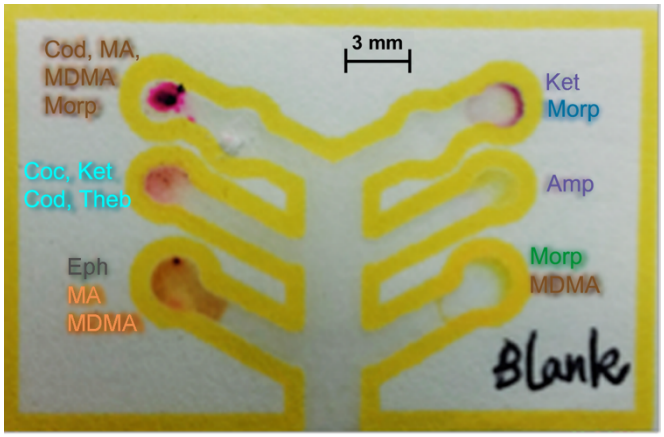

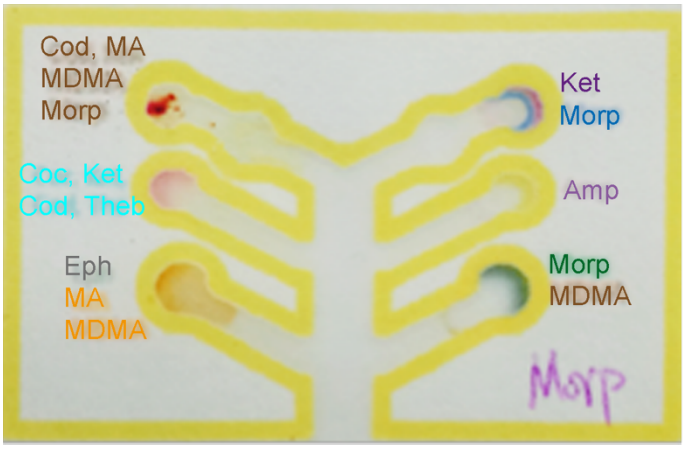

Figure 3.22: A demonstration of the μPAD developed to detect seized drugs: Top - Blank Sample; Bottom- a positive result for morphine. Each lane of the device is labeled with the name and color at which each analytes should appear Lane 1 ephedrine (Eph), metamphetamine (MA) and MDMA; Lane 2 cocaine (Coc), codeine (Cod), ketamine (Ket) and thebaine (The); Lane 3 codeine (Cod), metamphetamine (MA), MDMA and morphine (Morp); Lane 4 ketamine (Ket) and morphine (Morp); Lane 5 amphetamine (Amp); Lane 6 morphine (Morp) and MDMA.

D. Storage and Stability

We have examined various methods to enable long-term storage of the paper microfluidic chips. The first method was to save the paper chips in plastic envelopes. After 3 months, only the $Co(SCN)_2$/ NaOH - test and modified Scott's reagent remained effective. The other reagents did not immediately react with drug solutions; however they did produce a color change if they sat overnight. The second method was to seal the paper chips within a nylon film pouch. Since Ninihydrin reagent – paper chips changed color after heating during the sealing process, we heated the laminar sheets surround the paper chips but did not heat areas where reagents were spotted. The paper chips were kept in dark drawers and in the refrigerator. All chips reacted with target drugs after one month. After two months, all reagents produced the expected result in under 5 minutes with the exception of the Fast-Blue and ninhydrin reagents. These two reagents required an additional twenty-five minutes to produce a positive reaction.

5. Conclusions

Traditional screening tests using colorimetric reagents require a series of individual tests to produce a positive result, potentially wasting precious evidence and requiring time to manipulate samples and reagents. These traditional tests result in LODs that are above 10 ug, and the total cost for analysis is approximately 4 to 6 dollars per test. In this project, a rapid and sensitive method using a paper microfluidic device has been developed as an alternative to spot tests for the presumptive determination of a variety of illicit seized drugs. The device, not much larger than a postage stamp, produces observable color changes that are detectable by the naked-eye that are sufficient to detect a few micrograms of each compound, in under 5 minutes. The procedure uses low quantities of reagents in an easily stored format and demonstrates improved sensitivity when compared to solution based colorimetric testing. The cost for manufacture is minimal, approximately 20 cents per device. In addition, since the reagents are absorbed onto the paper the procedure is much easier to perform and less hazardous to use. The multichannel system permits the simultaneous detection of compounds using a variety different reagents. This process greatly increases the specificity of the method. The system also permits the user to distinguish between illicit drugs, drug diluents and common powders. Overall, we expect this procedure to greatly benefit forensic testing, customs and other applications where quick portable testing of unknown powders is necessary.

6. References

1. Preedy, V. R. *Neuropathology of Drug Addictions and Substance Misuse Volume 2: Stimulants, Club and Dissociative Drugs, Hallucinogens, Steroids, Inhalants and International Aspects*. Academic Press. 2016.

2. Namera, A., Nakamoto, A., Saito, T., & Nagao, M. Colorimetric detection and chromatographic analyses of designer drugs in biological materials: a comprehensive review. *Forensic toxicology*, **2011**, *29*(1), 1-24.

3. Masoud, A. N. Systematic identification of drugs of abuse I: Spot tests. *Journal of pharmaceutical sciences*, **1975**, *64*(5), 841-844.

4. Kolthoff, I. M. The Cobalt-Thiocyanate Reaction for the Detection of Cobalt and Thiocyanate. *Mikrochemie*, **1930**, *8*(1), 176-181.

5. Kovar, K. A., Laudszun, M. Chemistry and reaction mechanisms of rapid tests for drugs of abuse and precursors chemicals. *SCITEC/6, United Nations, Vienna*. 1989.

6. Fatah, A. A. Color Test Reagents/Kits for Preliminary Identification of Drugs of Abuse. *NIJ Standard-0604.01*. 2000.

7. O'Neal, C. L., Crouch, D. J., & Fatah, A. A. Validation of twelve chemical spot tests for the detection of drugs of abuse. *Forensic Science International*, 2000, *109*(3), 189-201.

8. Toole, K. E., Fu, S., Shimmon, R., Kraymen, N., & Casamento, S. G. Color tests for the preliminary identification of methcathinone and analogues of methcathinone. *Microgram Journal*. 2012.

9. Martinez, A. W., Phillips, S. T., Whitesides, G. M., & Carrilho, E. Diagnostics for the developing world: microfluidic paper-based analytical devices. 2009.

10. Houck, M. M., & Siegel, J. A. (2009). *Fundamentals of forensic science*. Academic Press.

11. Deakin, A. L. A study of acids used for the acidified cobalt thiocyanate test for cocaine base. *Microgram Journal*, **2003**, *1*(1-2), 40.

12. Dubey, P., Shukla, S. K., Gupta, K. C. Modified Scott's test for ketamine hydrochloride. *Australian Journal of Forensic Sciences*, **2013**, *45*(2), 165-171.

13. Rehse, K., Kawerau, H. G. Mechanism of the reaction of aromatic compounds with formaldehyde in concentrated sulfuric acid (Marquis reagent)(author's transl). *Archiv der Pharmazie*, **1974**, *307*(12), 934.

14. Fuller, H. C. *The Chemistry and analysis of drugs and medicines*. John Wiley & sons, Incorporated. 1920.

15. Andre, C., Vercruysse, A. Histochemical study of the stalked glandular hairs of the female Cannabis plants, using fast blue salt. *Planta medica*, **1976**, *29*(04), 361-366.

16. Komsta, L., Waksmundzka-Hajnos, M., Sherma, J. *Thin layer chromatography in drug analysis*. CRC Press. 2013.

17. Musile, G.; Wang, L.; Bottoms, J.; Tagliaro, F.; McCord, B., The development of paper microfluidic devices for presumptive drug detection, Analytical Methods, 2015, 7, 8025-8033.

Chapter 4. Gold nanoparticles/aptamers based paper microfluidic device designed to cocaine detection

1. Introduction

A. Gold nanoparticles

For more than 40 years, new uses for gold nanoparticles (AuNPs) have emerged within the fields of nanotechnology and nanoscience. Variation in the size and shapes of these nanoparticles result in a wide variety of chemical, electronic and optical properties that make them attractive for applications in chemistry, biology, physics and engineering.

a. Preparation of Gold Nanoparticles

The synthesis of gold nanoparticles can be separated into homogeneous and heterogeneous methods. Homogeneous methods involve Au^{III} reduction in aqueous or organic media followed by surface stabilization to minimize aggregation and precipitation. [1] Synthetic methods include chemical, photochemical, electrochemical, sonochemical and microwave-assisted reduction methods. [1] Chemical reduction is a popular and easy method, and this procedure is capable of producing a narrow size range of nanoparticles. For example, the Brust-Schiffrin method utilizes an organic phase and can produce 2-10 nm sized using $NaBH_4$ as reductant and organothiol as a surface protecting agent. [2] Alternatively, the Turkevich method occurs in aqueous phase and produces 10-20 nm gold nanoparticles using citrate both as a reductant and a surface protecting agent. [3] Larger nanoparticles (10-50 nm) can be created

using ascorbic acid and CTAB in the aqueous phase and particles with sizes up to 200 nm have also been created. [4]

When nanoparticle synthesis uses a surface support, deposition-reduction or reduction-deposition, can be used. [1] Each process has two steps. The deposition-reduction method involves the deposition of Au^{III} compounds onto the support, followed by reduction into metallic gold nanoparticles under thermal treatment. [1] The reduction-deposition method utilizes gold precursors followed by reduction with stabilizing agents and deposition of the resultant gold colloids onto the support. The deposition-reduction method is commonly used in the synthesis of small particles while the reduction-deposition method can synthesize different nanoparticle sizes depending on the different colloid preparations.

The method used in this project for the creation of gold nanoparticles involved the use of a citrate reduction. The citrate method can synthesize very stable gold nanoparticles with small sizes. The chemical reaction to produce the nanoparticles is shown below:

$$6Au^{3+} + C_6H_5O_7^{3-} + 15OH^- \rightarrow 6Au + 6CO_2 + 10H_2O$$

In the synthesis, trisodium citrate simultaneously acts as a reducing and stabilizing agent. The monodispersity and size of nanoparticles can be controlled through the modification of reaction conditions. For example, silver ions can adsorb to the surface of gold nanoparticles restricting the ultimate size of gold nanoparticles. [5]

Once prepared, the surface of citrate-coated gold nanoparticles can be

modified for use in biomedical applications. Citrate-capped spherical gold nanoparticles provide a negatively charged citrate surface, that can either bind to positive charges from proteins [6], react with cells via covalent conjugates [7], or functionalize with synthetic oligonucleotides [8].

b. Chemical and physical properties of gold nanoparticles

Gold nanoparticles are classified into three types based on their size range: clusters containing sizes less than 2 nm, catalytic particles with sizes 2-10 nm, and plasmonic crystals with sizes from 10-300nm. [1] Gold nanoparticles with diameters from 1-10 nm are described using the 'monolayer protected cluster'(MPC) model, in which gold nanoparticles couple with three layers, central atoms which contain the inner gold atoms with a close-packed crystal structure, surface atoms which stay in outer layers as the surface, and surface protecting organic ligands or surfactants. [1,9] (Figure 4.1) The surface atoms have more activity than the closed-packed atoms. [1]

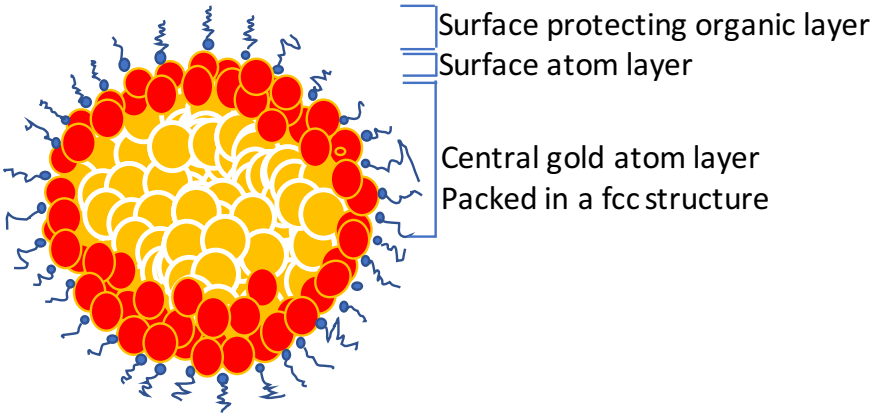

Figure 4.1. A structural model of a single gold nanoparticle. [1]

Shape is also an important parameter. Gold nanospheres are formed at

small sizes of 10 nm or less. As the size is increased, the particles can also take shape as nanoshells and gold nanorods. [10] Nanoparticles can be charge stabilized or sterically stabilized. Sterically stabilized gold nanoparticles are usually prepared with long-chain or dendritic polymers as the stabilizing agents. [11] These compounds produce steric stabilization in which polymers surround the surface of gold nanoparticles as layers. [9] (Figure 4.2) When the nanoparticles have zeta potentials from 20m V to -20 mV, insufficient electrostatic stabilization results in unstable nanoparticles; when the nanoparticles have sizes greater than 20 mV or less than ~ 20 mV of zeta potential, the particles have sufficient electrostatic repulsion in solution and they are stable. [9]

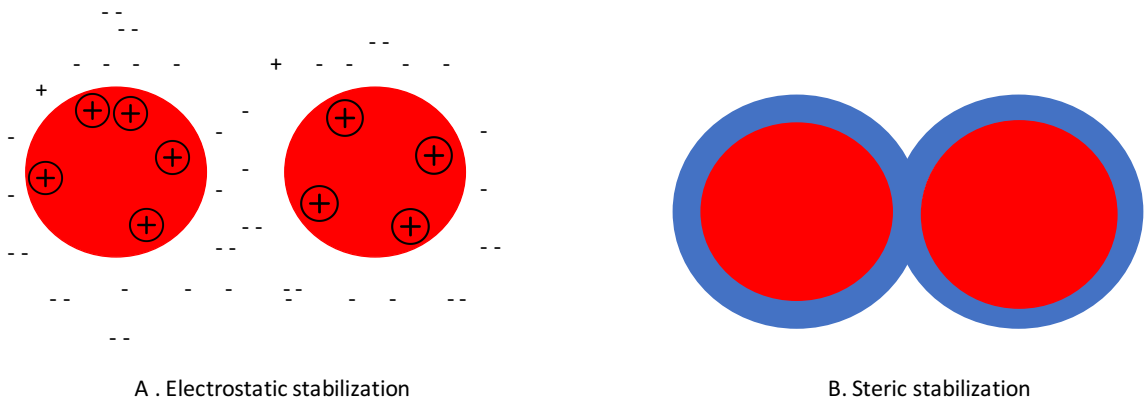

Figure 4.2 Stabilization mechanisms of monolayer nanoparticles: A. electrostatic stabilization; B. Steric stabilization. [9]

The zeta potential of nanoparticles can be affected by their environment or the presence of surface contaminants. High salt environments produce aggregations that result from an overlap of double layers between gold

nanoparticles. Alternatively, proteins and other biomolecules protect the surface charge of the gold nanoparticles making aggregation less likely. The chemical and physical properties of gold nanoparticles are dependent on their size and shape. The optical reflectivity and the conductivity of the metals depends on the movement of quasi-free electrons in the ground state through the metallic crystaline structure. When the nanoparticle size is smaller than 5 nm, the chemical/physical properties depend more on the surface effects than on internal characteristics. When the nanoparticles narrow to 10 nm or lower, their melting points, surface areas and interatomic separation decrease, and the binding ability to other molecules increases. Therefore, when nanoparticle sizes increase to 10-300 nm, the particles have a strong interaction with light as a result of the localized surface plasmon resonance (LSPR). [1,12]

c. Optical properties of gold nanoparticles

Gold nanoparticles have strong light absorption in the visible spectra because of the surface plasmon resonance (SPR) effect.[13] The optical properties of gold nanoparticles are determined by the resonance wavelength, the extinction cross-section, and the ratio of scattering to absorption on the nanoparticle dimensions.[9] Gold nanoparticles with a diameter smaller than 2 nm do not produce surface plasmon resonance because the plasmon bands almost completely quench in these nanoparticles.[9] Gold nanoparticles of 2-100 nm exhibit surface plasmon resonance (SPR) as the dominating optical feature and these

nanoparticles tend to produce a bright red color in colloidal form. When the gold nanoparticles increase the size, the wavelength of the maximum extinction shifts to longer wavelengths. These red shifts are also associated with an increase in peak intensity. [14] Gold nanoparticles larger than 2nm in size have an extinction cross-section with a light-to-heat conversion at nearly 100% efficiency, high photostability, and the ability to amplify electromagnetic fields near the metal surface. When gold particles are smaller than 60 nm, they have a balance between scattering and absorption. The particles have multipolar effects when the particle size is bigger than 60nm. [1]

Gold nanoshells have better optical cross-sections than nanospheres with the optical resonance occurring in the near-infrared region. In general, increasing the size of gold nanospheres increases the resonance wavelength. [10] Nanoshells also have a linear relationship between the size and their total extinction, and gold nanorods produce optical cross-sections with a smaller effective size. [1,10]

The size, polydispersity, and the shape of gold nanoparticles affects the SPR wavelength. Particle aggregation also effects the SPR wavelength and other optical properties. [13] For example, aggregation causes a red-shift in the maximum absorption. Color changes that result from particle aggregation have been used in many fields as a detection method. [1] The DNA-functionalized gold nanoparticles are widely used because of the color changes of red/blue of as the colorimetric indicator. [15,16]

d. Functionalized gold nanoparticles

Gold nanoparticles can be modified through derivatization of the surface of the gold monolayer. The addition of the surface functionalization involves an extra step in the synthesis of gold nanoparticles or through later mixing with other molecules. [1,9,17] The common functionalization methods include PEGylation[18], peptide/amino acid conjugation[19], oligonucleotide functionalization[20], and others[21]. Gold nanoparticles can be easily modified depending on specific binding to thiol groups. The physical and chemical properties of gold nanoparticles depend on the size of gold nanoparticles. The modifications on gold nanoparticles change the surface charges and the size as well as the physical and chemical properties of the particles. [9]

Overall, the method of synthesis, the size, and the surface charge affect the physical, chemical and optical properties of gold nanoparticles. Modifications to the surface change the properties of gold nanoparticles and increase their potential applications in biomedical fields. Gold nanoparticles can produce a salt-induced aggregation and cause color changes from red to blue. The salt based aggregation affects functionalized gold nanoparticles much less than pure gold nanoparticles, especially DNA-functionalized gold nanoparticles. This salt-induced effect can be important in the bio-related applications in which a target is determined based on a colorimetric reaction.

B. Aptamers

Aptamers are defined as small single-stranded DNA or RNA oligonucleotides which are able to bind target molecules with high specificity and affinity.[22] They usually have sizes ranging from 20 to 60 nucleotides, and they can bind different types of target samples which ranging from inorganic ions, small molecules such as pharmaceutical compounds, large protein complexes and even entire cells. [22,23] Aptamers are considered nucleotide analogues of antibodies, but their preparation is much easier and less expensive. [24,25] The earliest method for the production of aptamers was described by Tuerk and Gold in 1990 who designed gp43 binding sequences. [26] Their procedure became to be known as Systematic Evolution of Ligands by Exponential Enrichment (SELEX). [27] A target molecule is used to select the most specific sequences from a combinatorial nucleic acid library of random oligonucleotides These sequences are then PCR amplified and the process is until the most selective sequences are isolated. [27] The basic steps of the SELEX process are shown in Figure 4.3. The beginning of a SELEX process utilizes a pool of chemically synthesized random DNA or RNA oligonucleotides with 10^{13} to 10^{15} sequence. These sequences are incubated with the target. In the next step a binding complex is separated from the unbound and weakly bound oligonucleotides. The target bound oligonucleotides are removed and amplified by PCR (DNA SELEX) or reverse transcription-PCR (RNA SELEX). The amplified sequences added to a new oligonucleotide pool and another cycle of SELEX is

initiated. Several cycles of selection and amplification of the target oligonucleotides produces an increase in the affinity and specificity of the aptamer to the target. The number of cycles depends on the size and number of binding sites on the target. When matched oligonucleotides are cloned to create the aptamer clones, these aptamers are sequenced and analyzed to determine their binding properties. Some aptamers may require extra modifications to meet special requirements such as heterogeneous surface binding. [27]

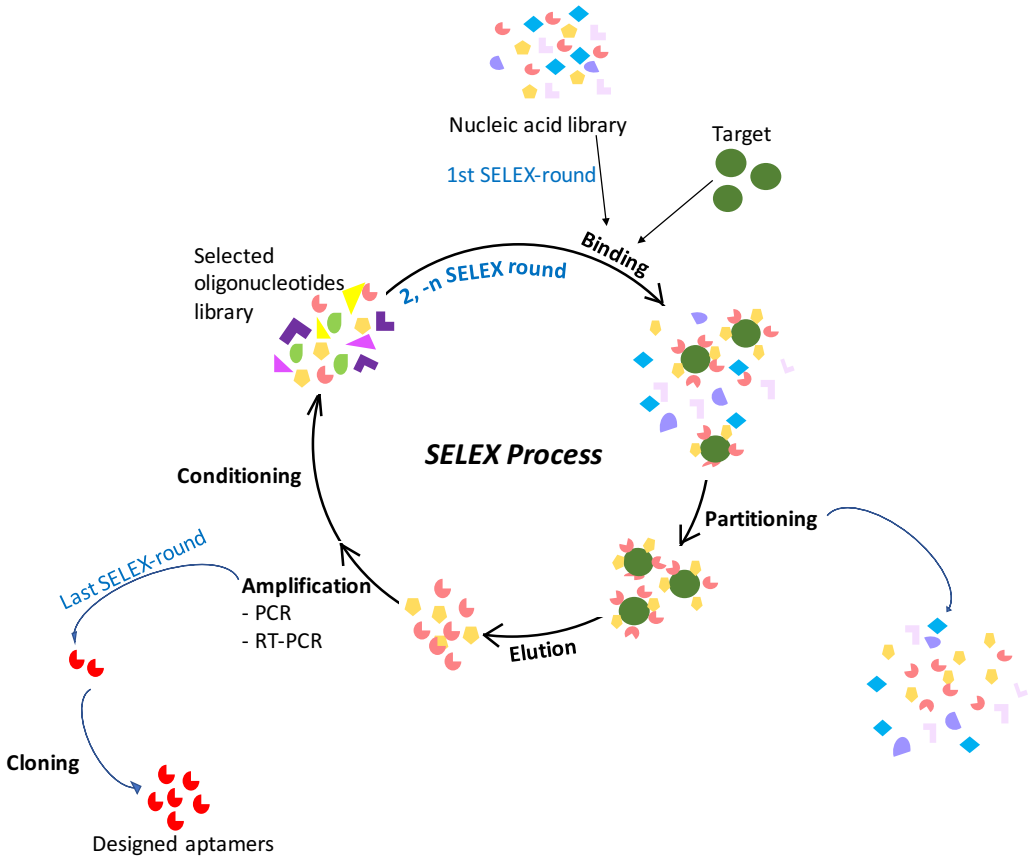

Figure 4.3. In vitro selection of target-specific aptamers using SELEX technology. [27] A synthetic random DNA library containing ~10^5 sequences is directly employed in the SELEX process for the selection of DNA aptamers. Each cycle includes selection, amplification, and conditioning. The target incubates in the library for binding, and the

unbound sequences are washed out from the binding complex. The target-bound oligonucleotides are then separated from the complex, copied and amplified by PCR. The amplified oligonucleotides add to the next DNA library, and a new cycle for the target happens again. Usually, an oligonucleotide with high affinity and specificity is prepared after 6-20 cycles.

Aptamers are a useful alternative to antibodies because their preparation is easier, more humane, and can be performed at a lower cost than antibodies. Over the past ten years, the development of aptamers has improved in terms of speed and selectivity. Many of these molecules are applied as optical sensors through the incorporation of enzymes, nanoparticles, quantum dots (QDs) and dyes. [22]

Aptamers have been successfully developed for the target molecules of inorganic ions [28], small organic molecules [29], nucleotides and derivatives [30], nucleic acids [31], peptides and proteins [27, 32] With appropriate labeling or downstream processing, this binding step can be used to indicate the presence of the target molecule in an unknown sample. [33] The detection of drugs and their metabolites is a particularly important applications in the use of aptamers. For example, a series of different aptamers have been developed to detect the presence of cocaine. Since the target is a small molecule of 303.353 g/mol, specificity can be a difficult to achieve and the sequences utilized include ssDNA and RNA based aptamers. The detection methods utilized for cocaine include fluorescence [34,35], electrochemistry [36,37] and colorimetric probes. Colorimetric methods can be separated into methods involving the

monomeric dyes [38] and gold nanoparticles aggregation. [39,40]

In summary, aptamers offer high selectivity and affinity to the target with easier preparation than current immunoassays. These oligonucleotide based biosensors can compete with other matrix elements to detect the target with minimal problems with interferences.

C. Lateral flow immunoassay

Many μPAD detection systems utilize the principle of lateral flow immunoassay (LFIA). In LFIA, a liquid sample is deposited on the sample pad and moves through the pad via capillary action. The analytes pass different zones where they are designed to interact with and/or bind to antibodies as well as gold nanoparticles. A LFIA device consists of several parts: (1) sample application pad; (2) conjugate release pad; (3) membrane; (4) test line and control line; (5) wicking-absorbent pad. (Figure 4.4) A sample reacts with at least two lines located on the strips: a test line and a control line. The test line captures and detects the complex of antibodies/analyte producing a color change resulting from nanoparticle aggregation while the control line detects unmodified analyte and/or indicates a proper flow of the liquid through the strip. As the end of the strip there is an absorbent pad which absorbs the excess solvent.[24]

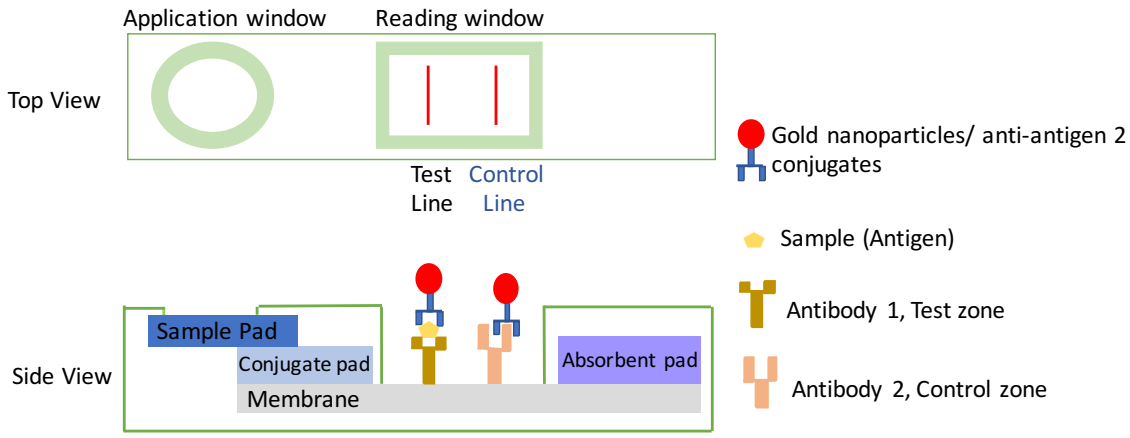

Figure 4.4 An example of a sandwich format of lateral flow immunoassay. [41] Samples are deposited on the sample pad and then move through capillary flow to the conjugated pad on membrane. When the AuNPs/anti-antigen 2 was captured by antibodies, it produced a red line in the antibody area.

The LFIAs are divided into two types of assays, competitive and sandwich. The former detects analytes having a single epitope and low molecular mass while the latter detects analytes with larger molecular weight containing more than one epitope. [41] The sandwich mechanism is more effective than the competitive assay. The sandwich assay has a test line with one analyte-specific antibody, and a conjugate release pad containing a second, labeled, anti-analyte antibody. The sample will bind during the primary process to the first antibody which is coupled to a gold nanoparticle. Then the sample-antibody conjugate is detected at the test line through the interaction between the second epitope and can be immobilized antibody at the test threshold. The response is directly proportional to the amount of analyte in the sample.

D. Gold nanoparticles/Aptamer based biosensors

Aptamers couple with enzymes, nanoparticles, QDs and dyes as the biosensors. Although QDs were first adapted to aptamer detection strategies by Levy and coworkers [42], gold nanoparticles become more increasingly popular because their absorption and optical properties change with the aggregation state. The color changes associated with the aggregation (purple-blue) and disaggregation (red) are easily visible to the naked eye without sophisticated instruments. In addition, gold nanoparticles are more biocompatible, easier to bio-conjugate, and less toxic than QDs. [1,9,34]

Gold nanoparticles will aggregate in the presence of added salt. However, gold nanoparticles can functionalize with biomolecules, and these functionalized nanoparticles can prevent the salt-induced aggregations from a low-salt solution even to an isotonic solution of salts. [43]

Several groups have developed different aptamer/ gold nanoparticles based biosensors. Most of published colorimetric methods utilizing AuNPs/aptamer based detection of cocaine are used in solution. Li et al. [44] modified a AuNPs/apatmer complex using biotin. In their device, biotinylated gold nanoparticle/aptamer complexes were added to a conjugation pad. Next cocaine was added. Upon reaching the conjugation pad, the drug was trapped by the biotinylated AuNPs/ aptamer complex. The results in release of nanoparticles, which continue to flow downstream

where a streptativdin test line captures the nanoparticles producing a red response.

In summary, gold nanoparticles can bind to aptamers with the result that these complexes can avoid salt-indicated aggregation. As a result, the DNA-functionalized gold nanoparticles maintain a red color in the presence of salt. In addition, the gold nanoparticles will aggregate together and produce a color change of blue in the presence of Mg salt solutions. Thus, functionalized nanoparticles can be used in colorimetric detection for target analytes.

2. Goals

The goal of the present project was to develop a paper-based microfluidic device to detect seized cocaine using specific drug binding aptamers and gold nanoparticles. The project included the determination of the capability of gold nanoparticles to move and aggregate on paper chips as well as characterizing the mobility and binding capability of anti-cocaine aptamers. In addition studies were performed on the potential modification of aptamers and gold nanoparticles for use in the detection of cocaine on paper microfluidic devices.

3. Chemicals and Methods

I. Chemicals

Gold (III) chloride trihydrate (≥ 99.9%) was purchased from Sigma-Aldrich (St Louis, MO). Sucrose, magnesium chloride hexahydrate and sodium citrate dihydrate were purchased from Fisher Scientific (Fair Lawn, NJ). The DNA sequences described by Fan et al.[40] were used to create the aptamers ACA-1: ACAGCAGGGTGAAGTAACTTCTTG and ACA-2: GGGAGTCAAGAAC, and the sequences were purchased from IDT (Coralville, IA). Cocaine standards were purchased from Sigma (St Louis, MO).

II. Synthesis of AuNPs

The preparation of AuNPs followed the reported produce. [45] All glasswares washed with aqua regia and d.i. water as well as the air drying before the synthesis. 0.039 grams of tetrachloraurate (III) hydrate was dissolved in 100 mL of d.i. water to 1 mM and 11.41 grams of sodium citrate dehydrate was dissolved in 10 mL of d.i. water to 38.8 mM. The solution of $HAuCl_4$ was heated to the reflux under stirring, and then the citrate solutions added to the reflux solution for another 10 minutes. After the addition of citrate, the pale yellow of the gold solution turned colorless and then black and finally wine-red in around 1 minute. The molar ratio of Au: citrate kept 1:3.8 in the solution. After 10 minutes, the flask with solutions sat in the ice bath for another 15 minutes. The AuNPs solution transferred to the volumetric flask and kept the volume of 100 mL with d.i.

water. The average particle size was determined by a dynamic light scattering measurement (ZetaSizer Nano, Malvern, UK).

III. Designs of μPADs

Two single channel μPADs were designed to detect cocaine samples. (Figure 4.5). The left design was used to detect the MDQ and the interference tests, and the right one was the design for the presumptive tests. Both designs have 2 zones A and B. Zone A was used to contain the AuNPs and the area was also used for colorimetric detection; zone B was the area used to deposit the aptamers. A second design (left hand side) had a third region, zone C, which was used for the deposition of sample solutions. A commercial wax printer (Xerox Color Cube 8750, Xerox, US) was used to print the single channel design on chromatography paper Whatman #1 (GE Healthcare, UK). The paper was wrapped in aluminum foil and passed through a laminator at 160 °C, a speed of 1.6 cm/sec (Tamercia Tashin Industrial Corp, TCC-6000) for 5 times. The laminator is used to melt the wax into the paper and create hydrophobic barriers. Samples and reagents are next deposited in the designed positions to optimize the color change on paper chips. Figure 5 showed the design of the device with letters indicating the potential locations of each reagent and samples. A 2 μL of AuNPs dropped on Position A and 3 μL of ACA-1 and ACA-2 were separately added to Position B. All reagents were added to μPADs and then dried. Otherwise the solution sample would spread along its corresponding channel. In the

detection tests, 1 µL of cocaine liquid samples were placed on Position C. In the reference tests, 1 µL of each sample was added to Position C. Vials were prepared for use with the carrier solution. Each vial contained 300 µL of 2.8M $MgCl_2$/ 0.15mM sucrose (v:v=1:1).

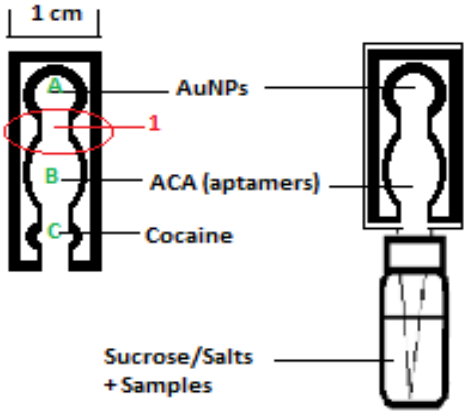

Figure 4.5. Left: The design of the AuNP/aptamer based µPAD used in these experiments. Zone A: AuNPs area; Zone B: aptamer (ACAs) area; Zone C: Sample area. Right: A presumptive test was developed for cocaine detection using this device. The process involves dipping a paper tab of the device into a solution containing the cocaine target. The circled region (1) is the connecting channel between gold nanoparticle area and aptamer area.

IV. Estimation of Visual LOD and MDQ

A modified paper chip (Figure 4.5 Left) was used in the determination of LOD. One µL of cocaine solution at a concentration from 1ng/mL to 10mg/mL was deposited onto the sample area (zone C - Figure 4.5, Left). Sample tests were repeated 9 times. The visual LOD was based on the color intensity at which greater than 90% of a group were able to detect the difference between a positive sample and a blank. [47] The camera-based LOD was performed using pictures recorded by a CCD

Camera from AmScope Inc. (Irvine, CA) attached to a Zeiss microscope (using a white background). The microscope was set at a magnification of 8x and a depth 1of 1.0 mm. The digital camera was set to an exposure setting of 120, exposure time 509, and gain 1.20; Color temperature was 6503 and Tint 1000. Data analysis was performed by ImageJ software 1.50i. The color analysis was performed in the AuNPs area. (zone A - Figure 4.5, Left) The camera based LOD was estimated as three times the standard deviation plus the blank signal (3s+b) of the quantity of drug at the inflection point for nanoparticle aggregation.

V. Interference tests

Publix granulated sugar, Arm & Hammer baking soda, ionized salt, Publix powdered sugar, King Arthur gluten free flour, Rumford aluminum-free baking powder, foot powder, tablets of Excedrin and ibuprofen, were purchased from supermarkets in Miami, FL. Procaine was purchased from Acros Organics (Waltham, MA). Caffeine, amphetamine, methamphetamine, ketamine, ephedrine were purchased from Sigma-Aldrich (St Louis, MO). Morphine and codeine were purchased from RBI (Natick, MA). All samples were prepared as 1mg/mL solutions in water for tests. Benzoylecgonine (1mg/mL) and ecognine methyl ester (0.1mg/mL) were purchased from Cerilliant (Round Rock, TX). The modified device (Figure 4.5, Left) was used in the interference tests. 1uL of each interference solution was added to the sample area (zone C - Figure 4.5, Left) and each test was repeated three times.

4. Results and Discussion

I. AuNPs/Aptamer detecting cocaine in solution tests

Two sets of cocaine aptamers were tested in the solution tests. [39,40] Zhang et al. [40] developed a set of anti-Cocaine aptamers (ACA-1 and ACA-2). This aptamer set included 2 unmodified DNA sequences, ACA-1 with 24 bases and ACA-2 with 13 bases. The mixture of ACAs and gold nanoparticles produced a color change from red to blue in the presence of cocaine and NaCl, but did not change with NaCl in the absence of cocaine. Alternatively, Liu et al. [39] developed three sequences for cocaine detection. According to their paper, the aggregated nanoparticles denature upon addition of cocaine and external heating, producing a color change from blue to red. We examined this process and were able to successfully incubate the gold nanoparticles with the aptamers, but the decomposition of the aptamer/gold nanoparticles did not occur on efficiently. Therefore, we reexamined the use of Zhang's ACA aptamers. The advantage of this set of aptamers was their sensitive to the presence of cocaine (as low as 2 μM [40]) and their quick reaction in solution tests. In addition, these aptamers were unmodified and less expensive to produce than those requiring biotin or thiol functional groups. The detection mechanism for the paper device was based on the capability of the free aptamers to bind cocaine or the surface of the gold nanoparticles. This binding process was thermodynamically favored and did not require external energy. In comparison, the aptamers created by Liu et al. [39],

could not be used in homogeneous assays as they required heating to separate the aptamers from the gold nanoparticles prior to binding cocaine, making the tests difficult to operate.

Picture 4.6 shows the production of color changes involving the change from a red-wine color to the purple color in the presence of cocaine.

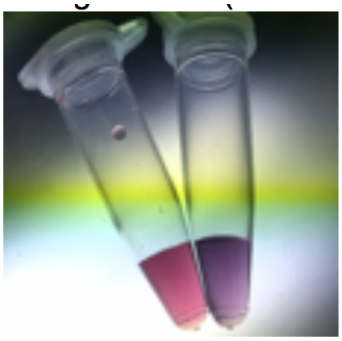

Figure 4.6. AuNPs/Aptamer based solution test for cocaine samples. In the absence of cocaine, the two ACA aptamers bind to the surface of gold nanoparticles and the complex does not aggregate with NaCl. The resultant mixture produces a red color. In the presence of cocaine, ACA aptamers bind to cocaine molecules and the gold nanoparticles aggregate producing a purple color. Left: Blank sample test; Right: cocaine sample test.

II. AuNPs on μPADs

The original μPADs design for cocaine detection was determined by changes in mobility causing aggregation of AuNPs on paper chips. Other applications of AuNPs on μPADs only used μPADs as a platform for detection [48,49], however, we have designed our system as a ready-to-use detector. The system permits sample analysis and detection based on capillary flow along a hydrophilic channel to the designed position where salt-induced self-aggregation and color development occurs.

a) Preparation of AuNPs on μPADs

A number of procedures were used in preparing the μPADs for analysis. These included immersion and deposition procedures. In the immersion method, the entire chromatographic paper was placed in a AuNP solution in which concentrations ranged from 1 mM to 0 mM for times ranging from 1 to 24 hours. When the immersion period was less than 12 hours, the AuNPs did not attach to the paper and the color of paper was pale pink to colorless. When the time was increased to 24 hours, the AuNPs appeared on chromatographic paper as a red color. The intensity of the color varied with concentration. Nanoparticles at a concentration from 0.5 mM to 0.6 mM, appeared dark red. Unfortunately, when AuNPs at concentrations of 0.5 mM or higher were used the color changed to purple-red or black when the paper dried, while AuNPs of 0.4 mM or lower appeared colorless on paper. Therefore, the immersion method can be used in the aggregation of AuNPs on paper for other purposes, but it was not appropriate for use the colorimetric detection.

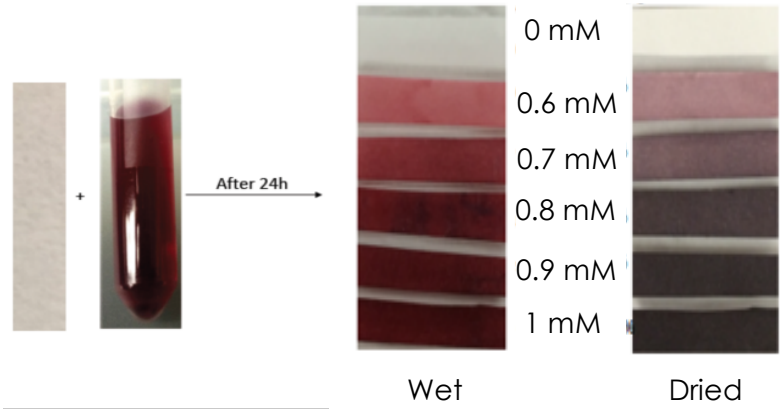

Picture 4.7. Effects of different concentration of AuNPs on chromatographic paper based on an immersion method. Gold nanoparticles were stable at concentrations below 0.6 mM in immersion methods on paper chips.

An alternate method for application to the paper was the deposition method. A zone was created on the paper with an inner diameter of 3.5mm (Figure 4.5) and 2 μL of a solution containing 1 mM, 0.5 mM, and 0.25 mM of AuNPs were tested in this area. The resulting color produced on the paper was a pink-red color with the 1mM solution while the 0.5 mM and 0.25 mM solutions produced a paler color which was hard to see. Therefore, 1 mM was the preferred concentration for the colorimetric detector.

When the synthesized AuNPs contained ~15% AuNPs of 15nm, the deposition of AuNPs appeared as red color on the AuNPs area but also produced a darker red or purple-red in the connecting areas. Depending on the distance between the point of application and the paper, sometimes the red color was darker in the external areas when compared to the middle of the deposition area. It was assumed that the darker spots on

the paper were due to the aggregation of the larger sizes of AuNPs.

To examine the effect of different quantities of AuNPs on paper, different volumes of 1mM AuNPs (2 μL, 4 μL, 6 μL, 2 μL *2 times, 2 μL*3 times) were added to the same position. When the volume of a single drop was higher than 2 μL, the AuNPs spread to the connecting channels and this region turned black. When multiple applications of small quantities of nanoparticles were added, the spreading effects decreased but the aggregation of the AuNPs in the designed positon increased and the area turned to purple-black. Therefore, a single deposition of 2 μL AuNPs of 1 mM was defined as the best method to optimize color effects on chromatographic paper.

b. Mobility of AuNPs on μPADs

In the original design, the AuNPs were expected to move to the end of the channel with the capillary flow. Unfortunately, the AuNPs did not move with the either water or sucrose on unmodified chromatographic paper. The AuNPs also aggregated on the micropads containing sucrose and water without any salt. (Figure 4.8)

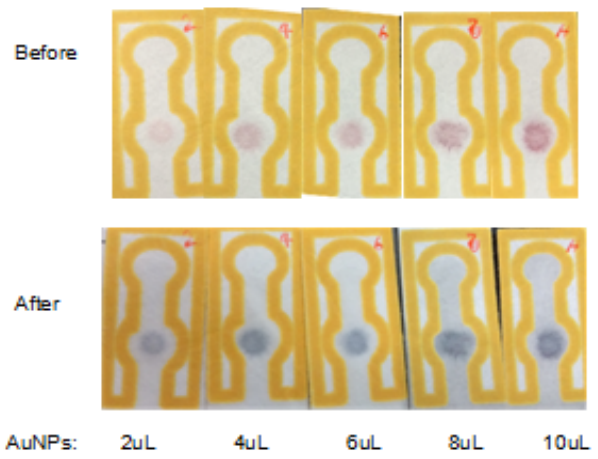

Figure 4.8. Effects of AuNPs paper without PVA/Tween 20 Treatments.

Therefore, it was necessary to perform surface modifications to the paper devices in order to increase the mobility and decrease the aggregation of AuNPs. Previous results using lateral flow devices [39] have indicated that AuNPs can move through membranes following the addition of sucrose. Surfactants such as Tween 20 and Tween 80, as well as the polymer poly(vinyl alcohol) (PVA) were also added to the paper to examine their effect on the mobility and aggregation of the nanoparticles. The modified paper was then immersed in the gold nanoparticles solutions for 24 hours. Tween 80 did not decrease the aggregation of AuNPs which turned to purple; Tween 20 decreased but did not eliminate the aggregation of AuNPs which turned to darker red while PVA minimized the aggregations yielding a pink-red color. Solutions of PVA from 0.01% to 1% provided the same color effects. However, AuNPs on PVA treated paper were too stable, these AuNPs did not move with capillary flow with

using sucrose solutions or distilled water.

To optimize the mobility and the stability of AuNPs on treated paper, we next examined mixtures of 0.01% PVA and 1% Tween 20 with different ratios (1:1, 1:9, 1:99). All treatments stabilized the AuNPs on paper, producing a red color. As the quantity of AuNPs on the paper increased, the darkness of the red color increased. To optimize the movement of the AuNPs, we examined different quantities of AuNPs at different ratios of PVA/Tween 20 and sucrose. The spotting positions are illustrated in Figure 4.9-top. With 0.15mM sucrose, the only successful condition was 1% Tween20/ 0.01% PVA (v:v=99:1) spotted in location 1 with AuNPs. As shown in Figure 4.9-a, we could observe color

Table 4.1. Effects of surfactant/ polymers modified AuNPs paper. PVA inhibited the aggregation of gold nanoparticles on paper, Tween 20 inhibited most of the aggregations of nanoparticles, Tween 80 does not inhibit nanoparticle aggregation.

	AuNPs/ PVA	AuNPs/ Tween 20	AuNPs/ Tween 80
Wet -> Dried	No Aggregation	Some Aggregation	Some Aggregation
Phenomena			
Deposited Water	No Aggregation	No Aggregation	Aggregation
Deposited 5M NaCl	No Aggregation	Some Aggregation	Aggregation
Deposited 0.15mM Sucrose/5M NaCl	No Aggregation	Some Aggregation	Aggregation

movements from position 1 (lower ball) to position 2 (top ball) with a solution containing 40mg/mL of sucrose, 50%Tween 20, and 1%PVA. More AuNPs moved to the end of the channel when the paper chips were treated with 50-30% Tween 20 mixed 1-0.1% PVA. (Figure 4.9-b) To optimize the movement of AuNPs, we tried different ratios of AuNPs to the PVA/Tween 20 along with 50 mg/mL sucrose. When the ratio of AuNPs: PVA/Tween 20 (v:v) was above 4:1, the moving distance and the darkness of the red color were obvious to the naked eye. (Figure 4.9) The whole procedure took around 10 minutes.

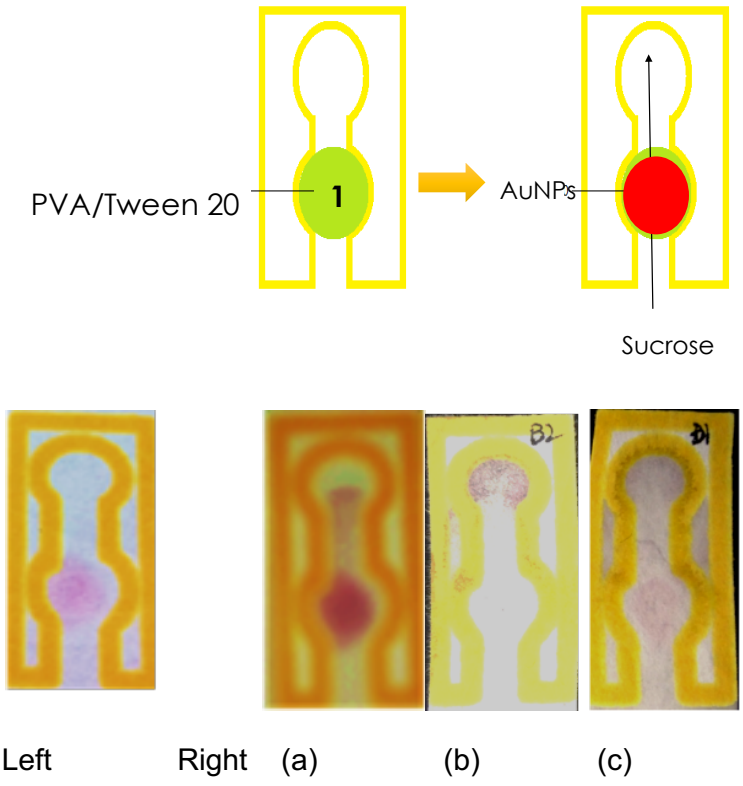

Figure 4.9. Effects of surface treatments on paper for AuNPs. Bottom: Left: AuNPs paper before test; Right: (a) 50mg/mL sucrose with the 1% Tween 20: 0.01% PVA in location 1; and (b): 40mg/mL sucrose with the 50% Tween 20: 0.01% PVA in location 1.

There were several problems when examining the mobility of the AuNPs on μPADs. The biggest issue was the low reproducibility of the moving AuNPs. We controlled all conditions in the preparations and operations, however, the same batch of AuNPs often produced different results. A larger quantity of AuNPs on the paper was required to achieve movement of AuNPs, but this process produced colors from red to purple in the designed position. If the width of the moving channel was reduced, the time increased to 1 hour and most AuNPs aggregated in the middle of the channel. If the moving channel was wider, the AuNPs moved past the wax barrier. Therefore, the design of this μPAD had to be changed.

c. Aggregations of AuNPs on μPADs

In earlier work, we found that a single deposition of 2 μL AuNPs of 1 mM produced a red color on chromatographic paper. Also as noted, AuNPs aggregate in solutions with the presence of salts. [1] Thus further testing was performed on the ability of different concentrations of AuNPs to produce aggregation. Table 4.2 shows that a concentration of 1 mM can produce complete aggregation in the presence of salts and sugars. Decreasing the concentration of gold nanoparticles reduced the aggregation effects. Sodium chloride and magnesium chloride were examined in both solution and on μPADs to examine their effect on aggregation. Magnesium chloride produced a more intense color of AuNPs aggregation in both tests. Therefore, magnesium chloride was used as the aggregating agent in the moving solution. Sucrose did not

cause aggregation in solution, however, gold nanoparticles did aggregate on the μPADs as a result of the capillary flow of sucrose into their zone. After tests of the mobility and aggregation, we utilized the aggregation of AuNPs on μPADs instead of their mobility on μPADs as the colorimetric detector. The next step was to determine if aptamers could bind AuNPs on μPADs.

Table 4.2. Aggregation effects of AuNPs on μPADs. The color in the table indicated the color change happened on μPADs. Black = Full aggregations, Purple = Partly aggregations, Brown-red = little aggregations, Red = No aggregations.

	Type	AuNPs #1	AuNPs #2	AuNPs #3
AuNPs concentrations		1mM	0.5mM	0.25mM
w/out Surface treatment	Sucrose			
	$MgCl_2$			
	NaCl			
	Sucrose + $MgCl_2$			
	Sucrose + NaCl			

III. Aptamers on μPADs

In our design, aptamers have two functions, (1) binding to gold nanoparticles to avoid aggregation in the presence of salts; (2) binding to cocaine. Gold aptamers should have sufficient mobility in the carrier solutions to permit moving through the channel via capillary action, and the ability to bind to the cocaine molecules.

Aptamers are colorless in solution so we needed a visual detection procedure for μPADs tests. To do this we used SYBR Gold and SYBR Green fluorescent DNA labeling dyes to track the presence and movements of aptamers on paper chips. 2uL of dye and the ACAs aptamer were separately dropped to the bottom-ball position on paper chips. (Figure 4.10) Sucrose can move the aptamers through the membrane, and the higher concentrations of sucrose can move even more aptamers on a solid matrix. [39] A series of sucrose with different concentrations were examined. 0.15mM of sucrose moved aptamers with a highest speed. When the paper dried, these paper chips were put in 50mg/mL of sucrose solution until the moving solution arrived at the end of the channel. A molecular imaging software of KODAK MI and a Gel Logic 100 were used to record the fluorescence of aptamers on paper chips. The detected fluorescence indicated the positions of the aptamers after the tests. Figure 4.10 showed that the dyes stayed in the bottom ball in the blank test, but the dyes moved up to the end of the channel in the presence of the aptamers. The moving fluorescence position

demonstrated that the aptamers can move through the channel on μPADs with sucrose. There was fluorescence in the middle of channel, indicating that the optimized conditions for the mobility of the aptamer should be either include a longer time for capillary action, or a shorter channel to transform more aptamers.

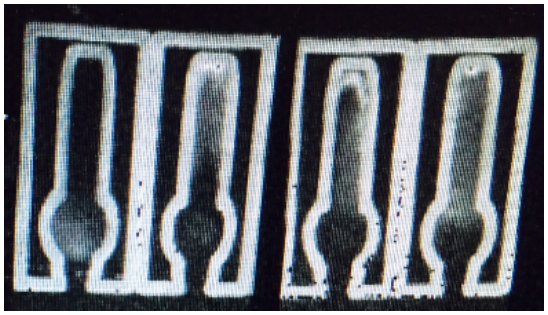

Figure 4.10. Movements of Dyes and Dye/Aptamer on paper chips with 50mg/mL of sucrose. Left: SYBR Gold only; Mid-left: SYBR Gold-ACA-1; Mid-right: SYBR+ACA-2; Right: SYBR Gold ACA1&ACA2.

The paper chips were next used to observe the binding of the ACAs aptamers with cocaine in Figure 4.11. SYBR Green 5x was used as the tracking dye. 4 uLof SYBR Green mixed ACA-1 and ACA-2 was deposited at the bottom ball. 1mg of Cocaine was dissolved in 40mg/mL sucrose. The bottom of the paper chip was placed in the sucrose solution for 10 minutes and the fluorescent response was photographed in each the channels as shown in Figure 4.6. The single aptamers or cocaine did not produce fluorescence with SYBR Green. The application of a mixture

of the two ACAs produced a fluorescence signal and the mixture of ACAs/cocaine enhanced the intensity of the fluorescence. ImageJ software was used to analyze the optical density of the top channels from Figure 4.11, and the average optical density of ACA mixture/SYBR Green was 0.005367, and the average optical density of ACA/SYBR Green/ Cocaine was 0.005521. The intensities indicated that ACAs can move through the channel of μPADs and they can also bind cocaine on μPADs.

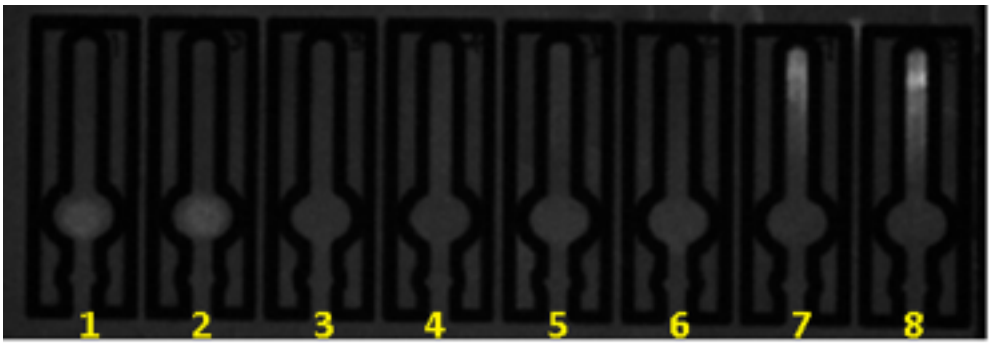

Figure 4.11: Results of SYBR Green with cocaine, ACAs and their mixtures.

1. Only SYBR Green 5X;

2. SYBR Green 5X + Cocaine, 1mmol

3. SYBR Green 5X + ACA-1, 1mmol;

4. SYBR Green 5X + ACA-1, 1mmol + Cocaine, 1mmol;

5. SYBR Green 5X + ACA-2, 1mmol;

6. SYBR Green 5X + ACA-2, 1mmol + Cocaine, 1mmol;

7. SYBR Green 5X + ACA-mixture, 0.5mmol of each ACA; ACA mixture/SYBR Green produced a fluorescence.

8. SYBR Green 5X + ACA-mixture, 0.5mmol of each ACA + Cocaine, 1mmol. ACAs/ SYBR Green/ Cocaine produced a brighter fluorescence in the end of channel.

IV. Aptamers/AuNPs complex on μPADs

a) Designs

The next step was to modify the aptamer/AuNPs assay to permit the usage in μPADs as demonstrated in Scheme 1 (Figure 4.12). A series of experiments were performed examining the stability and mobility of the various components of the detection scheme. Initial tests indicated that the gold nanoparticles bound strongly to the paper matrix. Thus, these were placed at the end of the channel. Aptamers were placed in a zone upstream of the AuNPs area. When the samples moved with the carrier solution, the ACAs bind to the targets and then the complex of aptamers/cocaine move toward the AuNPs area. Without the protection of the free aptamers, the AuNPs would aggregate under due to salt-induced aggregation. When the sample was not cocaine, the ACAs move with carrier solution and bind to the surface of the AuNPs eliminating the possibility of aggregation.

A series of experiments were next performed to test the stability and mobility of the various components of the detection scheme. The results were shown in Table 4.3. In the absence of aptamers, AuNPs on the μPADs produced a color change with the capillary flow of water, sucrose or sucrose/$MgCl_2$. In the presence of aptamers, the red color of AuNPs changed to purple when water was introduced. When the aqueous solution included sucrose, the red color turned to a darker red. With an aqueous solution containing sucrose and $MgCl_2$, the color changed to red-

purple. The next step was to optimize the concentration of the solution to produce an intense color change.

b) Moving solutions

The components of carrier solutions were important, as these contain the salt which produces the aggregation of AuNPs, and the sucrose which assists the movement of the AuNPs, and increases the binding of aptamers to AuNPs surfaces. A range of concentrations of salt and sucrose were examined. The best results occurred with a $MgCl_2$ concentration of 2.8m and 50mg/mL sucrose. Higher concentrations of sucrose reduced capillary flow while lower amounts of $MgCl_2$ did not produce full aggregation. These results suggested that the sucrose in the system helped to mobilize the aptamers towards the end of the channel [39], and that the $MgCl_2$ acted as the aggregating agent of the AuNPs. The optimized sucrose/$MgCl_2$ resulted in a salt-induced aggregation in the presence of cocaine. The aggregation was inhibited in the absence of cocaine, Table 4.3.

Table 4.3. The effect of different reagents on the aggregation of gold nanoparticles on the paper microfluidic device.

AuNPs	Aptamers	Moving S.	Cocaine	Color Result		Detection
2 nmol	n/a	Sucrose/ $MgCl_2$	n/a		Black	-
2 nmol	6 nmol	Sucrose/ $MgCl_2$	n/a		Red	Negative
2 nmol	6 nmol	Sucrose/ $MgCl_2$	Crack Cocaine		Black	Positive
2 nmol	6 nmol	Sucrose/ $MgCl_2$	Cocaine HCl		Black	Positive

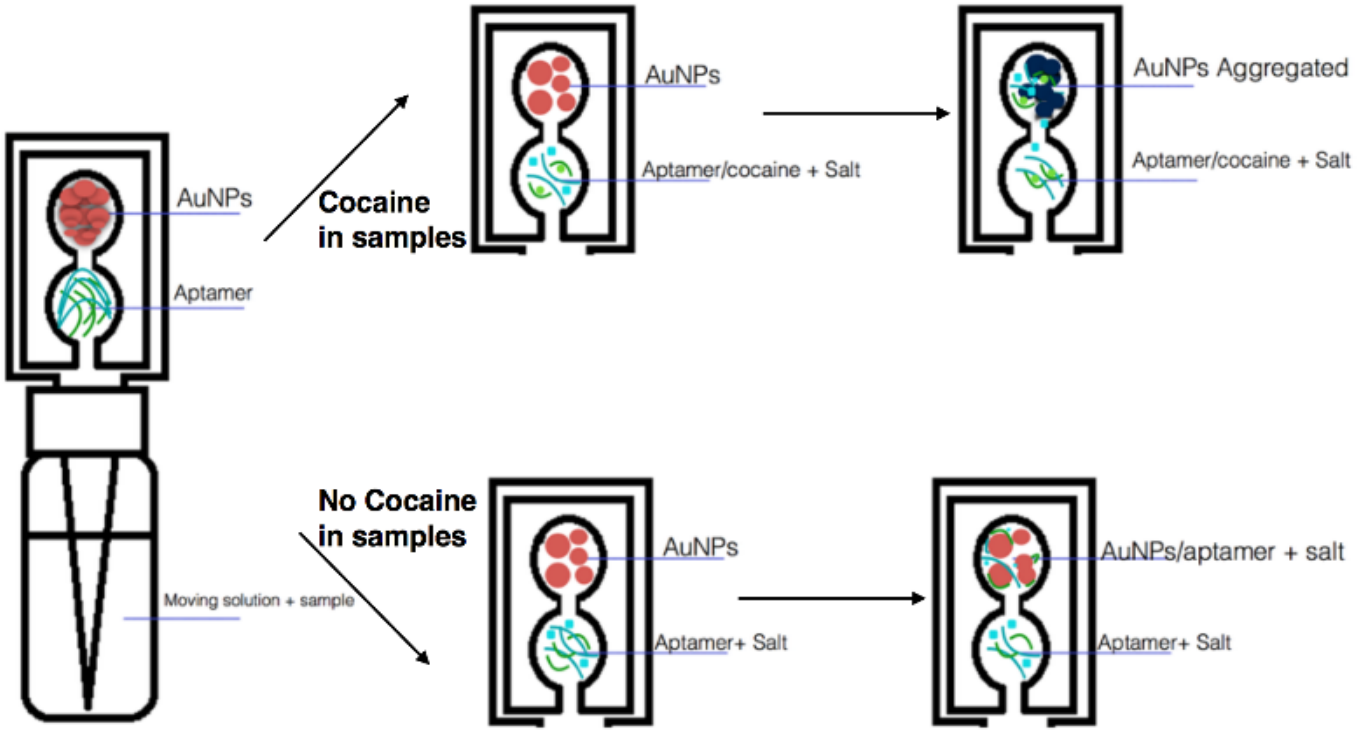

Figure 4.12. Schematic of the detection

c) AuNPs/Aptamers on μPADs

The visibility of the color change on the μPADs depended on the quantity of AuNPs and the method of addition. Lower concentrations of nanoparticles were difficult to detect once the colloidal gold solution dried on the paper. 2uL of 1 mM AuNPs deposited on the paper device with a size ranging 20 - 40nm produced a pink-red color on the μPADs visible to the naked eyes. The color changes that occured when AuNPs were used on μPADs in the absence of cocaine depended on the quantity of the two aptamers on the paper. AuNPs are sensitive to salts and produce salt-induced aggregation with the carrier solution of $MgCl_2$ if aptamers are not present. When present, the aptamers flow down the chip with the capillary flow of the $MgCl_2$/sucrose solution. When the aptamers arrive at the AuNPs area, they inhibit aggregation even in the presence of the salt solution. Figure 4.13 demonstrates that a linear relationship exists between the quantity of the two aptamers and the red colored response on the paper (red component of the RGB.) When the total amount of the two aptamers was less than 1.2 nmol, the deposited AuNPs turned to gray indicating that the quantity of the two aptamers was insufficient to bind to the surface of AuNPs and avoid aggregation. When the aptamer quantity was 1.2 nmol or more, the aggregation of AuNPs decreased and the color changed only from purple-red to light purple. At 8 nmol or higher, AuNPs area remained red, indicating that a sufficient quantity of aptamer was present to bind to the 2nmol AuNPs. This was judged to be the optimal amount of aptamer. (Figure 4.13)

At higher concentrations, a loss of sensitivity occurred. The binding effects between AuNPs and aptamers for solution tests required a 1:1 molar ratio. On paper however, a larger amount of aptamer was required to avoid the salt-induced aggregation. The color change of purple-red was hard to observe. The expected color was purple-black or black as an indicator for the presence of cocaine. The optimized amount was 1.2 nmol of ACAs which achieved the best sensitivity.

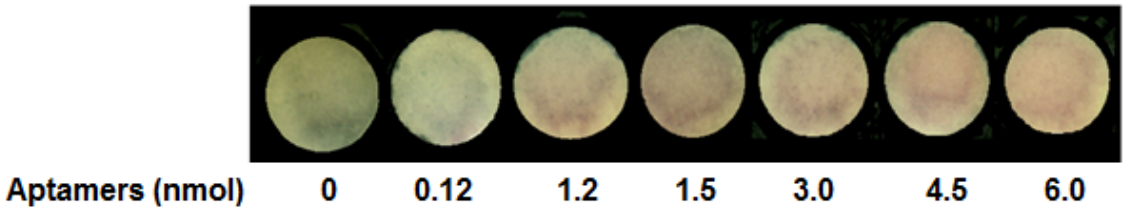

Figure 4.13. The effect of increasing quantities of the two aptamers applied to 2 nmol of the AuNPs on paper. As the concentration increases a red color appears. The optimum amount was 1.2 nmol of the aptamer mixture as this amount achieves the best sensitivity.

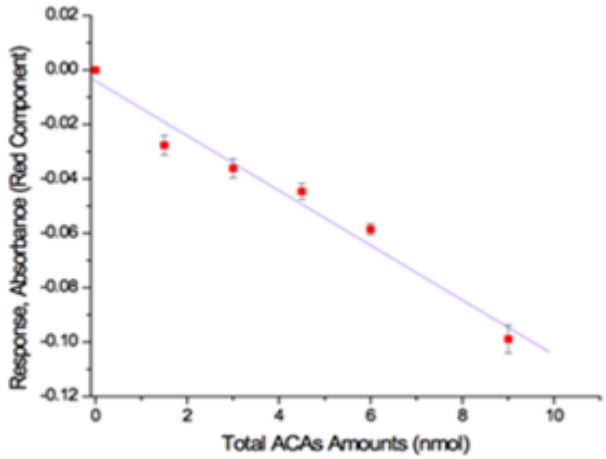

Figure 4.14. The color change produced when the sucrose/MgCl2 solvent front mixes with 2nmol AuNPs in the presence of differing amount of Aptamers on the μPAD. A linear response is obtained as y=-0.004 – 0.01x, R^2=-0.98. Error bars represent standard deviations of triplicate measurements.[46]

b) AuNPs/Aptamer based uPADs detecting cocaine

In these experiments a range of different designs were applied in the detection of cocaine. The channel design (length and width) affects run time and can affect the binding of cocaine/ACAs and the aggregation of AuNPs with salt. In the current design (Figure 4.5), the dimensions are 4mm (length) * 2mm (width) in the circled positions. These dimensions permit the carrier solution to move the samples through the chip within 5 minutes, and provide a visual LOD of 2.5 µg and an instrumental LOD of 2.4 µg. However, if this area is increased to 6mm (L) * 1mm (W), the visual LOD drops, however, the run time increases to 30 minutes or more

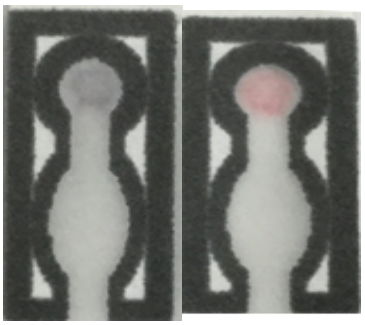

Figure 4.15. Example of the application of the µPAD in the detection of cocaine HCl. Left: 5mg/mL cocaine sample. Right: Blank sample.

In a typical experimental test, AuNPs (2nmol) and aptamers (ACA-1 and ACA-2, 0.6nmol each) were prepared and added to the µPADs. In the presence of 10µg cocaine, a solution of 2.8M $MgCl_2$/ 50mg/mL sucrose moved through the aptamer zone to the next location containing the AuNPs. Once this solution reached this region, the AuNPs turned from pink-red to gray in 5 minutes. In contrast, in the

absence of cocaine, the moving solution arrived at the end of the channel, and the AuNPs area remained red. (Figure 4.15) All color changes were apparent to the naked eye. The color changes of AuNPs indicated that aptamers could form a tertiary structure around the cocaine not only in the solution but also on the μPADs. Furthermore, AuNPs can produce a salt-induced aggregation on μPADs and aptamers can stabilize AuNPs against the aggregation on μPADs. (Figure 4.13) Experiments were next performed to define the optimized conditions for stabilization of the AuNPs and Aptamers on μPADs, while still permitting a sensitive and robust method to detect the presence of cocaine.

c) Estimation of visual LOD and MDQ

Figure 4.15 illustrates that the relationship between the response of the red component and the quantity of cocaine detected. When the cocaine amount was 0.1μg or lower, the AuNPs had a red/red-purple color. At amounts of cocaine of 0.5μg or higher a purple color change occurred and at 2.5μg or higher, the color became grey-purple. The visual LOD was based on the color intensity at which greater than 90% of a group of 13 individuals was able to detect the difference between a positive sample and a blank. The camera-based LOD was calculated at the inflection point for plot of red absorbance vs cocaine concentration. As is illustrated by the figure, at 1.7+/- 0.2 ug of cocaine a rapid transition occurs due the cocaine induced aggregation of the nanoparticles. This point was used to determine a camera-based LOD of 2.36 μg (3s+b). The LOD was consistent

over a range of 0.6 to 3.6nmol of each aptamer and 2 to 4 nmol AuNPs on the μPADs.

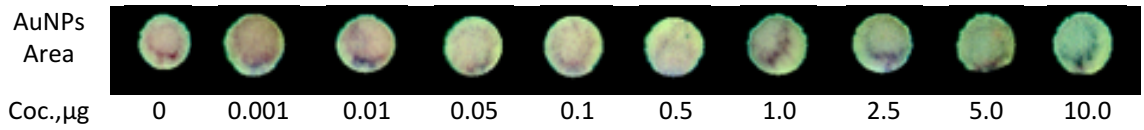

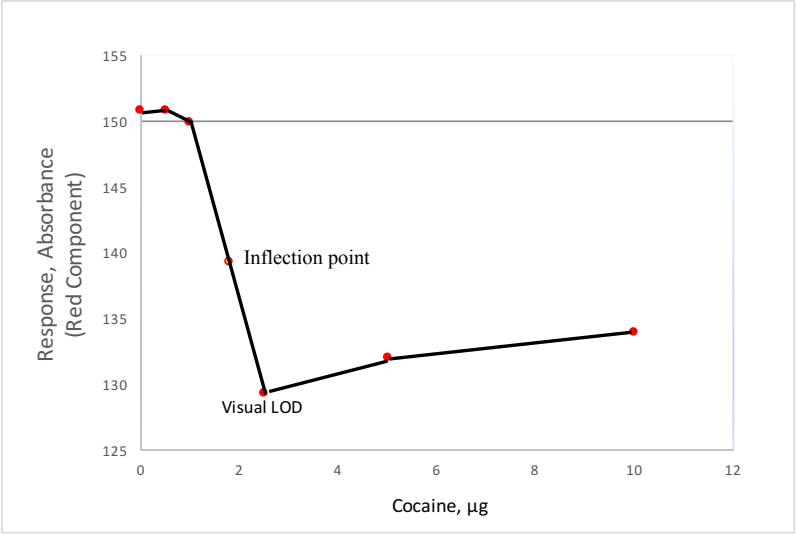

Figure 4.16. The effect of increasing quantity of cocaine on the response of red component (RGB) from image J. As seen in the figure, at a signal intensity of 139, an inflection point occurs. This point is used to estimate the camera based LOD of 2.36. The standard deviation of the estimate at the inflection point was 0.20 ug. The visual LOD was estimated based on a signal sufficient for 90% of subjects to detect the color change and was 2.5 ug of cocaine.

Table 4.4. Estimation of instrumental LOD and visual LOD.

Drug	Instrumental LOD	Visual LOD
Cocaine	2.36 μg	2.5μg

b) Interference tests

Common white powders including baking soda, salt, powder sugar, flour, baking powder, foot powder, Excedrin and ibuprofen were tested as potential

interferences. All tested interferences maintained an intense red color indicating a negative result. Common diluents used in illicit samples,

Table 4.5. Interference tests. All listed interference materials produced negative results of red colors

Interference Compounds	Types	Amount (ug)	Results
Benzoylecgonine	Metabolite	1.5	No Aggregation
Ecgonine methyl ester	Metabolite	0.15	No Aggregation
Ketamine	Drug	1.5	No Aggregation
Codeine	Drug	1.5	No Aggregation
Morphine	Drug	1.5	No Aggregation
Ephedrine	Drug	1.5	No Aggregation
Amphetamine	Drug	1.5	No Aggregation
Methamphetamine	Drug	1.5	No Aggregation
JWH-073	Drug	1.5	No Aggregation
Caffeine	Adulterant	1.5	No Aggregation
Procaine HCl	Adulterant	1.5	No Aggregation
Sugar	Diluent	1.5	No Aggregation
Sucrose	Diluent	1.5	No Aggregation
Inositol	Diluent	1.5	No Aggregation
Excedrine	Common powder	1.5	No Aggregation
Ibuprofen	Common powder	1.5	No Aggregation
Foot powder	Common powder	1.5	No Aggregation
Baking soda	Common powder	1.5	No Aggregation
Sea Salts	Common powder	1.5	No Aggregation
Flour	Common powder	1.5	No Aggregation
Powder sugar	Common powder	1.5	No Aggregation

such as sugar, procaine, caffeine and inositol also produced a negative result. Illicit drugs such as ephedrine, codeine, ketamine, amphetamine, morphine, and

JWH-073 did not produce a color change; methamphetamine produced a reddish-purple color. Metabolites of cocaine, benzoylecgonine and ecgonine methyl ester were also negative. (Table 4.5)

5. Conclusions

A rapid and specific method using an AuNPs/aptamer based paper microfluidic device has been developed for the field tests of seized cocaine. The stamp-size paper device produces a detectable color change by the naked-eye or camera. The method can detect microgram levels of cocaine in under 5 minutes. The procedure uses environmentally friendly reagents in a flexible format. Compared to current colorimetric testing procedures, the newly developed μPADs are inexpensive and easy to use. When tested against a wide variety of potential interferences, the μPAD has shown a high specificity and sensitivity. Furthermore, this strategy has the potential to detect other illicit drugs as new aptamers are developed. Overall, we believe this general procedure can benefit the forensic detection of many types of illicit drugs.

6. References

1. Louis, C. and O. Pluchery, Gold nanoparticles for physics, chemistry and biology. 2012: World Scientific.

2. Brust, M., Walker, M., Bethell, D., Schiffrin, D. J., & Whyman, R. Synthesis of thiol-derivatised gold nanoparticles in a two-phase liquid–liquid system. *Journal of the Chemical Society, Chemical Communications*, **1994**, (7), 801-802.

3. Kimling, J., Maier, M., Okenve, B., Kotaidis, V., Ballot, H., & Plech, A. Turkevich method for gold nanoparticle synthesis revisited. *The Journal of Physical Chemistry B*, **2006**, *110*(32), 15700-15707.

4. Jana, N. R., Gearheart, L., & Murphy, C. J. Seed-mediated growth approach for shape-controlled synthesis of spheroidal and rod-like gold nanoparticles using a surfactant template. *Advanced Materials*, **2001**, *13*(18), 1389.

5. Grzelczak, M., Pérez-Juste, J., Mulvaney, P., & Liz-Marzán, L. M. Shape control in gold nanoparticle synthesis. *Chemical Society Reviews*, **2008**, *37*(9), 1783-1791.

6. Niemeyer, C. M. Nanoparticles, proteins, and nucleic acids: biotechnology meets materials science. *Angewandte Chemie International Edition*, **2001**, *40*(22), 4128-4158.

7. Chithrani, B. D., Ghazani, A. A., & Chan, W. C. Determining the size and shape dependence of gold nanoparticle uptake into mammalian cells. *Nano lett*, **2006**, *6*(4), 662-668

8. Giljohann, D. A., Seferos, D. S., Daniel, W. L., Massich, M. D., Patel, P. C., & Mirkin, C. A. Gold nanoparticles for biology and medicine. *Angewandte Chemie International Edition*, **2010**, *49*(19), 3280-3294.

9. Valcárcel, Miguel, and Ángela I. López-Lorente. Gold nanoparticles in analytical chemistry. Vol. 66. Elsevier, 2014.

10. Jain, P. K., Lee, K. S., El-Sayed, I. H., & El-Sayed, M. A. Calculated absorption and scattering properties of gold nanoparticles of different size, shape, and composition: applications in biological imaging and biomedicine. *J. Phys. Chem. B*, **2006**, *110*(14), 7238-7248.

11. Hecold, M., Buczkowska, R., Mucha, A., Grzesiak, J., Rac-Rumijowska, O., Teterycz, H., & Marycz, K. The Effect of PEI and PVP-Stabilized Gold Nanoparticles on Equine Platelets Activation: Potential Application in Equine Regenerative Medicine. *Journal of Nanomaterials*, *2017*.

12. Khlebtsov, N., & Dykman, L. Biodistribution and toxicity of engineered gold nanoparticles: a review of in vitro and in vivo studies. *Chemical Society Reviews*, **2001**, *40*(3), 1647-1671.

13. Benkovičová, M., Végsö, K., Šiffalovič, P., Jergel, M., Majková, E., Luby, Š., & Šatka, A. Preparation of sterically stabilized gold nanoparticles for plasmonic applications. *Chemical Papers*, **2013**, *67*(9), 1225-1230.

14. Rayford, C. E., Schatz, G., & Shuford, K. Optical properties of gold nanospheres. *Nanoscape*, **2005**, *2*(1), 27-33.

15. Lee, J. S., Han, M. S., & Mirkin, C. A. Colorimetric detection of mercuric ion (Hg2+) in aqueous media using DNA-functionalized gold nanoparticles. *Angewandte Chemie*, **2007**, *119*(22), 4171-4174.

16. Sato, K., Hosokawa, K., & Maeda, M. Rapid aggregation of gold nanoparticles induced by non-cross-linking DNA hybridization. *Journal of the American Chemical Society*, **2003**, *125*(27), 8102-8103.

17. Zhou, J., Ralston, J., Sedev, R., & Beattie, D. A. Functionalized gold nanoparticles: synthesis, structure and colloid stability. *Journal of Colloid and Interface Science*, **2009**, *331*(2), 251-262.

18. Takae, S., Akiyama, Y., Otsuka, H., Nakamura, T., Nagasaki, Y., & Kataoka, K. Ligand density effect on biorecognition by PEGylated gold nanoparticles: regulated interaction of RCA120 lectin with lactose installed to the distal end of tethered PEG strands on gold surface. *Biomacromolecules*, **2005**, *6*(2), 818-824.

19. Lee, S. H., Bae, K. H., Kim, S. H., Lee, K. R., & Park, T. G. Amine-functionalized gold nanoparticles as non-cytotoxic and efficient intracellular siRNA delivery carriers. *International journal of pharmaceutics*, **2008**, *364*(1), 94-101.

20. Chen, C., Wang, W., Ge, J., & Zhao, X. S. Kinetics and thermodynamics of DNA hybridization on gold nanoparticles. *Nucleic acids research*, **2009**, *37*(11), 3756-3765.

21. Tiwari, P. M., Vig, K., Dennis, V. A., & Singh, S. R. Functionalized gold nanoparticles and their biomedical applications. *Nanomaterials*, **2001**, *1*(1), 31-63.

22. Lakhin, A. V., Tarantul, V. Z., & Gening, L. V. Aptamers: problems, solutions and prospects. *Acta Naturae (англоязычная версия)*, **2013**, *5*(4),19.

23. Bouchard, P. R., Hutabarat, R. M., & Thompson, K. M. Discovery and development of therapeutic aptamers. *Annual review of pharmacology and toxicology*, **2010**, *50*, 237-257.

24. Kulbachinskiy, A. V. Methods for selection of aptamers to protein targets. *Biochemistry (Moscow)*, **2007**, *72*(13), 1505-1518.

25. Conrad, R. C., Giver, L., Tian, Y., & Ellington, A. D. In vitro selection of nucleic acid aptamers that bind proteins. *Methods in enzymology*, **1996**, *267*, 336-367.

26. Tuerk, C., & Gold, L. Systematic evolution of ligands by exponential enrichment: RNA ligands to bacteriophage T4 DNA polymerase. *Science*, **1990**, *249*(4968), 505-510.

27. Stoltenburg, R., Reinemann, C., & Strehlitz, B. SELEX—a (r) evolutionary method to generate high-affinity nucleic acid ligands. *Biomolecular engineering*, **2007**, *24*(4), 381-403.

28. Freeman, R., Liu, X., & Willner, I. Chemiluminescent and chemiluminescence resonance energy transfer (CRET) detection of DNA, metal ions, and aptamer–substrate complexes using hemin/G-quadruplexes and CdSe/ZnS quantum dots. *Journal of the American Chemical Society*, **2001**, *133*(30), 11597-11604.

29. Liu, D., Wang, Z., & Jiang, X. Gold nanoparticles for the colorimetric and fluorescent detection of ions and small organic molecules. *Nanoscale*, 2011, *3*(4), 1421-1433.

30. Latham, J. A., Johnson, R., & Toole, J. J. The application of a modified nucleotide in aptamer selection: novel thrombin aptamers containing-(1-pentynyl)-2′-deoxyuridine. *Nucleic Acids Research*, **1994**, *22*(14), 2817-2822.

31. Sekkai, D., Dausse, E., Di Primo, C., Darfeuille, F., Boiziau, C., & Toulmé, J. J. In vitro selection of DNA aptamers against the HIV-1 TAR

RNA hairpin. *Antisense and Nucleic Acid Drug Development*, **2002**, *12*(4), 265-274.

32. Hamaguchi, N., Ellington, A., & Stanton, M. Aptamer beacons for the direct detection of proteins. *Analytical biochemistry*, **2001**, *294*(2), 126-131.

33. Cho, E. J., Lee, J. W., & Ellington, A. D. Applications of aptamers as sensors. *Annual Review of Analytical Chemistry*, **2009**, *2*, 241-264.

34. Zhou, J., Ellis, A. V., Kobus, H., & Voelcker, N. H. Aptamer sensor for cocaine using minor groove binder based energy transfer. *Analytica chimica acta*, **2012**, *719*, 76-81.

35. Stojanovic, M. N., De Prada, P., & Landry, D. W. Aptamer-based folding fluorescent sensor for cocaine. *Journal of the American Chemical Society*, **2001**, *123*(21), 4928-4931.

36. Li, X., Ballerini, D. R., & Shen, W. A perspective on paper-based microfluidics: current status and future trends. *Biomicrofluidics*, **2012**, *6*(1), 011301.

37. Swensen, J. S., Xiao, Y., Ferguson, B. S., Lubin, A. A., Lai, R. Y., Heeger, A. J., Soh, H. T. Continuous, real-time monitoring of cocaine in undiluted blood serum via a microfluidic, electrochemical aptamer-based sensor. *Journal of the American Chemical Society*, **2009**, *131*(12), 4262-4266.

38. Stojanovic, M. N., & Landry, D. W. Aptamer-based colorimetric probe for cocaine. *Journal of the American Chemical Society*, **2002**, *124*(33), 9678-9679.

39. Liu, J., & Lu, Y. Fast colorimetric sensing of adenosine and cocaine based on a general sensor design involving aptamers and nanoparticles. *Angewandte Chemie*, **2006**, *118*(1), 96-100.

40. Zhang, J., Wang, L., Pan, D., Song, S., Boey, F. Y., Zhang, H., & Fan, C. Visual cocaine detection with gold nanoparticles and rationally engineered aptamer structures. *Small*, **2008**, *4*(8), 1196-1200.

41. Posthuma-Trumpie, G. A., Korf, J., & van Amerongen, A. Lateral flow (immuno) assay: its strengths, weaknesses, opportunities and threats. A literature survey. *Analytical and bioanalytical chemistry*, **2009**, *393*(2), 569-582.

42. Levy, M., Cater, S. F., & Ellington, A. D. Quantum-dot aptamer beacons for the detection of proteins. *ChemBioChem*, **2005**, *6*(12), 2163-2166.

43. Zhao, W., Lin, L., Hsing, I. M. Rapid synthesis of DNA-functionalized gold nanoparticles in salt solution using mononucleotide-mediated conjugation. *Bioconjugate chemistry*, **2009**, *20*(6), 1218-1222.

44. Liu, J., Mazumdar, D., Lu, Y. A Simple and Sensitive “Dipstick” Test in Serum Based on Lateral Flow Separation of Aptamer-Linked Nanostructures. *Angewandte Chemie*, **2006**, *118*(47), 8123-8127.

45. Schubert, U., Hüsing, N., Laine, R. *Materials syntheses: a practical guide*. Springer Science & Business Media. 2008.

46. Kompany-Zareh, M., Mansourian, M., Ravaee, F. Simple method for colorimetric spot-test quantitative analysis of Fe (III) using a computer controlled hand-scanner. *Analytica Chimica Acta*, **2002**, *471*(1), 97-104.

47. Scherr, T. F., Gupta, S., Wright, D. W., Haselton, F. R. Mobile phone imaging and cloud-based analysis for standardized malaria detection and reporting. *Scientific reports*, **2016**, *6*, 28645.

48. Chen, G. H., Chen, W. Y., Yen, Y. C., Wang, C. W., Chang, H. T., & Chen, C. F. Detection of mercury (II) ions using colorimetric gold nanoparticles on paper-based analytical devices. *Analytical chemistry*, **2014**, *86*(14), 6843-6849.

49. Zhao, W., Ali, M. M., Aguirre, S. D., Brook, M. A., & Li, Y. Paper based bioassays using gold nanoparticle colorimetric probes. *Analytical chemistry*, **200**8, *80*(22), 8431-8437.

Chapter 5. Conclusions and Future Work

1. Conclusions

In forensic analysis, presumptive tests for drugs of abuse may be performed on-site or in a laboratory setting. With increasing laboratory backlogs, on-site and point-of-care based testing have become important ways to prescreen samples as well as to provide probable cause that a crime has taken place. The colorimetric response from this type of presumptive test depends on the sensitivity of the test and the sample type. Colorimetric tests are typically used for seized drugs, while antibody-based, lateral flow immunoassay techniques are used for trace detection of drugs in toxicological samples such as saliva, sweat and urine. Although these methods are cheap and easy to use, they generally lack multiplex capabilities, thus several individual tests are required to determine the range of potential analytes. Since these procedures are presumptive, false positive results can occur due to lack of specificity, and false negative results can occur due to environmental interferences.

This project was designed to improve the specificity and sensitivity of screening tests through the development of paper-based microfluidic devices for drug detection. These tests will be cheap, simple to use, and will provide rapid response times. Two different paper-based devices have been developed. The first device was based on adapting current colorimetric tests to a paper based format. Analytes included classes of seized drug samples such as opiates, phenethyl amines, amphetamines and cocaines. The second type of device was

developed for on-site detection of cocaine with aptamer based lateral flow assays designed to utilize gold-nanoparticle coupled reagents.

The construction of the paper-based microfluidic devices was relatively simple and only required chromatographic paper, wax-ink and a laminator. Wax ink provides a hydrophobic barrier and the paper substrate creates hydrophilic channels. This device utilizes capillary action to move the solvents, reagents and drugs to the designed position, where previously deposited sample reagents produce a color change, indicating a positive result. An advantage of the paper based approach is that multiple channels can be designed to simultaneously detect the presence of different analytes in a mixture.

(1) Colorimetric reagents based uPADs

Standard colorimetric reagents used in drug testing were modified for use with paper chips. These reagents are generally based on the detection of certain functional groups and commonly involve interaction with transition metals. We have developed a modified set of colorimetric reagents for the presumptive detection of seized drugs to permit their use with paper microfluidic devices. Reagents are placed in series along the length of each channel to permit reactions to occur at set locations and times. The result is a safe and easy to store device that permits detection of a wide variety of controlled substances and just slightly bigger than the size of a postage stamp. The multiplex test can be read in under 5 minutes and is stable for up to 3 months. The paper microfluidic tests are inexpensive and simple to operate.

(2) Gold nanoparticles/aptamers

Aptamers are alternatives to the lateral flow immunoassays that are currently used. Aptamers have the capability to bind specific target molecules, they have high selectivity and affinity. The change between dispersion and aggregation of gold nanoparticles produces a color change from red to blue. The color appears when hybridized DNA coupled nanoparticles are released from the aptamers, following the binding of the aptamer to a target drug. A rapid and specific method using a AuNPs/aptamers within a paper microfludic device has been developed for the field testing of seized cocaine. The stamp-size paper device produces a detectable color change by the naked eye or camera and can detect microgram levels of cocaine in under 5 minutes. The procedure was found to be selective against a wide variety of potential interferences. Furthermore, this strategy has the potential to detect other illicit drugs as new aptamers are being developed.

2. Future Work

The current work provides proof of concept for paper microfluidic devices as useful platforms for seized drug determination. Prior to implementation, a more extensive the validation of the current paper microfluidic devices would be necessary before implementation in laboratory operations. This would include testing of a wide range of drug substances and interferences. In addition, round robin tests of reproducibility and sensitivity as well as determinations of false positive/false negative rates should be undertaken. The effect of variations in

reagent concentration and accuracy should also be performed. It is important to note that for the multichannel device, most of the reactions have previously been well characterized in terms of sensitivity and specificity for many years. [1,2] Aptamer tests are relatively new, but there is a great body of literature on their application. [3]

Future studies for drug analysis may also involve new color tests and channels for other dangerous drugs such as cathiones and cannabinoids can be developed. Lastly, aptamers designed for the determination methamphetamine and codeine have been published. Initial laboratory studies have demonstrated that the approach used for the determination of cocaine will also work in methamphetamine and codeine determination. Thus this general procedure should prove useful for a wide range of analytes so long as similar aptamer based binding mechanisms can be developed.

3. References

1. Wong, R.L., Mytych, D., Jacobs, S., Bordens, R. and Swanson, S.J. Validation parameters for a novel biosensor assay which simultaneously measures serum concentrations of a humanized monoclonal antibody and detects induced antibodies. *Journal of immunological methods*, **1997**, *209*(1), 1-15

2. Piety, N. Z., Yang, X., Kanter, J., Vignes, S. M., George, A., Shevkoplyas, S. S. Validation of a low-cost paper-based screening test for sickle cell anemia. *PloS one,* **2016**, 11(1): e0144901.

3. Mairal, T., Özalp, V. C., Sánchez, P. L., Mir, M., Katakis, I., O'Sullivan, C. K. Aptamers: molecular tools for analytical applications. *Analytical and bioanalytical chemistry***, 2008**, *390*(4), 989-1007.

APPENDIX I

Table 4.5 The original records of the interferences tests.

Chemicals	AuNPs	
	Color change	Aggregation
Ketamine		No Aggregation
Codeine		No Aggregation
Morphine		No Aggregation
Ephedrine		No Aggregation
Amphetamine		No Aggregation
Methamphetamine		No Aggregation
JWH-073		No Aggregation
Caffeine	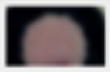	No Aggregation
Procaine HCl		No Aggregation
Sugar		No Aggregation
Sucrose	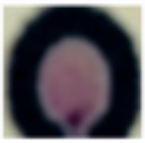	No Aggregation

Chemicals	AuNPs	
	Color change	Aggregation
Inositol	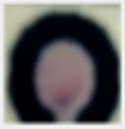	No Aggregation
Excedrine		No Aggregation
Ibuprofen	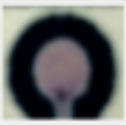	No Aggregation
Foot powder		No Aggregation
Baking soda	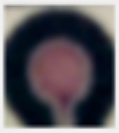	No Aggregation
Baking powder		No Aggregation
Sea salts	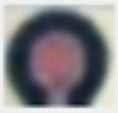	No Aggregation
Flour		No Aggregation
Powder sugar	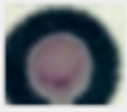	No Aggregation

APPENDIX II

Calculation of the cost of paper microfluidic devices in this project.

a. AuNPs/Aptamers based paper chips

For each chip: 10 cents

- Aptamer = $ 0.07548 (ACA-1, $22.10/umole, $40.80/umole)
  $ 62.9/umole * 1.2 nmole = $ 0.07548
  Total $ 0.07548/chip
- AuNPs
  $HAuCl_4$, $56.982/g * 0.039g/100mL * 2uL = $ 0.00004445
  Sodium citrate, $ 0.039/g*11.41g/100mLl*2Ul = $ 0.0000088
  Total $ 0.000053/chip
- Chromatographic Paper & Wax ink = $ 0.00923 (1cm * 2cm)
  $ 0.6595/ A4 size chromatographic paper, each A4 size paper can prepare 72 chips, each chip = $ 0.00915
  Xerox, ColorQube 8570 Black solid ink, $154.99/ 4 packs,
  each pack $38.7475, each ink pack yields approximately 8600 pages from their website data,we assume each pack prints 8000 pages, each page cost $ 0.00484, each page prepare 72 chips, each chip will cost $0.000067 for ink
  Total $ 0.0092
- $MgCl_2$ = $ 0.0025
  $0.1822/ gram * 5.6M * 150 μL = $ 0.00250
- Sucrose = $ 0.0005
  $ 0.03122/ gram * 100mg/mL * 150μL = $ 0.0004683

Above all, the total cost is = $ 0.0877

b. Colorimetric reagent based paper chips

For each chip: 10 cents

Chromatographic Paper & Wax ink = $ 0.00923 (1cm * 2cm)

All chemicals using in the test costs less 10 cents.

Appendix III

A comparison of detection limits for colorimetric tests and the paper microfluidic device developed in this work.

Reagent	Standard regents		Modified reagents	
	Components	NIJ detection limit	Components	Instrumental MDQ
Ferric chloride	$FeCl_3$, 20 mg/mL	50-200 µg morphine	$Fecl_3$, 100 mg/mL	3.2 µg morphine
Cobalt thiocyanate	$Co(SCN)_2$,10mg/mL Glycerol (v:v = 1:1)	60 µg cocaine	$Co(SCN)_2$,100mg/mL Glycerl (v:v = 3:2)	1.4 µg cocaine
Froede Reagent	MoO_3, 5mg/mL in hot conc. H_2SO_4	50 µg codeine	Permanganate(Paste) Molybdic acid(Paste)	2.0 µg codeine
Basified cobalt thiocyanate	$CoCl_2$, 2.9mg/mL NH_4SCN,3.04mg/mL NaOH 0.1M	N/A	$Co(SCN)_2$, 100mg/mL NaOH 2%	4.1 µg ketamine
Fast Blue B	Fast Blue B, 1mg/mL	10-100 µg methamphetamine	Fast Blue B 10mg/mL Na_2SO_4 100mg/mL	5.6 µg methamphetamine
Ninhydrin	Ninhydrin, 1 mg/mL	10-20 µg amphetamine	Ninhydrin, 50mg/mL NaOH, 1M	1.2 µg amphetamine

Appendix IV

Comparison of sensors for cocaine detection

Detection Method	Strategy	Detection limit
Visual (NIJ Standard reagent): Pink (negative) to Blue (positive)	Cobalt thiocyanate chemical reaction	60 µg with visual detection
Visual (Fan et al.) : Red (negative) to Blue (positive)	Aptamer and gold nanoparticle in solution tests	2 µM = 0.06 µg with UV-Vis detection
Visual (Lu et al): Blue (positive) to Red (negative)	Aptamer and gold nanoparticle in solution tests	50 µM = 1.5 µg with UV-Vis detection
This work: AuNPs/ Aptamers device Red (negative) to Blue (positive)	Aptamer and gold nanoparticle	2.36 µg

Appendix V. Comparison of screening tests for seized drugs and toxicological samples

	Spot Tests	TLC	Lateral flow Immunoassay	Colorimetric reagent based uPADs
Detection Method	Visual	Visual	Visual	Visual
Target	Seized drugs	Bulk drug material & toxicology sample[1]	Toxicology samples	Seized drugs
Market product	NARCO Pouch (Union Hall, VA)	Toxi-Lab (Irvine, CA)	TesTcard 9® (Brooklyn, NY)	-
Cost	$ 1.8-2.3 / single test	$ 8-15 / piece (since 2014 unmanufactured)	$ 4.25 / Device	$ 0.2 / Device
Detection Limit	Seized drugs [2] - Cocaine HCl 60 µg - d-methamphetamine HCl 10-100µg - d-amphetamine HCl 10-20 µg - morphine monohydrate 50-100 µg - codeine 1-50 µg - THC 5 µg	Urine sample Cannabinoid 2.5 µg [7] Codeine 5 µg [8] Morphine 10 µg [8] Cocaine metabolites 2µg [9]	Cut-off for urine samples [3]: Marijuana metabolites 2.5 ng* Cocaine metabolites 15 ng* Opiates 100 ng* Phencyclidine 1.25 ng* Aptametamines 50 ng*	Seized drugs - Cocaine HCl 1.4 µg - d-methamphetamine HCl 5.6 µg - d-amphetamine HCl 1.2 µg - morphine 3.2 µg - codeine 2.0 µg
Field Tests	Cocaine-specific field testing: [4] No comprehensive data available. False positives mentioned for certain compounds at levels above 2 mg input.	Toxilab commercial product Urine samples [5] False positive = 0.3-3.1%	TesTcard commercial product N= 80 urine samples [6]: False positive = 0-20% False negative = 0-1.25%	9 drugs tested, 18 interferences tested (no false positives detected at 1mg/ml input)

* Cut-off concentration * 50 uL

References

[1] Ojanpera, I. Forensic toxicology: Thin-layer (Planar) chromatography, **2000**, 2879-2885
[2] Color Test Reagents/Kits for Preliminary Identification of Drugs of Abuse, NIJ Standard-0604.01, 2000
[3] Schütz, H., Paine, A., Erdmann, F., Weiler, G., Verhoff, M. A. Immunoassays for drug screening in urine. *Forensic science, medicine, and pathology*, **2006**, *2*(2), 75-83.
[4] Tsumura, Y., Mitome, T. and Kimoto, S. False positives and false negatives with a cocaine-specific field test and modification of test protocol to reduce false decision. *Forensic science international*, **2005**, *155*(2), pp.158-164.
[5] Nora, P.R. Drug tests, nreilly.asp.radford.edu/drug%20tests.doc (accessed by July 11, 2017)
[6] Drug Test, http://courses.washington.edu/medch535/NEW/PDFs/535_13DrugTesting_2016.pdf (accessed by July 11, 2017)
[7] Dextraze, P.A.U.L., Griffiths, W.C., Camara, P., Audette, L. and Rosner, M., Comparison of fluorescence polarization immunoassay, enzyme immunoassay, and thin-layer chromatography for urine cannabinoid screening. Effects of analyte adsorption and vigorous mixing of specimen on detectability. *Annals of Clinical & Laboratory Science*, **1989**,*19*(2), pp.133-138.
[8] Simpson, D., Jarvie, D. R., & Heyworth, R.An evaluation of six methods for the detection of drugs of abuse in urine. *Annals of clinical biochemistry*, **1989,** *26*(2), 172-181.
[9] Adamovics, J. A. Analysis of addictive and misused drugs. CRC Press. 1994, pp 45

VITA

LING WANG

Born, Shanghai, China

2004-2008	B.S., Applied Chemistry Jiangsu Polytechnic University Changzhou, Jiangsu, China
2008-2009	Dye Technician Gabrain (Shanghai) Company, Shanghai, China
2009-2012	M.S., Analytical Chemsitry Florida Agricultural and Mechanical University Tallahassee, Florida Teaching Assistant Research Assistant
2012-2017	Ph.D., Chemistry with a Forensic Science Track M.S.F.S. Florida International University Miami, Florida Teaching Assistant Research Assistant

PUBLICATIONS AND PRESENTATIONS

Wang, L., Musile, G., McCord, B., An aptamer based paper microfluidic device for the colorimetric determination of cocaine (accepted)

Musile, G., Wang, L.(co-first), Bottoms, J., Tagliaro, F., McCord, B. The development of paper microfluidic devices for presumptive drug detection. Analytical Methods, Issue 19, 2015

Archibong, E., Wang, L., Ivanov, I., Lita, A., Redda, K., Mateeva, N., Investigation of the binding of dioxin selective pentapeptides to a polyaniline matrix, Synthetic Metals, June 2012

Wang, L., McCord, B., Applications of paper microfluidic devices in the field tests of seized drugs, 6th Annual IFRI Symposium, Miami, FL, May 9-10, 2017

Wang, L., McCord, B., Gold Nanoparticles (AuNPs)/Aptamer-Based Paper Microfluidic Devices Developed for the Detection of Cocaine, Pitccon,Conference & EXPO, March 5-9, 2017

Wang, L., McCord, B., Gold Nanoparticles (AuNPs)/Aptamer-Based Paper Microfluidic Devices Developed for the Detection of Cocaine, AAFS 69th Annual Scientific Meeting, New Orleans, LA, February 13-18, 2017

Wang, L., Musile, G., Bottoms, J., Tagliaro, F., McCord, B., Colorimetric based paper microfluidic devices for the presumptive determination of seized drugs, 5th Annual IFRI Symposium, Miami, FL, March 15-16, 2016

Wang, L., Musile, G., Bottoms, J., Tagliaro, F., McCord, B., Colorimetric based paper microfluidic devices for the presumptive determination of seized drugs, AAFS 68th Annual Scientific Meeting, Las Vegas, NV, February 22-27, 2016

Wang, L., Musile, G., Bottoms, J., Tagliaro, F., McCord, B., Presumptive determination of seized drugs using paper microfluidic devices, Florida Annual Meeting and Exposition 2015, Palm Harbor, Florida, May 8, 2015

Wang, L., Musile, G., Bottoms, J., Tagliaro, F., McCord, B., Presumptive determination of seized drugs using paper microfluidic devices, 4th Annual IFRI Forensic Science Symposium, Miami, Florida, May 5, 2015

Wang, L., Musile, G., Bottoms, J., Tagliaro, F., McCord, B., Presumptive determination of seized drugs using paper microfluidic devices, AAFS 67th Annual Scientific Meeting, Orlando, Florida, February 18, 2015

Wang, L., McCord, B., Detection for drugs of abuses with paper microfluidic devices assisted colorimetric tests. Florida Annual Meeting and Exposition 20014, Palm Harbor, Florida, May 8, 2014

Wang, L., Archibong, E., Ivanov, I., Lita, A., Redda, K., Mateeva, N., Binding of chlorinated toxins to selective peptides in solution, 88th FAME, Palm Harbor, FL, May 19, 2012

Wang, L., Archibong, E., Mateeva, N., Spectroscopic Investigation of the Binding of PCBs and Dioxins to Selective Peptides on Polyaniline Matrix, 87th FAME, Palm Harbor, FL, May 13-15, 2011